

Automated Scour Detection Arrays using Bio-Inspired Magnetostrictive Flow Sensors

Deliverable 12B
Report: Final Technical Report
January 29, 2016

Michigan Technological University
USDOT Cooperative Agreement No. RITARS-12-H-MTU

Principal Investigator: Dr. R. Andrew Swartz, Assistant Professor
Department of Civil and Environmental Engineering
Michigan Technological University
1400 Townsend Drive
Houghton, MI 49931
(906) 487-2439
raswartz@mtu.edu

Program Manager: Caesar Singh, P.E.
Lead Engineer/Program Manager
Office of the Assistant Secretary for Research and Technology
1200 New Jersey Avenue, SE, E33-123
Washington, DC 20590
(202) 366-3252

Caesar.Singh@dot.gov

MichiganTech

Project Personnel

Principle Investigators

Michigan Technological University

PI – R. Andrew Swartz (Assistant Professor)

Co-PI – Brian Barkdoll (Professor)

Michigan Tech Research Institution

Co-PI – Colin Brooks (Research Scientist)

University of Maryland

Co-PI – Alison Flatau (Professor)

Other Contributors

Michigan Technological University

Benjamin Winter (Graduate Student)

Baibhav Rajbhandari (Graduate Student)

Jennie Tyrrell (Graduate Student)

Megan MacNeill (Graduate Student)

Michigan Tech Research Institution

Reid Sawtell

K. Arthur Endsley

University of Maryland

Steven Day (Graduate Student)

Ganesh Raghunath (Graduate Student)

Suok-Min Na (Post-doctorate Fellow)

Technical Advisory Committee

Tim Ularich (Utah DOT)

Robert Ettema (University of Wyoming)

David Claman (Iowa DOT)

Rebecca Curtis (Michigan DOT)

Stanley Davis (Maryland DOT)

Acknowledgements and Disclaimer

This work is supported by the Commercial Remote Sensing and Spatial Information Technologies program of the U.S. Department of Transportation (USDOT) Office of the Assistant Secretary for Research and Technology, Cooperative Agreement #RITARS-12-H-MTU, with additional support provided by the Michigan Department of Transportation (MDOT), the Maryland State Highway Administration (MDSHA), Michigan Technological University, the Michigan Tech Research Institute, Civionics, and the Center for Automotive Research.

The views, opinions, findings, and conclusions reflected in this presentation are the responsibility of the authors only and do not represent the official policy or position of the USDOT/OST-R, MDOT, MDSHA, or any other entity.

Abstract

Scour is the most common cause of catastrophic bridge failures worldwide. Approximately over 60% of bridge failures reported in the United States from 1966 to 2005 are scour related. To ensure the continued safe operation of bridges, monitoring bridge scour is of paramount importance. Most monitoring regimes that are widely used are based on expensive underwater instrumentation. This research focuses on scour detection using automated remote flow detection arrays based on bio-inspired flow sensors. This study employs an array of bio inspired flow sensors that are inexpensive and robust versions of buried-rod scour sensor arrays, coupled with low-power wireless sensor network utilizing civil-engineering domain wireless sensing units to detect scour around bridge piers and abutments. Sensors within the network that report dynamic flow signals are considered to be waterborne or located above the sediment and sensors reporting static signals are characterized as buried or as being located in sediment. The *a priori* information of sensor depth will help to establish the sediment level in real time. An automated data interrogation system collects data, processes the raw sensor data using in-network data interrogation methods, then and communicates the results to the on-site base station. The relative directness of this data interrogation adds to the robustness of the system. The main purpose of the scour detection system is to provide remote scour information to bridge owners in a format that is easy to comprehend as an aid in decision making. In this project, only processed results, not raw data, are transmitted to the user. The system under study utilizes a cellular data link to relay simplified data to the bridge owner to aid in decision making.

A robust program of validation has been conducted to define the limits of the approach in the laboratory in the field. This reports details research activities on whisker development for sensitivity and robustness, signal processing, hardware development, installation methods, automation, and visualization of results.

Table of Contents

Project Personnel	i
Acknowledgements and Disclaimer	ii
Abstract.....	iii
1 Introduction.....	1
1.1 Scour.....	1
1.2 Impact of Scour	2
1.3 Detecting and Monitoring of Scour.....	3
1.4 Scour Monitoring system under study	3
1.5 Technical Challenges	4
1.6 Objectives and Scope	7
2 Literature Review.....	8
2.1 Portable Instrumentation Method.....	8
2.1.1 Diving	8
2.1.2 Sounding Rods or weights	8
2.2 Embedded Instrumentation Method.....	9
2.2.1 Sonar-Based Sensors Method	9
2.2.2 Time Domain Reflectometer (TDR) Method	10
2.2.3 Tilt -Meters Method.....	10
2.2.4 Magnetic sliding collar Method	11
2.2.5 Buried RF Sensor Method	12
2.2.6 Vibration-Based Method.....	12
2.2.7 Acoustic Doppler Current Profiler Method	12
2.2.8 Subsurface Geophysical Methods.....	13
3 Summary of DOT Survey Results	1
3.1 Procedure.....	2
3.2 Methods.....	5
3.3 Results	8
3.4 Conclusions	17
4 Post Sensor Survivability – Wired MD Installations.....	19

4.1	Scope	19
4.2	Phase 1 Installation.....	20
4.2.1	Installation plan.....	21
4.3	Results from Phase 1	30
4.4	Phase 2 Installation.....	32
4.4.1	New holders designed for new install procedure	32
4.4.2	Construction of scour post	32
4.4.3	Installation.....	33
4.5	Conversion to Autonomous Cellular Data Collection.....	34
4.5.1	Problems unique to wired system	35
4.6	Bathymetric Surveys for 2013 & 2014	36
5	Results of Laboratory Study	39
5.1	Objectives.....	39
5.2	Laboratory Facility.....	40
5.2.1	Flume (Water channel)	40
5.2.2	Scour experiment structure	42
5.3	Proposed Scour Detection System	44
5.4	Equipment for scour monitoring and detection.....	44
5.4.1	Transducers	44
5.5	Scour Measurement (Hydrology).....	47
5.6	Experimental Setup	47
5.6.1	Pier and abutment experiment	47
5.6.2	River bank experiment	48
5.6.3	Experimental Procedure.....	49
5.7	Results	50
5.7.1	Data collection analysis of laboratory experiment: model pier and abutment 52	
5.7.2	Data collection analysis of laboratory experiment: model post.....	53
5.8	Conclusions	55
6	Embedded System Design	56
6.1	Sensors	56

6.1.1	Whisker inspired magnetostrictive Galfenol sensors.....	56
6.2	Wireless sensing unit for scour sensing posts	58
6.2.1	Assembled smart scour sensing posts	61
6.3	Base Station.....	62
6.3.1	Single Board Computer.....	62
6.3.2	Cellular Data Link.....	63
6.3.3	Narada Base Station.....	63
6.3.4	Assembled Base Station.....	64
7	Scour Sensor Design – Corrosion Protection and Fluid	66
7.1	Development of Magnetostrictive Transducers	66
7.1.2	Fracture mode of Alfenol whiskers.....	76
7.1.3	Increasing response from Galfenol whiskers	79
7.2	Slow/Steady Flow and Seaweed Transducer Geometry	86
8	Signal Processing for Scour Detection	87
8.1	Objectives for autonomous detection algorithm	88
8.2	Platforms	88
8.3	Operation.....	88
8.3.1	Data acquisition (DAQ).....	89
8.3.2	Statistical computation.....	90
8.3.3	Fast Fourier transform and frequency-domain analysis.....	90
8.3.4	Decision file and application of thresholds.....	91
9	Decision Support Engine for Scour Monitoring	93
9.1	DSS Server	93
9.2	DSS Client Process.....	94
9.3	DSS Client Software	95
9.4	Conclusions	98
10	Field Validation of Magnetostrictive Scour Monitoring	99
10.1	Installation Plan	99
10.1.1	MI Bridge Number 1 – US41 crossing of the Pilgrim River	99
10.1.2	Bridge Number 2 – M38 crossing of the Sturgeon River	103
10.2	Installation	108

10.3	Operation – Problems Encountered.....	111
10.4	Conclusions	112
11	Conclusions.....	113
12	References.....	114

1 Introduction

Scour is a process of channel erosion around structural supports that can result in development of scour holes around the bridge structures that significantly reduce the foundation stiffness which may lead to abrupt collapse of the structure. It is not easy to prevent scour [1]. However, scour can be monitored over time and, if required, remediation measures can be implemented to avert the collapse of the structure or prevent the public from using it.

This section presents an introduction to scour and details its impact on civil structures such as bridges, abutments, and ridge piers. It also introduces the difficulties that are faced during the monitoring and measurement of scour, and this section briefly describes the conventional methods of scour detection that are commonly used (a topic presented in more detail in literature portion of this document). This section also gives an introduction to scour detection using automated remote flow detection arrays based on bio-inspired magnetostrictive flow sensors that this research focuses on.

1.1 Scour

“Scour is the result of the erosive action of flowing water, excavating and carrying away material from the bed and banks of streams and from around the piers and abutments of bridges” [2]. As such, scour can precipitate bridge collapse when the depth of scour hole formed near the foundations make them unstable. Scour can be categorized into three forms according to its occurrence as general scour, contraction scour, and local scour [3]. The depth of scour around a bridge structure is due to a combined effect of general, contraction and local scour. Scour that is caused as a result of lowering of the stream bed elevation over a short period of time or due increase in the elevation of bed is known as general scour. Change in elevation of the stream bed may occur naturally due to slow transport of sediment which results in lowering of elevation or due to slope failure in the upstream causing deposition of soil downstream, increasing the elevation of the stream bed. General scour can also occur due to simulated causes such as artificial straightening of river. Contraction scour occurs due to the increase in the water velocity which is caused by the decrease in cross-sectional area of the channel. The decrease in cross-sectional area is generally caused by construction of structures such as bridge piers and abutments or approach embankments. The increases in water velocity amplify the erosive action of water resulting in increased scour at the locality of a bridge [3]. Local scour takes place around the vicinity of the structure when a structure obstructs the flow of water or causes a change in pattern of the flow pattern. The change in flow pattern disrupts the equilibrium between actual sediment load and the capacity of the flow to carry sediment resulting in scour to restore equilibrium [4].

Civil structures sit on foundations which are, ideally, constant over time and their presence prevents collapse. Any course of action or natural process that undermines the foundations or the soil around them also causes damage to the structure. Bridge structures as well as embankments near roadways are mainly susceptible to this kind of attack when high-velocity water flows and transfer sediment away from the bridge foundation. Bridge

substructures consist of piers, abutments, and foundations, which are vital elements for safe operation of bridges. A bridge is considered scour critical when its foundations have been determined to be unstable for the calculated or observed scour condition [5]. Such bridges require extra attention from bridge owners.

1.2 Impact of Scour

Scour is considered one of the major causes of bridge failures in the United States. More than 20,000 bridges in the United States are considered scour critical [6]. More bridge failures are due to scour than to all other factors combined. Fig. 1.1 shows the contribution of different causes of bridge failure during 1996 to 2005 in the United States. It can be clearly seen that scour resulted in the highest number of bridge failure during this time period compared to other contributing causes. The 1987 catastrophic collapse of the Schoharie Creek Bridge in the state of New York is a prominent example of bridge failure due to scour (Fig. 1.2). The chief cause of the Schoharie Creek Bridge failure was reported to be scour under a plain concrete pier footing [7]. This incident showed the devastating nature of scour damage and signified the need and importance of proper scour monitoring.

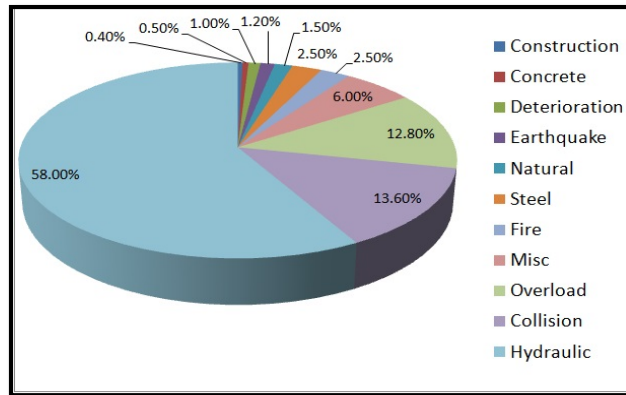


Fig. 1.1: Cause of Bridge Failure (1966-2005) (Data Source: New York State DOT and Texas A&M University)

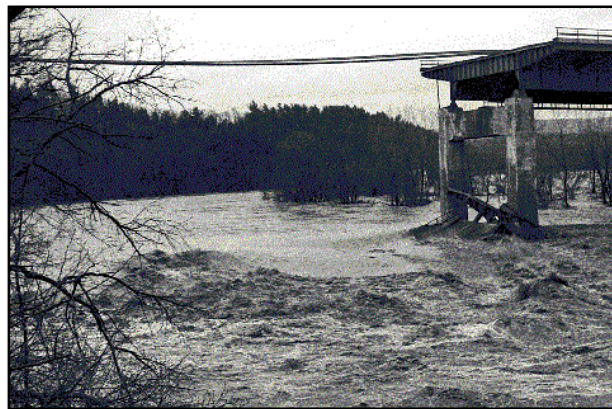


Fig. 1.2: Schoharie Creek Bridge Collapse (Used with permission from http://en.wikipedia.org/wiki/Schoharie_Creek_Bridge_collapse)

1.3 Detecting and Monitoring of Scour

Monitoring scour is a very useful countermeasure to deal with bridge failure caused by scour, as potential scour problems can be identified early and required course-of-action can be taken. However, since scour occurs under the channel flow and usually cannot be visually detected, it is not easily discernible [8]. The flow of water may deposit or erode the sediments in the river bed over time making it more difficult to detect scour.

Scour monitoring allows for action to be taken before the potential failure of a bridge which may endanger the safety of the public. Nearly all of the methods that are currently used to measure scour suffer from some drawback in that they are either expensive, are only capable of measuring maximum scour (thus they do not monitor scour continuously), or do not work in difficult but common water conditions, such as turbulent, sediment-filled, or icy water conditions. The most commonly used methods to measure scour are visual inspection, sonar technology, sounding rod, and diving method, along with a few embedded instrumentation methods such as magnetic sliding collar and Tilt sensors. The relative merits of these approaches are presented in literature review portion of this document.

1.4 Scour Monitoring system under study

The approach of scour monitoring under study is automated, remotely operated embedded sensor networks that have the ability to measure and record scour conditions on a continuous basis. The scour sensor network in study utilizes an array of bio-inspired flow sensors along with low power, inexpensive sensor network. A diagram of the system under study is shown in Fig. 1.3.

The scour monitoring system under study is aimed at being inexpensive, easy to install, and low maintenance. The system is being designed to be robust, which will make it difficult to damage and suitable for different working conditions such as turbulent water flow and conditions with large amount of debris and sediment. The robust nature of the transducers adds to the robustness of the system. The system will also be remotely operated and automated, making it easier to monitor scour on different conditions and also eliminating the requirement of having experienced personnel at site.

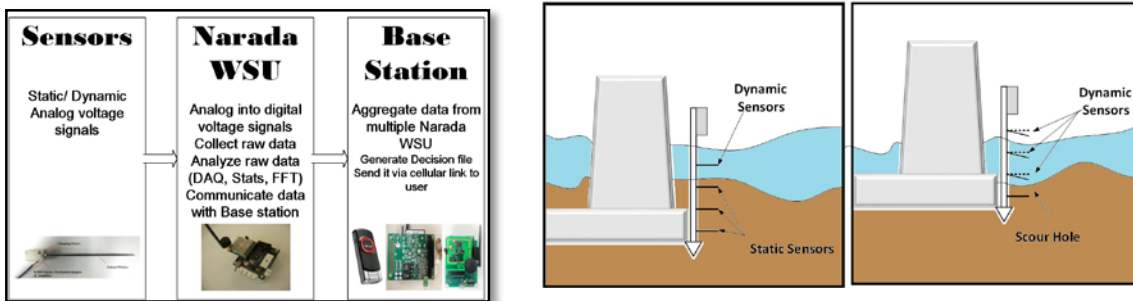


Fig. 1.3: Working of Proposed System: (left) concept schematic and (right) installation

1.5 Technical Challenges

Numerous technical barriers were investigated during the course of the project. This section will discuss these barriers and the approach taken for overcoming them in four broad categories: 1) those barriers associated with sensor protection; 2) those associated with signal generation; 3) those associated with signal processing and classification; and 4) those associated with flow of data/information and decision support. Each of these categories of challenges is discussed below.

Sensor Protection: Despite their inherent mechanical robustness, protection of the proposed magnetostrictive sensors from corrosion is an issue that required study for use in the proposed application. Galfenol is an iron-based alloy which has corrosion properties that are similar to those of steel. The flow sensor design must incorporate sufficient corrosion protection for the Galfenol whiskers to have a life expectancy that is matched to the life expectancy of the batteries that power the wireless data acquisition system.

Previously, Tata Steel (tatasteel.com) had a comprehensive publication to provide “guidance on the corrosion and protection of H-section (steel) universal bearing piles”. They note that fresh water can contain dissolved salts, gases or pollutants that are harmful to ferrous alloys (like Galfenol). And although corrosion loss from river water immersion is generally lower than for seawater, their report shows results from studies of H-section steel bearing pile corrosion that exhibited corrosion rates in fresh water of 0.02 – 0.05mm/side/year, and in corrosive soils of up to 0.015mm/side/year. With these corrosion rates, if made from an unprotected Galfenol strip with a thickness of 0.50 mm, the proposed whiskers would vanish several years (<5) after installation.

Canadian researchers have conducted the only prior known studies on the corrosion of Galfenol. Their studies suggest iron provides a good basis for initial Galfenol corrosion design considerations. They indicated a negligible corrosion rate for Galfenol (with gallium content that ranges from 15% to 27%) in de-aerated 3.5%NaCl solution at 25°C. They suggest that this because a protective film is formed on the alloy surface causing its potential (E) to fall below -0.79~-0.86, which is below the cathodic protection criterion for iron.

This protective film resulted in a plateau potential region during the anodic polarization scan. Gallium oxide (Ga_2O_3) layer as a major component of the protective film formed like dense aluminum oxide (Al_2O_3) layer on aluminum, and the increase of gallium content in Galfenol is more effective for protecting on the surface. However, they observed pitting and crevice corrosion on Galfenol with gallium content greater than 18.4% after cyclic polarization scan. The average corrosion rate of Galfenol in naturally aerated 3.5%NaCl solution is approximately four times lower than that of AISI 1012 steel, while it is higher than that of 304 stainless steel.

In this study, cathodic protection is explored in order to further improve the corrosion life of Galfenol whiskers. Alfenol (Iron-Aluminum) whiskers, with lower magnetostrictive coupling properties but improved robustness are also examined.

The smart scour-sensing post concept requires that the magnetostrictive flow sensors be capable of surviving the installation process which will involve being driven into the soil near abutments, culverts, and in river banks. Flanges installed just below the sensors will protect their bases during driving. It was initially proposed to install them in a coiled condition utilizing a water-soluble tie to hold the entire whisker within the protective shadow of the base flange; that tie will dissolve after installation when water is present. Ultimately a number of installation approaches were found to be effective. Use of a hollow-stem auger allowed posts to be installed in wet conditions without exposing whiskers to driving damage. In dry conditions (riverbanks), a standard auger was found to deliver the same benefit. In driven applications (the worked in both wet and dry conditions), flanges protected the whiskers when using a low-power, handheld pneumatic hammer to provide the driving force. An alternative to the magnetostrictive whisker sensor, a magnetic sea weed sensor (composed of a cloth strip and rare-earth magnet) was also deployed that could survive all three installation processes.

Signal Generation: Generation of appropriate signals under certain conditions was envisioned to be another potential barrier to successful implementation of the proposed approach. For low-flow conditions, there may be little dynamic signal generated by the whisker sensor which may make unburied sensors appear to be buried sensors. The project team performed extensive laboratory studies to quantify which conditions have sufficiently low enough flow levels to create false indications of the trapped condition to understand where these conditions may occur in the field. In addition, the geometric properties of the whiskers as well as their support conditions provided some avenues for alleviating this problem. By varying the whisker profile to increase fluid-structure instability and by altering the roughness around the base of the whisker, additional turbulence can be introduced into the system that will benefit free-condition detection. The aforementioned alternative transducer design, the magnetic sea weed sensor, proved to be especially useful in low-flow conditions as well.

Signal Processing and Classification: Several signal processing and classification barriers were overcome for the successful validation of this approach. To accomplish low-power operation of the remote sensing hardware it is important to take advantage of embedded processing techniques. Embedded processing techniques are important in low-power and wireless application as transmission of raw data represents the most energy intensive process for such systems. Local, embedded data processing allows sensors to transmit only results from the engineering algorithms rather than lengthy time-history records saving energy and extending battery life.

The most basic embedded processing task is flow detection. The system operates by differentiating between static and dynamic flow signals returned from the magnetostrictive whiskers. For fast moving and turbulent water bodies, such a distinction is relatively trivial to make from highly varying sensor data. For slow moving bodies exhibiting laminar flow around piers, application of sophisticated autonomous signal processing techniques can help to distinguish genuine perturbations from noise. The laboratory experimental study was used to highlight conditions under which flow detection becomes difficult. Here, basic

signal processing (discrete Fourier transform) and data classification (naive Bayes classifier) techniques were used to differentiate between noise and very low signals based on the vibrational properties of the whisker sensors themselves.

The array of magnetostrictive whisker sensors was designed to provide sufficient measurement points to provide useful scour measurements in real time. The automated system monitors the locations of sensors returning static and dynamic data and maintain a map of the estimated channel bed profile. The system also notes sensors that are topographical outliers: either dynamic sensors surrounded by static sensors, or static sensors surrounded by dynamic sensors. Such sensors may indicate unusual scour, impingement of whiskers by trees or other debris, or a sensor fault condition. Because some applications for these sensors require installation below the water line (*e.g.*, bridge piers), the cost of installing the system becomes a concern. The team worked with state DOT partners to establish the optimal number and placement of sensors depending on the application and establish installation guidelines according to feedback received from these agencies as well as through feedback gained from a national survey of state DOTs.

In any long-term installation, sensor reliability and sensor failure are important problems. To reduce false alarms due to transducer failure, there has been significant progress made in the field of fault detection for permanently installed sensor arrays. The issue of sensor failure is particularly troublesome in systems such as the proposed scour monitoring system in which static, or noise only, sensor signals are used as an important indicator (in this case, presence of sediment). Without embedded sensor fault detection algorithms, signals measured from damaged sensors may be easily interpreted as dynamic data potentially triggering false alarms, or worse, as static data, potentially missing hazardous scour events. Sensor failure detection algorithms were also implemented to look for common failure modes including excessive noise, loss of signal, intermittent railing, and drift.

Data/information flow and decision support: The purpose of the proposed system is, rather than overwhelm them in raw data, to present remote scour information to bridge owners in an easy to use, easy to understand format to aid in decision making. Coordination of the flow of data and information between the remote sensing system and the decision support client was a major challenge. The bulk of data processing is embedded in the sensors themselves. The actionable and decision-enabling outputs that are produced from sensor hardware are: flow or no-flow (static versus dynamic) state of the sensor (or a sensor fault condition detected), the channel bed profile, and the time-series of scour depth over a user-defined time period. In addition, user-defined parameters and thresholds will contribute even more to a rich, decision-making workflow. An example of added-value processes and products is the provision of critical scour depth alerts (*e.g.* an e-mail or application pop-up to notify decision makers about a recent critical scour depth measurement) based on user-defined thresholds. Another example are report templates, stored on the server, dynamically populated with up-to-date bridge information, and generated quickly upon request in a variety of formats (*e.g.* Microsoft Word Document or Adobe PDF).

The project team worked closely with its cost-share partners, the Michigan Departments of Transportation and Maryland State Highway Administration (MDSHA) as well as the TAC

and survey respondents to develop visualization and analysis routines that best support decision makers, and establish sample intervals and alarm conditions.

1.6 Objectives and Scope

The main objectives of the research are:

1. Development of a robust sensors, sensor network, and economical installation approaches.
2. Laboratory validation of the automated scour detection and monitoring system that is based on bio-inspired flow sensing sensors.
3. Signal processing, which includes building library of signals at different flow conditions such as turbulent flow, laminar flow. Characterize typical dynamic signatures for varying conditions and establish classification criterion and thresholds.
4. Embedded, automated data collection and interrogation system integration.
5. Validation work on data collection, installation strategies, and decision making support tools.
6. Installation of field validation system at existing bridges.

2 Literature Review

This literature review outlines the conventional instrumentation existing for monitoring and measurement of scour and their characteristics based on literature review of sensors used and instrumentation technologies that are utilized for monitoring scour at the specific site condition. During the past decade, monitoring concepts for structural systems have been subjected to a rapid development process. They play a huge role in the intervention planning of new and existing structures [6]. Similarly, in the past few decades a number of interesting methods for detection and monitoring of scour have been developed. This section of the document briefly describes a few of the conventional methods that are widely used for scour monitoring and measurement.

Scour detection methods can be classified by several factors including function, purpose, measurement technologies, and instrumentation. They are classified into two categories according to instruments utilized is portable instrumentation methods and embedded instrumentation methods. Portable instrumentation method include diving, sounding rods, *etc.*, and fixed or embedded instrumentation method consists of buried RF sensors, sonar, *etc.*

2.1 Portable Instrumentation Method

Portable instrumentation methods basically depend on visual inspections conducted by professionally trained inspectors with experience. Although this method of scour monitoring has served well for many years, this approach may not be the best to implement as the data from this method may not be very accurate and this approach can be dangerous in some cases.

Portable instrumentation methods are well suited for use by bridge maintenance and inspection crews for detecting scour conditions at piers and abutments and taking cross sections of the channel at problem bridges [9]. However, these methods have many drawbacks such as difficulty in mobilizing a crew of well trained workers and experienced supervisors and safety and requirement of traffic control for tests.

2.1.1 Diving

Diving is a simple method of scour monitoring in which a qualified bridge inspector performs a manual inspection of bridge underwater. Scour data can be collected from many locations using this method and the water clarity does not affect the data collection process. However, the drawback of this method is that it can be expensive and thus this method is mostly suitable only for worst case scenarios. It also includes considerable potential danger. Additionally, the data obtained by such visual inspections can contain a high degree of variability due to the subjectivity of the inspectors.

2.1.2 Sounding Rods or weights

Sounding-rod or falling-rod instruments are manual or mechanical gravity-based physical probes. In this method a qualified bridge inspector performs a manual inspection by dropping a rod or weight on the streambed to measure the sediment depth, as depicted in Fig. 2.1. The bottom of the rod needs to be wide in order to prevent the rod from penetrating

the streambed caused by the weight of the rod and the vibration due to flowing water. Sounding rods tend to go through the streambed when the river bed consists of sand which influences their accuracy. The main drawback of this method is the inaccuracy of the data samples acquired and the potential danger involved in this method. Moreover, this method can be expensive and does not have the ability of automated alerts [10].

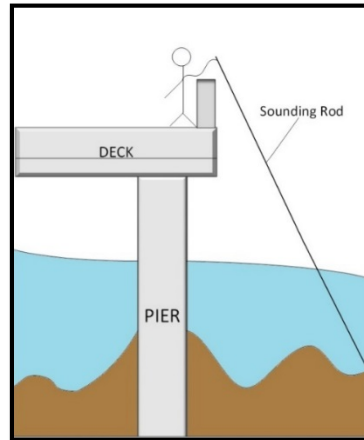


Fig. 2.1: Sounding rod instrumentation

2.2 Embedded Instrumentation Method

Fixed instrumentation methods, also known as embedded instrumentation of scour monitoring, include instrument that are placed in the vicinity of the bridge or in the bridge structure itself, typically at piers and abutments, to record data for the purpose of alerting the concerned personnel when the scour depth becomes excessive. The instrument is installed at preselected bridge sites to monitor and measure scour. Most commonly used embedded instrumentation monitoring methods include sonar based sensors, magnetic sliding collars, float-out devices, sounding rods and tilt meters. The type of fixed scour monitoring system adopted depends on the kind of information desired.

Embedded instrumentation generally measures scour only in the vicinity of the area where they are installed [11]. This method of scour monitoring does not require a field crew to be at site for monitoring or measurement or to record data.

2.2.1 Sonar-Based Sensors Method

Sonar-based sensors are fixed instruments and are typically mounted, as shown in Fig. 2.2, at the pier and abutment locations. Sonar emits pulse waves and calculates the round trip travel time of a pulse from the riverbed to measure scour depth. Sonar sensors have the capability of measuring both scour and deposition of sediments. The major limitation of sonar as a scour measuring instrument is that their readings are negatively affected in water with high sediment and turbulent flow. High end sonars with high depth capacity and resolution can be expensive [12].

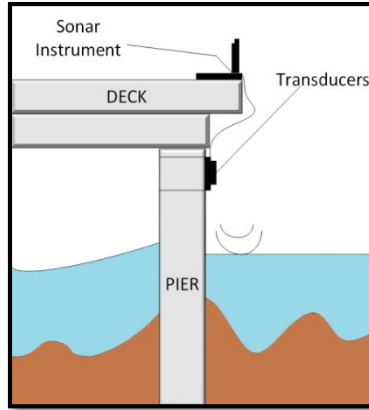


Fig. 2.2: Sonar-based sensor scour instrumentation

2.2.2 Time Domain Reflectometer (TDR) Method

Time domain reflectometer (TDR) based methods utilize similar method to sonar to measure scour. However, in TDR, a magnetic pulse is sent through sensor conduits and the magnetic pulse helps to determine the portion of the conduits buried in the stream bed. TDRs are capable of performing repeatable tests and are very robust. However, the tests conducted by this method require large amount of power, making them expensive. Furthermore, the signal analysis instruments associated with Time domain Reflectometer are extremely complicated and are difficult to calibrate [13]. An illustration of the TDR instrumentation *in situ* is provided in Fig. 2.3.

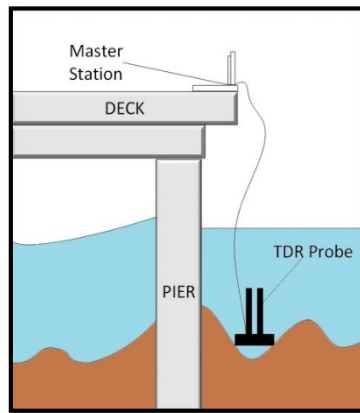


Fig. 2.3: Time Domain Reflectometer for scour sensing

2.2.3 Tilt -Meters Method

Tiltmeters, also known as inclinometers, use a very simple method for scour measurement. Tilt-meters are fixed to a bridge structure such as an abutment or pier, depicted in Fig. 2.4. When the structure leans or tilts due to scour, the Tilt-meters sense this change to measure scour. This method is relatively simple and is appropriate for extreme scour cases. However, this method measures extreme case scour and it can be difficult to distinguish

between scour movements from the common movements of the structure caused by traffic, thermal, wind, and other causes [10].

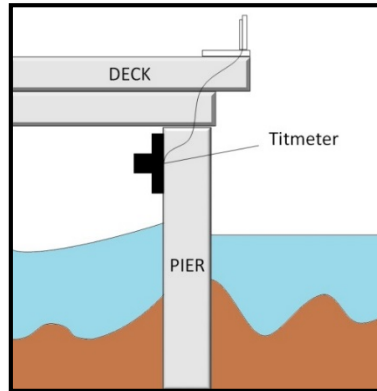


Fig. 2.4: Tilt-meter scour detection schematic

2.2.4 Magnetic sliding collar Method

Magnetic sliding collars are another effective device used for detection of scour. This instrument consists of a heavy collar mounted on a magnetic rod. The rod is driven into the streambed (Fig. 2.5) and the collar rests on the streambed. During scour, as sediment is washed away from the streambed, the collar slides down the magnetic rod with the decreases in level. A base station detects this change in height of the collar, which is used to deduce scour. It is a direct method of measurement and its reading are not affected by the quality of water. Although this method is very useful in measuring scour depth, the main drawback of this method is that its sensors can be used only once and they are not capable of measure sediment deposition [14].

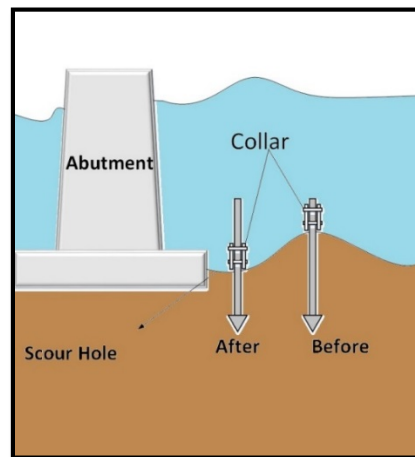


Fig. 2.5: Sliding collar scour sensing

2.2.5 Buried RF Sensor Method

Buried RF sensors are floating electronic devices that are buried in sediment at predetermined depths. When the sediment is scoured away, the devices rise to the surface and transmit RF signal (Fig. 2.6). The Base station senses signal and notes a scour event. The main advantage of this method is that it is not affected by the quality of water and it is a direct scour measurement. The main disadvantage associated with this method is that it uses single use sensors, making them costly. The sensors also require long lasting battery power to be able to transmit signals when they resurface to the top. Distinguishing between healthy devices and faulty ones can also be very difficult in this method [10].

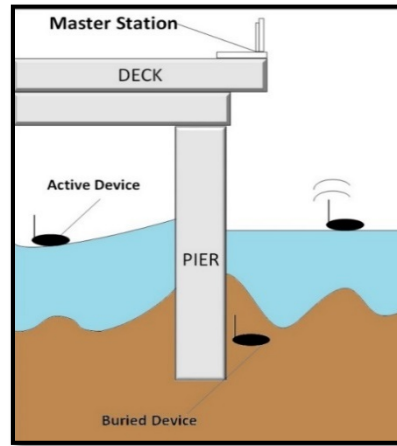


Fig. 2.6: Buried RF Sensors

2.2.6 Vibration-Based Method

This method utilizes the concept of measuring the fundamental frequency of a rod embedded in the riverbed. The inverse relationship between fundamental frequency and the length of the sensor rod is used for the detection of scour depth. It uses structural vibration sensors including accelerometers or fiber optic Bragg-grating (FBG) for use as the dynamic sensing element of the scour sensor. However, this method is yet to be fully validated. It is an ongoing research and tests are being performed on it [15].

2.2.7 Acoustic Doppler Current Profiler Method

This method is based on the Doppler Effect, i.e., the relative change in frequency of the wave. Acoustic Doppler Current Profilers use the Doppler Effect to measure the depth of water and to determine the velocity profile (Fig. 2.7), which assists in scour forecasting. Scour is then determined from the velocity of the flow. It is an indirect method of scour measurement. Additionally, this method of scour measurement is not feasible for areas with snow and the device used in this method are not rugged [16].

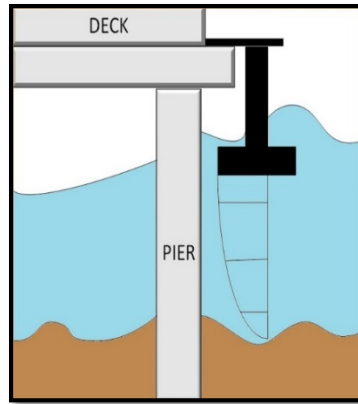


Fig. 2.7: Acoustic Doppler

2.2.8 Subsurface Geophysical Methods

Geophysical instruments are based on wave propagation and reflection measurements. Geophysical instruments combine continuous seismic-reflection profiling and ground penetrating radar. They have the ability to provide accurate results and are capable of real time scour measurements. However, these instruments are expensive, very complicated to use, and require expertise to analyze the resulting data. The instrument is very hard to automate and it is not very effective in deep water. This method is mainly used after flood during lower flow conditions to locate scour holes and areas of infilling [17].

Other instruments for scour measurement include float out sensors and accelerometers. The accelerometer is used to measure the acceleration of the member it is attached to. It measures the vibration properties of the bridge which is caused by the change in support conditions of the bridge due to scour. Accelerometers are very easy to install and maintain but accelerometers require lot of power to transmit and require considerable post-processing. Float out sensors are similar to buried RF sensors.

An ideal scour monitoring and detection system should integrate all the advantages of various type monitoring systems to obtain more useful information on scour depth through direct monitoring and should be able to aid the decision-makers with the obtained information. In other words, they should be permanent, automated, robust, inexpensive, and should have a long life. Conventional scour monitoring instrumentation often necessitates costly installation and maintenance. They can also be vulnerable to debris damage during flooding. Often, the data from these instruments can be difficult to read and can be time consuming to process.

My research is focused on developing a low-maintenance system to detect and monitor scour development. The advantages of the system under study over traditional instrumentation are the ease of installation and the low maintenance.

The system studied in this research (automated scour detection array using magnetostrictive flow sensors) is automated, has the capability to capture transient events and can issue warnings. It is in continuous operation and the system uses low-power

hardware components coupled with an appropriate power harvesting technology. It is highly robust (withstand adverse weather conditions) and inexpensive compared to other monitoring systems. Moreover, it uses low power and the data analysis is very simple. It harvests sustainable power by using solar cells. The sensors used are magnetostrictive sensors, which are attractive for scour measurement purpose due to their robustness and their low corrosion property. The proposed wireless monitoring system utilizes and takes advantage of a low-power wireless sensor network constructed from *Narada* wireless sensing modules and utilizes a cellular data link for secure data transfer.

3 Summary of DOT Survey Results

A 14 question survey was distributed to 79 state DOT hydraulics and bridge management personnel soliciting their opinions regarding the aspects of the proposed bioinspired scour monitoring system including questions about application, usefulness, installation concerns, desired system resolution, and commercialization issues. Responses are not individually identifiable by individual of DOT agency by the investigators or in this report.

Based on the responses from the DOT Bridge and Hydraulic Engineers listed above it can be concluded that:

1. Scour is a problem in fewer than 10% of bridges, primarily due to successful monitoring and/or countermeasures.
2. Most bridges do not use permanently-embedded scour detection sensors.
3. Of those that use permanent sensors, all states only used them on ‘scour critical’ bridges.
4. When used, permanent sensors are mounted on piers or abutments and at the scour depth considered critical to collapse, with a few applications on the deck beams.
5. Sensors are mainly buried in the riverbed with some bolted onto the bridge.
6. The most common method of scour detection was a survey rod from the bridge deck for shallow flows and divers for deeper flows, with some using sonar.
7. At least one sensor is needed near the scour-critical elevation but more are also necessary at other elevations and near the bridge beams.
8. At least one sensor is needed at the front of the structure but more are also helpful at the sides and rear of the structure.
9. Scour levels need not be reported more often than hourly.
10. Scour information should be sent when a threshold level is crossed but continuous data should also be available via the internet.
11. Annual monitoring costs should be kept to under \$1,000, if possible, but no more than \$10,000.
12. Installation by burying in the riverbed is preferred with other acceptable methods being bolted onto the bridge and in a post. Installation in flowing water is acceptable.
13. Sensors are needed on piers and abutments, but not necessarily on riverbanks, or culverts.
14. There was not a significant preference for ownership arrangements with both DOT owned and private service provider being acceptable.

The full set of questions and responses is presented in this report.

Real-time scour monitoring on bridges for scour can lead to the saving of property and lives. In this regard, Michigan Technological University is conducting research into the feasibility of using magnetostrictive sensors for this purpose.

This section of the research project includes the following:

The team will canvass the state DOT agencies to solicit additional information regarding the needs of bridge owners for scour monitoring as state DOT agencies represent a large

and influential group of bridge owners. We hope to achieve three goals: 1) understand the costs associated with their current scour inspection paradigm for the final project cost/benefit analysis; 2) understand the information they would require from a remote monitoring system in terms of sensor density and location, sampling frequency, information, visualization, service life, and cost; and 3) establish acceptable installation methods for sensors, particularly at piers. State DOT's response rate will be a critical evaluation criterion; the team will follow up with respondents for additional information when appropriate.

Outputs include:

Improved understanding of bridge owner costs associated with scour.

Improved understanding of system requirements.

3.1 Procedure

The survey questions were as follows:

Question 1. On what percent of bridges is bridge scour a problem for your agency?

Percentage (1-100%)_____

_____None, due to successful monitoring and/or countermeasures

_____None, due to favorable site conditions

Question 2. Do you use permanently-embedded scour detection sensors?

_____Yes

_____No

Question 3. How is it decided if scour sensors are needed on a particular bridge?

_____Bridge is considered 'scour critical'

_____River is subject to high flow velocity.

Question 4. If used, where are the sensor(s) located on the bridges, and why?

_____Bridge deck

_____Deck beams

_____Pier or abutment

_____Near critical scour depth of pier or abutment

Question 5. If used, how are the scour sensors installed?

_____ Bolted onto bridge

_____ Buried in riverbed

_____ Flow diverted first

_____ Installed in flowing water

_____ Other (please specify)

Question 6. What are the scour inspection methods commonly used for typical bridges in your inventory and their approximate costs per bridge?

_____ Survey rod from bridge deck (cost)

_____ Divers (cost)

_____ Other (please specify)

Question 7. What are the desired number and location of sensor systems?

_____ Only one sensor is needed near the scour-critical elevation

_____ Sensors are needed at many elevations

_____ Sensors near the bridge beams to monitor water surface

Question 8. Sensors are needed at the structure:

_____ Front

_____ Sides

_____ Rear

Question 9. How often is the scour condition needed?

_____ Once a minute

_____ Once a hour

_____Once a day

_____Once a month

Question 10. How should the info be displayed to DOT engineers to make the best use of it?

_____Message when sensor is triggered

_____Continuous sensor status

_____Cell phone message

_____Log onto a sensor website with sensor status

_____Other (please specify)

Question 11: What annual cost per bridge is reasonable for monitoring?

_____Under \$100

_____Under \$500

_____Under \$1,000

_____Over \$10,000

_____Other (please specify)

Question 12: What installation methods are acceptable for permanently-embedded sensors?

_____Bolted onto bridge

_____Buried in riverbed

_____Sensors in a post that is installed near the structure (perhaps using a hollow stem auger)

_____Flow diverted first

_____Installed in flowing water

Question 13. Are scour sensors needed on the following structures?

- _____Piers
- _____Abutments
- _____River banks
- _____Culverts
- _____Other

Question 14. Ownership of sensor system preference:

- _____Owned and maintained by your DOT
- _____Owned and maintained by a private service provider
- _____No preference

3.2 Methods

The survey questions as listed above were sent out using SurveyMonkey in such a way that the respondent was anonymous. The survey email was sent to all DOT Bridge and Hydraulic Engineers in all 50 states at the following email addresses (obtained from Dan Ghere at FHWA and at: <http://design.transportation.org/Documents/AASHTO%20State%20Hydraulics%20Contact%20Info%20Summer%202011.xlsx>)

- flournoyg@dot.state.al.us <mailto:flournoyg@dot.state.al.us>
- ramseyd@dot.state.al.us <mailto:ramseyd@dot.state.al.us>
- michael.knapp@alaska.gov <mailto:michael.knapp@alaska.gov>
- lItty@azdot.gov <mailto:lItty@azdot.gov>
- Mark.Earl@arkansashighways.com <mailto:Mark.Earl@arkansashighways.com>
- glenn_s_decou@dot.ca.gov <mailto:glenn_s_decou@dot.ca.gov>
- kevin_flora@dot.ca.gov <mailto:kevin_flora@dot.ca.gov>
- steve_ng@dot.ca.gov <mailto:steve_ng@dot.ca.gov>
- amanullah.mommandi@dot.state.co.us
<mailto:amanullah.mommandi@dot.state.co.us>
- michael.masayda@ct.gov <mailto:michael.masayda@ct.gov>
- barry.benton@state.de.us <mailto:barry.benton@state.de.us>
- reginald.arno@dc.gov <mailto:reginald.arno@dc.gov>
- rick.renna@dot.state.fl.us <mailto:rick.renna@dot.state.fl.us>

bmcmanus@dot.ga.gov <mailto:bmcmanus@dot.ga.gov>
sbeck@dot.ga.gov <mailto:sbeck@dot.ga.gov>
curtis.matsuda@hawaii.gov <mailto:curtis.matsuda@hawaii.gov>
lotwick.reese@itd.idaho.gov <mailto:lotwick.reese@itd.idaho.gov>
matthew.oconnor@illinois.gov <mailto:matthew.oconnor@illinois.gov>
cmweaver@indot.in.gov <mailto:cmweaver@indot.in.gov>
david.claman@dot.iowa.gov <mailto:david.claman@dot.iowa.gov>
orth@ksdot.org <mailto:orth@ksdot.org>
ronald.matar@ky.gov <mailto:ronald.matar@ky.gov>
mitra.hashemieh@la.gov <mailto:mitra.hashemieh@la.gov>
michael.wight@maine.gov <mailto:michael.wight@maine.gov>
akosicki@sha.state.md.us <mailto:akosicki@sha.state.md.us>
kpujara@sha.state.md.us <mailto:kpujara@sha.state.md.us>
richard.g.murphy@state.ma.us <mailto:richard.g.murphy@state.ma.us>
potvinc@michigan.gov <mailto:potvinc@michigan.gov>
andrea.hendrickson@state.mn.us <mailto:andrea.hendrickson@state.mn.us>
rwesterfield@mdot.state.ms.us <mailto:rwesterfield@mdot.state.ms.us>
dale.henderson@modot.mo.gov <mailto:dale.henderson@modot.mo.gov>
mgoodman@mt.gov <mailto:mgoodman@mt.gov>
kevin.donahoo@nebraska.gov <mailto:kevin.donahoo@nebraska.gov>
kirk.harvey@nebraska.gov <mailto:kirk.harvey@nebraska.gov>
cwolf@dot.state.nv.us <mailto:cwolf@dot.state.nv.us>
sswana@dot.state.nh.us <mailto:sswana@dot.state.nh.us>
mrichardson@dot.state.nh.us <mailto:mrichardson@dot.state.nh.us>
tmallete@dot.state.nh.us <mailto:tmallete@dot.state.nh.us>
david.ahdout@dot.state.nj.us <mailto:david.ahdout@dot.state.nj.us>
wgannett@dot.state.ny.us <mailto:wgannett@dot.state.ny.us>
dmorse@dot.state.ny.us <mailto:dmorse@dot.state.ny.us>
dchang@ncdot.gov <mailto:dchang@ncdot.gov>
bpfeifer@nd.gov <mailto:bpfeifer@nd.gov>
jeffrey.syar@dot.state.oh.us <mailto:jeffrey.syar@dot.state.oh.us>
tngo@odot.org <mailto:tngo@odot.org>

llewis@odot.org <mailto:llewis@odot.org>
alvin.shoblom@odot.state.or.us <mailto:alvin.shoblom@odot.state.or.us>
ed.foltyn@odot.state.or.us <mailto:ed.foltyn@odot.state.or.us>
cnewcomer@state.pa.us <mailto:cnewcomer@state.pa.us>
c-dnewell@state.pa.us <mailto:c-dnewell@state.pa.us>
lusantos@dtop.gov.pr <mailto:lusantos@dtop.gov.pr>
vpalumbo@dot.ri.gov <mailto:vpalumbo@dot.ri.gov>
rfura@dot.ri.gov <mailto:rfura@dot.ri.gov>
helmspw@scdot.org <mailto:helmspw@scdot.org>
smoakck@scdot.org <mailto:smoakck@scdot.org>
kevin.marton@state.sd.us <mailto:kevin.marton@state.sd.us>
ali.hangul@tn.gov <mailto:ali.hangul@tn.gov>
jon.zirkle@tn.gov <mailto:jon.zirkle@tn.gov>
aronnfel@txdot.gov <mailto:aronnfel@txdot.gov>
jamesbaird@utah.gov <mailto:jamesbaird@utah.gov>
nick.wark@state.vt.us <mailto:nick.wark@state.vt.us>
ba.thrasher@vdot.virginia.gov <mailto:ba.thrasher@vdot.virginia.gov>
kramerc@wsdot.wa.gov <mailto:kramerc@wsdot.wa.gov>
darrin.a.holmes@wv.gov <mailto:darrin.a.holmes@wv.gov>
douglas.w.kirk@wv.gov <mailto:douglas.w.kirk@wv.gov>
najoua.ksontini@dot.state.wi.us
<mailto:najoua.ksontini@dot.state.wi.us>
AnnMarieE.Kirsch@dot.wi.gov <mailto:AnnMarieE.Kirsch@dot.wi.gov>
william.bailey@dot.state.wy.us <mailto:william.bailey@dot.state.wy.us>
william.ray@la.gov <mailto:william.ray@la.gov>
Parviz.eftekhari@state.nm.us <mailto:Parviz.eftekhari@state.nm.us>
john.r.woodroof@odot.state.or.us
<mailto:john.r.woodroof@odot.state.or.us>
jon.zirkle@tn.gov <mailto:jon.zirkle@tn.gov>
dstuhff@utah.gov <mailto:dstuhff@utah.gov>
rodney.taylor@dot.state.wi.us <mailto:rodney.taylor@dot.state.wi.us>
najoua.ksontini@dot.state.wi.us

The initial survey was sent out for respondents to fill out by SurveyMonkey on March 26, 2013, after which reminder emails were sent out on April 10, 2013 and April 30, 2013.

The following results were collated on May 30, 2013.

3.3 Results

There were 33 respondents to the survey, probably reflecting the views of 33 out of the 50 states, although it is possible that more than one DOT engineer from a state responded to the survey.

Table 3.1: Question 1- On what percent of bridges is bridge scour a problem for your agency?*

	(1-5)%	(6-10)%	(11-15)%	(16-20)%	(21-25)%	Response Count
Percentage	46.15% (12)	30.77% (8)	7.70% (2)	7.70% (2)	7.70% (2)	26
None, due to successful monitoring and/or countermeasures	8					8
None, due to favorable site conditions	3					3
answered question						30
skipped question						3
Comments						15

*Some respondents chose one of the “None” options but also chose a numerical percentage. These were considered in the respective “None” groups.

Comments:

1. Scour critical bridges.
2. The percentage is low because of efforts to install mitigation at problem sites and for liberal use of riprap on new bridges
3. Estimated.
4. All remaining SC bridges are scheduled for replacement in next 8 yrs
5. Sort of depends on what you consider a "problem". This is an educated guess, and also depends on if we include all of the bridges in the state, or just those that we (the state) own.
6. Didn't we fill this same survey out a few weeks ago?
7. WAG. Monitoring is not considered a long term solution.
8. Only about 5 percent of the bridges over water in the state are listed as scour critical and all are monitored using the Bridgewatch monitoring program.
9. Countermeasures protect others
10. PennDOT does use monitoring and scour countermeasures on scour critical bridges. However, this does not eliminate scour failures.
11. Just under 5 percent of our bridges over water are rated scour critical. All of our scour critical bridges have POAs according to FHWA requirements and are monitored using the Bridgewatch Program from US Engineering Solutions.
12. As defined by have a scour rating of 4 or less.

13. Unclear how to respond to 2 other input boxes. 3-5% of our bridges have scour concerns
14. 50% of waterway bridges
15. All scour critical bridges (unknown foundations, shallow foundations, etc) have had countermeasures placed. All new bridges have scour calcs done as part of the design, to make sure foundation is below Q500 scour. All other bridges are checked for scour when a rehab is planned. Eventually we'll check every bridge in the state.

Table 3.2: Question 2- Do you use permanently-embedded scour detection sensors?

	Response Percent	Response Count
Yes	15.60%	5
No	84.40%	27
answered question		32
skipped question		1
comments		9

Comments:

1. We have a research project in progress with Clemson University installing real time scour devices. One device is in with 3 more being installed this year.
2. Float out were used in the past without much success.
3. We have one location where float out devices were installed.
4. sliding collar or sonar
5. Overhead, climatic Conditions and vandalism are the impediments
6. The Bridgwatch system can monitor in place scour devices and send alerts to our inspectors when a threshold is exceeded however we have not a bridge where in place monitoring was justified for the associated cost to date.
7. On 1 structure.
8. Not currently, but we would like to.
9. We use a lot of tilt sensors which technically isn't measuring any scour; just the result of scour

Table 3.3: Question 3- How is it decided if scour sensors are needed on a particular bridge?

	Response Percent	Response Count
Bridge is considered 'scour critical'.	100.00%	14
River is subject to high flow velocity.	0.00%	0
answered question		14
skipped question		19
Other replies		15

Other replies:

1. N/A
2. May be other factors, including scour history at the site and route importance (ADT, etc.).
3. The bridges also have real time USGS discharge gages and as-built plans.
4. Depending on scour risk rating, sufficiency rating and ADT of the bridge.
5. The bridge is scour prone
6. Float out device was installed on a bridge with a failed countermeasure as an interim measure until funding could be found and a mitigation contract completed. The float out devices are now under the riprap.
7. N/A
8. We don't use sensors
9. Dependent on risk assessment, so far we have used this on major river bridges with high ADT or bridges with chronic scour issues that can't be monitored easily by other methods.
10. Would be case by case.
11. N/A
12. Long term monitoring would be required in lieu of very expensive or otherwise difficult scour mitigation techniques.
13. This structure has sandy soil which made it a concern.
14. Don't use scour sensors
15. N/A

Table 3.4: Question 4- If used, where are the sensor(s) located on the bridges, and why?

	Yes	No	Rating Count
Bridge deck	11.1% (1)	88.9% (8)	9
Deck beams	22.2% (2)	77.8% (7)	9
Pier or abutment	76.9% (10)	23.1% (3)	13
Near critical scour depth of pier or abutment	68.8% (11)	31.3% (5)	16
answered question			18
skipped question			15
Other (please specify)			7

Other replies:

1. Not used
2. Buried under the riprap protection (float-outs)
3. Not on simply supported members. Trying to monitor for settlement, so pier members better. Some float-outs (limited battery life) installed at scour depth.
4. Can be site specific, safety of the inspector is a key component
5. N/A
6. The sensors are located on the upstream end of the pier and abutment that historically have had scour issues at two levels. The first level is to warn us of an issue the second level requires the bridge be closed.
7. N/A

Table 3.5: Question 5- If used, how are the scour sensors installed?

	Response Percent	Response Count
Bolted onto bridge	29.40%	5
Buried in riverbed	41.20%	7
Flow diverted first	5.90%	1
Installed in flowing water	5.90%	1
Other (please specify)	17.60%	3
answered question		
skipped question		

Other replies:

1. Not used
2. We have done it multiple ways, I wanted to select: Bolted onto bridge, buried in riverbed, and installed in flowing water.
3. Bolted and buried. Dry conditions allow buried devices.

Table 3.6: Question 6- What are the scour inspection methods commonly used for typical bridges in your inventory and their approximate costs per bridge?

	Response Percent	Response Count
Survey rod from bridge deck (cost)	31.00%	9
Divers (cost)	10.30%	3
Other (please specify)	58.60%	17
answered question		29
skipped question		4

Other replies:

1. Survey rod is used, divers are used, bathymetric survey.
2. Routine bridge inspection and maintance reports also divers perform underwater inspection every 5 year and post floods as well.
3. We Use both methods listed depending on site conditions.
4. Survey rod, and divers for deep rivers
5. Probing of streambed during inspection. Also have used sidescan sonar
6. We use bridge inspection including underwater inspection.
7. In water probing or divers. approx cost 2,000
8. Tape down from bridge deck, sonar imaging
9. Sonar
10. We inspect dropping weighted measuring tape from bridge deck and underwater scour using divers
11. We monitor using both methods. The regular inspections are typically done with divers, flood monitoring is generally done from the bridge deck. We have also used some side scan sonar (very limited). Cost - on deck monitoring is done with our own forces, no cost data available. Underwater inspections with divers typically cost about \$2000.
12. In house bridge inspectors wade all creeks with water depths of 3 ft or less and probe with survey rod. Divers are used on bridges with depths greater than 3 ft.
13. For wadable channels, scour inspection is performed by bridge safety inspection teams using probe rods. For deeper channels, scour inspection is performed by divers.
14. TDOT's bridge inspections are done with in house inspection teams. Underwater inspections are done for piers in excess of 3 feet of water depth and all those are done by contract divers.
15. Structures that require an underwater inspection sonar and sidescan sonar are used; which the equipment is owned by the State. (equipment cost less than \$10,000) Structures with water less than 4 feet visual and probing methods are used.
16. Laser from below or weighted tape from the deck when dry is most common. Cost is trivial. Sonar from boat and divers are secondary means with a wide range of cost associated.
17. Divers are used for deeper waters. Others can be inspected by wading or are dry or in shallow water during low flows.

Table 3.7: Question 7- What are the desired number and location of sensor systems?

	Yes	No	Rating Count
Only one sensor is needed near the scour-critical elevation	90.9% (10)	9.1% (1)	11
Sensors are needed at many elevations	78.6% (11)	21.4% (3)	14
Sensors near the bridge beams to monitor water surface	63.6% (7)	36.4% (4)	11
answered question			19
skipped question			14
Comments:			8

Comments:

1. Depends on instrument type.
2. We currently use electronic transducers for scour monitoring at the bridges where we have determined that they are the best suited.
3. Float out devices were installed at two levels. The first level is a "warning". The second is placed lower.
4. N/A
5. Depends on what you are monitoring: riprap protection, water surface elevation, or the riverbed. I'd say typically we would use one sensor located a few feet below the water surface to avoid ice and debris (with a sonar system).
6. Used Ultrasonic to measure water surface elevations. Not sure of your question.
7. N/A
8. You need a warning level so you can get to the bridge and close it before it becomes unsafe.

Table 3.8: Question 8 – Sensors are needed at the structure:

	Yes	No	Rating Count
Front:	100.0% (21)	0.0% (0)	21
Sides:	78.6% (11)	28.6% (4)	14
Rear:	61.5% (8)	38.5% (5)	13
Other (please specify)			8
answered question			21
skipped question			12

Other replies:

1. Typically where the worst scour occurs - at the leading edge of the piers.
2. Site specific. Sensor locations are determined on a case by case basis.
3. It's really a case by case decision
4. We have seen scour at all of these locations.
5. N/A
6. Normally front, maybe sides, normally not the rear.
7. N/A
8. Most problems appear at the nose, but hydraulic skew can move this location depending on the site conditions.

Table 3.9: Question 9- How often is the scour condition needed?

	Response Percent	Response Count
Once a minute	12.50%	2
Once an hour	68.80%	11
Once a day	18.80%	3
Once a month	0.00%	0
answered question		16
skipped question		17
Comments:		11

Comments:

1. Every 1-3 hours during high flow events. Otherwise, every week or month to ensure the instrument is still working.
2. During flash floods and during spring snow melt.
3. Seasonally dependant.
4. Under high flow conditions, otherwise once a month
5. Not sure what this question is asking.
6. N/A
7. During significant rain events and established inspection frequencies.
8. Every 4-8 hours should suffice
9. Measure often, but may only need reporting hourly or daily if nothing is moving.
10. N/A
11. The buried devices will send an alert when activated. In addition we have implemented BridgeWatch which lets us know when enough rainfall and/or flow (from USGS gauge stations) is likely to produce scour which is approximately within a minute of live data.

Table 3.10: Question 10- How should the info be displayed to MDOT engineers to make the best use of it?

	Response Percent	Response Count
Message when sensor is triggered	21.70%	5
Continuous sensor status	17.40%	4
Cell phone message	8.70%	2
Long onto a sensor website with sensor status	17.40%	4
Other (please specify)	34.80%	8
answered question		23
skipped question		10

Other replies:

1. I don't know. I'm a PennDOT engineer.
2. All good options. Automated e-mail/text message when a threshold is reached. Continuous monitoring via website is good option also.
3. More than one option should be used, incase of power outage or cell phone service is down duringg the time of need.
4. N/A

5. Best to have message when sensor is triggered, but also have the continuous data available on a website to view when interested/needed.
6. All of the above. Need overlapping notification to make the correct determination of the bridge status.
7. N/A
8. We receive a message when the sensor or threshold is triggered through e-mail or text message. In addition we can log into a web site to monitor rainfall NWS and flow USGS through BridgeWatch.

Table 3.11: Question 11- What annual cost per bridge is reasonable for monitoring?

	Response Percent	Response Count
Under \$100	4.30%	1
Under \$500	21.70%	5
Under \$1,000	39.10%	9
Under \$10,000	0.00%	0
Over \$10,000	0.00%	0
Other (please specify)	34.80%	8
answered question		23
skipped question		10

Other replies:

1. Varies, depending on the importance of the bridge and the scour history at the site. \$1,000 is reasonable for "important" bridges.
2. For small bridges ideally under \$1K while \$10K for larger bridges may be okay
3. Currently using BridgeWatch to monitor rainfall intensities. It is hard to estimate cost because we have internal overhead to administer the system
4. N/A
5. Do you include the capital cost here (spread out over the life for cost)? I'm a little confused, but I would say in the \$500 range seems appropriate with capital and maintenance costs (and phone plans, etc).
6. N/A
7. Our current monitoring with the Bridgewatch program is under \$10 per month per bridge.
8. The float out devices for one bridge were approximately \$15,000 counting labor to install and maintain the system for seven years a total of \$24,500 or \$3,500 per year. BridgeWatch was implemented for \$350 per bridge per year.

Table 3.12: Question 12- What installation methods are acceptable for permanently-embedded sensors?

	Yes	No	Rating Count
Bolted onto bridge	92.9% (13)	7.1% (1)	14
Buried in riverbed	100.0% (15)	0.0% (0)	15
Sensors in a post that is installed near the structure (perhaps using a hollow-stem auger)	68.8% (11)	31.3% (5)	16
Flow diverted first	42.9% (3)	57.1% (4)	7
Installed in flowing water	100.0% (8)	0.0% (0)	8
Other (please specify)			6
answered question			21
skipped question			12

Other replies:

1. Sensor must have minimal protrusion. Otherwise, it might cause scour itself due to vortices/turbulence. Also, any sensor that is separate from the substructure unit is simply another obstruction that could cause scour itself or will become a debris catch point.
2. All good options. Depends greatly on the concerns the site and things you want to monitor.
3. Will vary depending on site conditions and the project (new vs existing structure)
4. Debris and ice are significant problems
5. N/A
6. N/A

Table 3.13: Question 13- Are scour sensors needed on the following structures:

	Yes	No	Rating Count
Piers	100.0% (22)	0.0% (0)	22
Abutments	76.2% (16)	23.8% (5)	21
River banks	35.7% (5)	64.3% (9)	14
Culverts	20.0% (2)	80.0% (8)	10
Other	20.0% (1)	80.0% (4)	5
answered question			22
skipped question			11
Comments:			5

Comments:

1. Typically concerned most with piers in live-bed conditions. The rest can usually be monitored and repaired following the event.
2. N/A
3. Typically we only use these on Piers or sometimes abutments. We haven't used any on banks or culverts.
4. Culverts not part of my area. River banks normally extend outside of right of way.
5. PennDOT does not use scour sensors.

Table 3.14: Question 14- Ownership of sensor system preference:

	Yes	No	Rating Count
Owned and maintained by your DOT	93.3% (14)	6.7% (1)	15
Owned and maintained by a private service provider	80.0% (4)	20.0% (1)	5
No preference	75.0% (6)	25.0% (2)	8
answered question			21
skipped question			12
Comments:			7

Comments:

1. Whichever is most economical
2. Depends on costs, maintenance required. Instrument should require very little maintenance to be useful. Should also consider USGS, since this is what they do well.
3. N/A
4. I think this is the second time this survey has been filled out. Can you please send survey results and information on your project to:

Wayne Gannett, P. E.
 Hydraulic Engineering Unit
 NYS Department of Transportation
 50 Wolf Rd., Pod 4-3
 Albany, NY 12232
 518-457-9215

5. Hard to maintain.
6. PennDOT does not use scour sensors.
7. Both the DOT and private have their advantages and disadvantages

3.4 Conclusions

Based on the responses from the DOT Bridge and Hydraulic Engineers listed above it can be concluded that:

1. Scour is a problem in fewer than 10% of bridges, primarily due to successful monitoring and/or countermeasures.
2. Most bridges do not use permanently-embedded scour detection sensors.
3. Of those that use permanent sensors, all states only used them on ‘scour critical’ bridges.
4. When used, permanent sensors are mounted on piers or abutments and at the scour depth considered critical to collapse, with a few applications on the deck beams.
5. Sensors are mainly buried in the riverbed with some bolted onto the bridge.
6. The most common method of scour detection was a survey rod from the bridge deck for shallow flows and divers for deeper flows, with some using sonar.
7. At least one sensor is needed near the scour-critical elevation but more are also necessary at other elevations and near the bridge beams.
8. At least one sensor is needed at the front of the structure but more are also helpful at the sides and rear of the structure.

9. Scour levels need not be reported more often than hourly.
10. Scour information should be sent when a threshold level is crossed but continuous data should also be available via the internet.
11. Annual monitoring costs should be kept to under \$1,000, if possible, but no more than \$10,000.
12. Installation by burying in the riverbed is preferred with other acceptable methods being bolted onto the bridge and in a post. Installation in flowing water is acceptable.
13. Sensors are needed on piers and abutments, but not necessarily on riverbanks, or culverts.
14. There was not a significant preference for ownership arrangements with both DOT owned and private service provider being acceptable.

4 Post Sensor Survivability – Wired MD Installations

In the interest of facilitating some field testing in the first year of the project, development of the smart scour-sensing posts was been split between several sections of this document: Section 4; Section 6; and Section 10. In this section, a wired version utilizing laptop-based National Instruments data acquisition systems was be developed for initial field data collection campaigns. In this section, the scour-sensing post assemblies were be constructed without the wireless and embedded data interrogation components as purely a data collection device. During this work discussed in this section, different sensor protection flange geometries and post installation approaches were tested with whisker survivability during the driving process used as the primary evaluation metric. Initial field campaigns in Maryland began in October of 2013. After installation, UMD students and MDSHA personnel made (at a minimum) quarterly trips to the instrumented bridge abutment and riverbed migration sites and used laptops to collect data from the hard wired scour-sensing posts.

This data was used to evaluate the behavior and survivability of the scour-post sensors in the field, and to compare and contrast scour-post data with the routine site evaluations performed by the MDSHA staff at these scour-prone sites as well as with MDSHA scour model predictions. Phased installations were made, 2 bridges at a time. In the first installation phase, hollow-stem augers were used to install posts that were then wired to a central access point located on the bridge. It was found that excessively tight clearances in the posts around the whisker sensors confined the materials leading to excessive strains and breakage. Whisker sensors were replaced and larger clearances given to protect the whisker sensors. In the second phase, a driven approach using segmental posts and a handheld hydraulic hammer was used for post installation, leading to faster and less expensive installations. During the final year of the project, the manual data acquisition systems were replaced with cellular-enabled automated systems, though wiring between the posts and base station was retained.

Output(s):

- Demonstration of successful installation of the scour-sensing posts with survival of the whiskers.
- Improved installation methods.
- Whisker protection flange design improvements.
- Manually collected field data.
- Conversion to autonomous cellular (remote) system.

4.1 Scope

Four bridges in the State of Maryland were instrumented using early versions of the scour sensing post system. The objectives of the work included in Section 4 were to demonstrate post installation, collect early scour data, and study whisker survivability for varying installation approached. Mean and implementation for meeting the objectives of this work were executed in 2 Phases, with the first phase focused on prototype design/development and hollow-stem auger installation, and the second on a more economical driven post approach. The sites used are listed below in Table 4.1.

Table 4.1: Maryland post instrumentation sites.

Bridge #0301900 MD 25 over Georges Run Baltimore County Location: http://maps.google.com/?ll=39.615291,-76.790078&spn=0.00137,0.00283&t=h&z=19
Bridge #15053 MD 355 over Little Bennett Creek Montgomery County Location: http://maps.google.com/?ll=39.279264,-77.314761&spn=0.001385,0.00283&t=h&z=19
Bridge #1008600 MD 355 over Bennett Creek Montgomery County Location: http://maps.google.com/?ll=39.317898,-77.332635&spn=0.007835,0.016479&t=h&z=16
Bridge #1200900 MD 7 over James Run Harford County Location: http://maps.google.com/?ll=39.476643,-76.260341&spn=0.002762,0.005659&t=h&z=18

4.2 Phase 1 Installation

In the first installation phase, the Maryland team developed the smart scour sensing post prototype. Based on performance of the GMR based whisker sensor that was initially proposed, it was decided to use Hall-effect sensors owing to the appropriateness of its range and greater sensitivity. Different configurations of the sensors were tested to decide the optimal location of the biasing magnet and Hall-effect sensor with respect to the whisker. Once the basic principle was finalized, different compositions of the whisker were tested with the inclusion of tertiary additives including Niobium Carbide and Molybdenum. The performances of these whiskers were compared to one and other. Other than Galfenol, Alfenol (an alloy of Iron and Aluminum) was also tested owing to its sustainability and cost effectiveness. The best performing whiskers have been chosen to be used in the scour post prototype. It has been decided that the prototype has both Galfenol and Alfenol whiskers to allow the team the opportunity to compare the performance and survivability of both compositions in the field.

Since oscillations were difficult to observe in the bare whiskers at extremely low-flow velocities, various alternative geometries were tested to induce oscillations. These included tree-like whiskers, whiskers with different 2D plates attached to the free end, whiskers with zip-ties attached, and placement bluff bodies upstream of the post. A design of the post with the Hall effect sensor attached to the post and a spring with a permanent magnet oscillating in the water was tested for low water speeds. Also, attached airfoils to the free end of the whisker were also tested for low water velocities (see laboratory study).

It was decided to change the material for the scour post from PVC (original concept) to galvanized steel to avoid failure upon impact during storms. Studies have been initiated to test to whether the magnetic signal is lost due to the post. This consideration proved crucial in deciding whether galvanized steel will ultimately be appropriate for the prototype.

For the first iteration of the scour sensing post, the team used Arduino microcontrollers to collect field data. One Arduino will be connected to each of the sensors, and will reside within the post. From this unit, a wire was run to the shore, connecting to another Arduino with the ability to record data onto an SD card. This data, sent via serial communication, consisted of raw voltage readings that can be post processed on a computer after being downloaded from an SD card. For this first iteration, power was also be supplied from the shore using large batteries that could be accessed to recharge, when needed.

4.2.1 Installation plan

Based on feedback received from the TAC, revised installation plans were developed to eliminate pile driving (and reduce the chances of whisker damage) and instead use hollow-stem augering. Creation of a casing around the top portion of the post is desired to protect the whiskers and avoid having to back fill hollow stem auger with dirt is the auger is removed. This casing needed to be an ecofriendly substance that would dissolve quickly when the post is exposed to water. To accomplish this goal, the team experimented with Sodium Acetate solutions (an ecologically friendly salt) mixed with dirt and rock. Sodium Acetate has the ability to supersaturate in water, causing rapid crystallization with the introduction of a seed crystal. The team found that when we pour the hot super saturated solution over the dirt and rock, it creates a solid structure upon cooling. This structure then rapidly dissolves in water leaving only dirt behind.

Initially, the team had planned on using a PVC post for mounting our sensors. But, due to uncertainties regarding the structural integrity of the PVC post during a storm with rocks hurtling around, the team decided to use a galvanized steel post. Since galvanized steel is magnetic, the team had to make sure that there was no loss of sensitivity of the sensors which depends heavily on magnetics of the environment. For this, the team tested a bench-top setup with a whisker sensor inside galvanized steel pipe to ensure that the sensors would still work as expected. This setup is shown in Fig. 4.1. Results from this test showed that the sensors would still exhibit good sensitivity despite the use of galvanized steel. Two galvanized steel pipes 14'6" long (3.5" outer dia.) were ordered and after many rounds of discussions, a CAD drawing of the post was created to nail down the location of the holes for sensors on the post. The bottom 7ft of the post was going to be filled with concrete (8" outer dia.) to act as ballast once it gets drilled into the river bed. It was decided to drill 22 holes for Galfenol and Alfenol whiskers (11 each at intervals of 6" for the first 4ft and at 1ft intervals for the last 3 ft) as shown in Fig. 4.1.

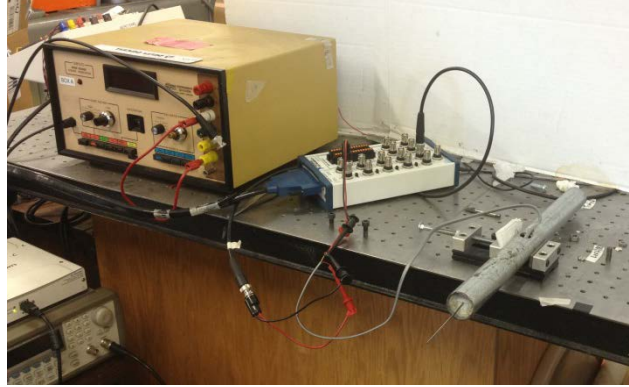


Fig. 4.1: Bench top setup to test use of galvanized steel.

Since there was curvature and dimensions were too unwieldy, the team had to drill the holes manually. Apart from the holes for the whiskers, the team decided to incorporate 4 low speed sea weed like sensors on the post. The location of these sensors was in the first 2ft of the post at 6" intervals just below the whisker sensors. Additional smaller holes had to be drilled for the jig which would hold the sea weed sensor components. In addition to these holes, a hole needed to be drilled at the top of the post for a shackle which would be used to lift the post up using the excavator and dropped in to the hole drilled using the auger. A hole had to be drilled at the bottom of the exposed top of the post for wires to run from the sensors to the shore through a conduit. Fig. 4.2 (a-c) show the holes drilled for the whiskers, shackle and seaweed sensors respectively.



(a)



(b)



(c)

Fig. 4.2: (a) Holes drilled for the whiskers; (b) shackle, and; (c) seaweed sensors.

Holes were also drilled in all directions in the lower 7' of the post for rebar to pour the concrete. A coat of galvanizing spray paint and a coating of water resistant paint were used

to prevent the drilled region from rusting due to prolonged exposure to water. The rebar was cut into 8" long pieces using a hack saw machine and inserted into the holes and the post was now ready for concrete. This post is shown in Fig. 4.3.



Fig. 4.3: Post coated with waterproof paint with rebar inserted for pouring concrete.

The post was then taped up with duct tape in the top 7'6" to prevent concrete from getting into the holes. An 8" outer diameter Sonotube was inserted into a PVC pipe of 8" inner diameter and the post was lowered into this. This setup is mounted vertically into a bucket and secured to a frame using harnesses to hold it in place. The space between the bucket and the PVC pipe is filled with paver base to support the structure. This setup is shown in Fig. 4.4. The post is centered in the Sonotube using styrofoam.



Fig. 4.4: Post set up vertically for pouring concrete.

Concrete was mixed in a wheelbarrow as shown in Fig. 4.5 and was transported to the top of the frame from where it was poured into the Sonotube. This is shown in Fig. 4.6. Periodically the tube was hammered so that the concrete settles. This was done to avoid air bubbles in the ballast which might compromise the integrity of the structure.



Fig. 4.5: Concrete mixed in a wheel barrow.



Fig. 4.6: Concrete poured into Sonotube to create ballast for scour post.

Once the desired height of 7ft for the ballast was reached, the concrete in the post was allowed to cure for 24 hours under constant supervision. After the concrete had dried, the post was lowered on to a pallet from the frame by loosening the harness and the Sonotube was ripped out after pulling out the PVC sleeve. The final post with the 8" dia. concrete ballast is shown in Fig. 4.7.



Fig. 4.7: Post with cured concrete ballast.

This post was moved indoors to install wires. The post had to accommodate 11 wires (with 3 channels each: Voltage input, Ground and Signal out) for each of the sensors. Hence, the length of wire required for each sensor was calculated based on its location on the post and pre-cut. The wiring from the electrical box which would be on the shore was made of 4 wires containing 3, 3, 3 and 4 channels. Two channels on the wire with 4 channels were dedicated ground and power channels. The remaining 11 channels were meant to carry signal from each of the 11 sensors on the post to the Arduino processor in the box which was used to record data on to an SD card. These 4 wires (50ft long, calculated based on the tentative length of the sensor post to the electrical box on the shore) had to be fed through a harsh weather conduit to protect the wires from hurting rocks in case of a storm event. This work was accomplished using fish tape. One end of the 4 wires was staggered and then hooked up to the pulling end of the fish tape and taped up using electrical tape. Soap was used as a lubricant and applied to the entire 50ft length. The other end of the mule tape was tied to a pillar and the conduit was slipped on over the 4 wires for the entire length. Once fed through the conduit as shown in Fig. 4.8, the end that was at the post was soldered on to an electrical circuit board.



Fig. 4.8: Wires fed in to harsh weather conduit.

The dedicated Ground and Power channels were split into 11 terminals at the board to which the power and ground wires from each of the sensors was connected as shown in Fig. 4.9. The signal from each of the 11 sensors was connected to the 11 channels between the 4 wires running to the shore using the board as well. (*i.e.*, the circuit board was used to create a common ground and a common power line for all the sensors that would go on the post and each sensor had a separate channel for signal).

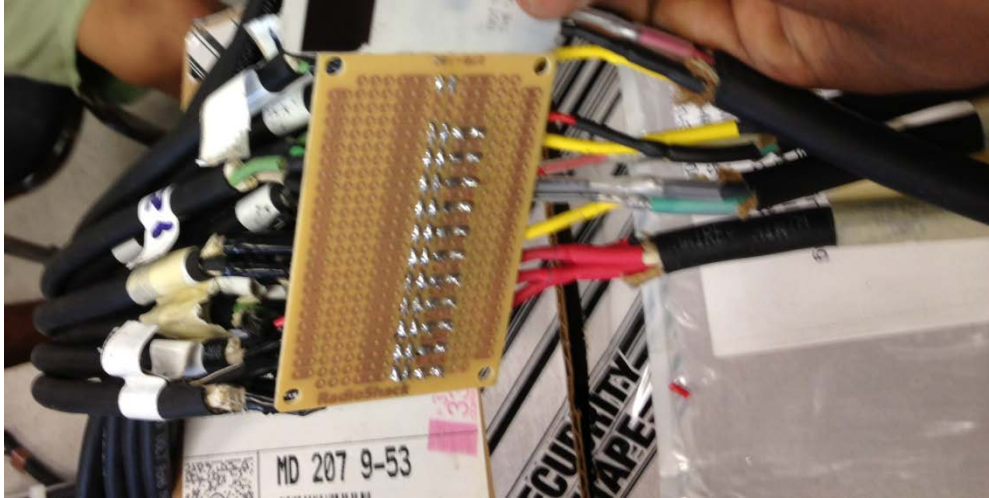


Fig. 4.9: Electrical circuit board to create common power and ground for whisker sensors.

Hence, 11 wires with 3 channels each from the sensors were connected to 4 wires with 13 channels running to the electrical box at the shore through the circuit board. This can also be seen in Fig. 4.9. The circuit board had to be waterproofed to avoid shorting when in water. Hence, a mold was created and this circuit board was dunked into epoxy and allowed to cure overnight as shown in Fig. 4.10.



Fig. 4.10: Epoxy mold created to waterproof circuit board.

The free end of the wires meant for attaching the whisker sensor was pulled through the holes on the post using string and fish tape (Fig. 4.11).



Fig. 4.11: Wires ready to be pulled into the scour post using fish tape and string.

Once they were pulled out through their respective holes, the sensors were soldered on and the holders were press fit into the designated holes. The sea weed sensors were also attached to their holders and mounted on to the post.

At this stage, a mold made of sodium acetate and rock-salt had to be created to protect the sensors during installation. To do this, the post was to be lowered horizontally into a wooden tub filled with the solution. But at this stage, once the whisker sensors were press fit into the holes, the whiskers started snapping off even with minimal contact. Most of the whiskers had broken off due what has subsequently been identified as excess stress associated with the process of press fitting the holders into the galvanized post holes. Hence, it was decided that whisker sensors have to be called off for the first installation. This approach was acceptable because the site at Bacon Ridge Branch was tidal and multiple measurements of flow velocities indicated that the water was flowing at very low velocities which would be too low for the whiskers to detect on a daily basis, and for which the sea weed sensors would still provide adequate data for assessment of the general sensor post concept.

Since the team only going to install the sea weed sensors, the wiring for the second post was simplified further. The circuit board was done away with and a more direct method of hard wiring was used. The team had manufactured 4 sets of sea weed sensors for each post, each requiring a wire with 3 channels. The wire from the shore had 13 channels which meant that we had a spare channel. The wires were directly fed into the post from the bottom hole meant for the conduit once it was sleeved using soap as described for the first post.

The wires were pulled out using fish tape but it was decided to use the large holes meant for the whiskers right above the ones for the sea weed sensors since it was easier to pull through the larger holes which weren't going to be used. The holders were secured on the post using water resistant metal epoxy. The power from the battery and the ground were split in the electrical box using a circuit board into the 4 channels required by the 4 seaweed sensors. As the seaweed sensors had holders that could withstand the installation, the posts didn't have to be protected using the rock-salt and sodium acetate structure. Shackles with washers to compensate for the extra length of the clevis pin were used for both the posts to lift them using an engine lift. The posts were loaded on to a truck to be transported to the site.

At the site, an excavator was used to drill into the river bed using augers shown in Fig. 4.12. For the first post there was a major setback in the installation process owing to a malfunction in the hydraulics of the excavator. Once this was rectified, a hole was drilled for the first post. The problem with the hole that was drilled was that the dirt at the bottom of the river started filling up this hole when the auger was removed. This consumed most of Day 1 of the install.



Fig. 4.12: Augers used to drill holes into the river bed.

The bridge construction team from Connecticut had several rounds of meetings that evening to combat this issue and came up with a slightly different way of drilling the hole. This method was tried the next day and it worked perfectly. Once the first hole was drilled, the scour sensor post was lowered and the auger was detached from its base using the excavator and pulled out leaving behind the auger base at the bottom.

The second post on the south side went in without any glitches. The conduits from both the posts were pulled to the shore and the electronics in the box was hooked up. Wiring and boards as installed in the box are shown in Fig. 4.13. Tests were performed to ensure that the sensors were giving a reading and it was also checked if the Arduino was recording this data on to the SD card.

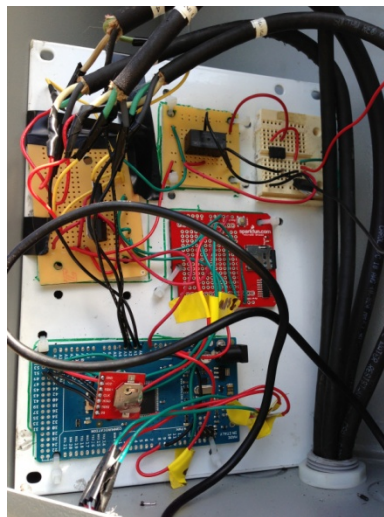


Fig. 4.13: Electronics in electrical box and wire to sensors in riverbed.

Frequent trips were later made to the site to pour sand around the posts to make up for any scour the post might have induced. Survey of the floor profile around the post was also made during each visit.

4.3 Results from Phase 1

As mentioned, early whisker breakage was observed despite the use of the hollow-stem auger for installation. After some consideration, it was discovered that the post openings that were designed for the whiskers were too small. The holes had been made slightly smaller than the whisker with the objective of reducing the ability of water to flow freely into and out of the post. However, this condition created stresses in the whisker bases that were excessive and lead to breakage. Because the interior components of the posts were waterproofed, it was decided that the hole size could be increased on future posts, reducing stresses, and protecting the whiskers. The posts from phase one utilized the sea weed style transducers developed for low-flow environments.

Additional scour posts were installed in a second site (Bennett Creek) in Maryland to monitor slope stability of the riverbank (Fig. 4.14) during the past quarter.



Fig. 4.14: Riverbank migration post installation.

One post was installed below the nominal water level and another above (but below the high-water line) to study the contrast between signals returned from the free transducers (Fig. 4.15 and Fig. 4.16). Here, even the qualitative difference between the buried and water-borne transducers is stark indicating good performance of the sensing system. Air-borne sensors also show good differentiation for dynamic signals for low-wind conditions.

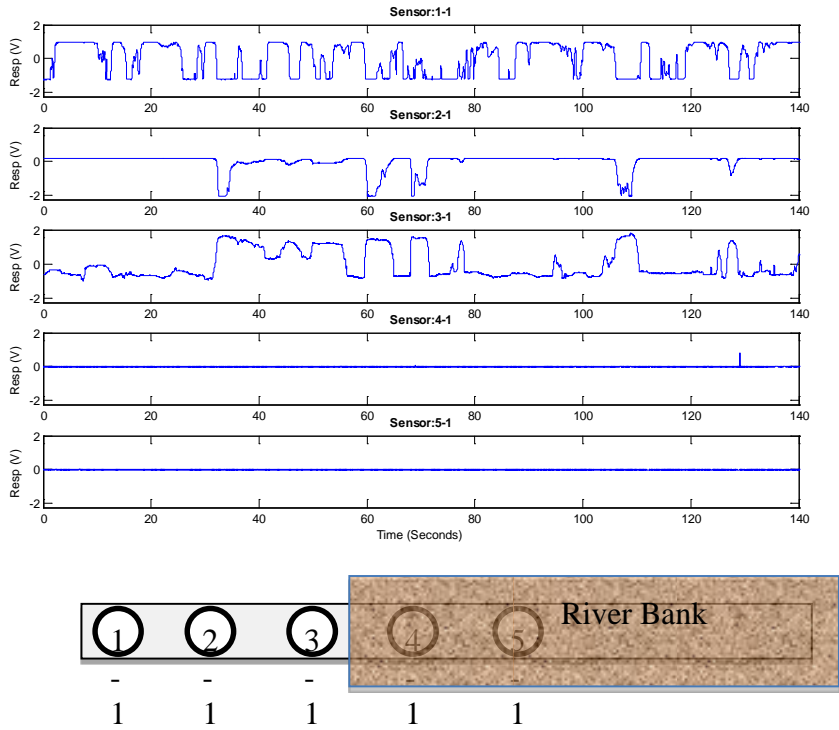


Fig. 4.15: Riverbank installation, sample underwater response.

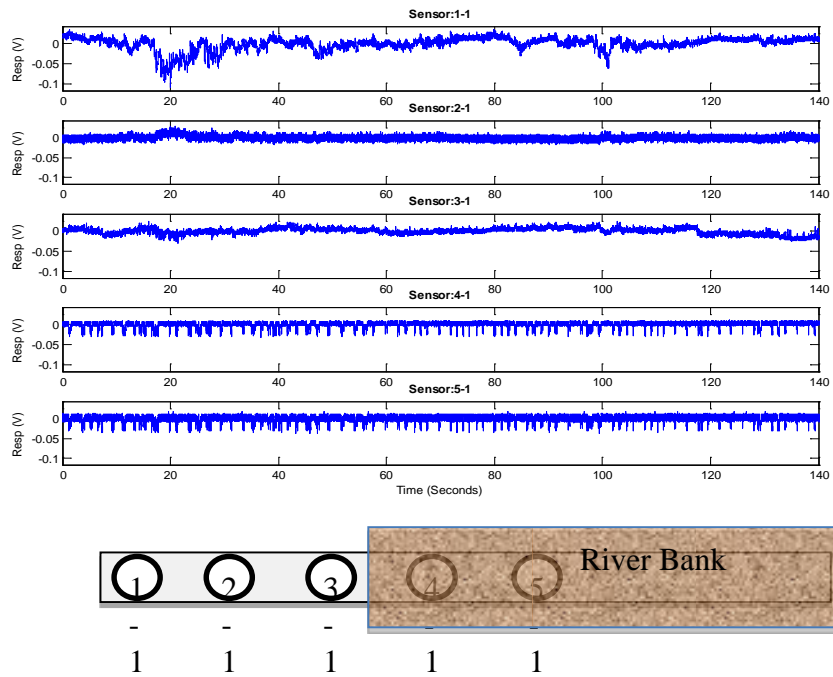


Fig. 4.16: Riverbank installation, sample in-air response (low-wind conditions).

Data was collected periodically from the site though the bottom post was eventually completely buried (aggradation).

4.4 Phase 2 Installation

A new post configuration not requiring use of a hollow-stem auger for installation was designed to facilitate a cheaper and faster installation process. For this new design, a steel sheath with a driving point will be driven into the ground using a pile driver. The scour post will be inserted into the sheath and the sheath will then be removed leaving the driving point and the post in place. This new approach is expected to save considerable time and lead to cheaper post installations. Modifications to the sensor holders and posts were made based on prior experience in order to improve the ease of installation of the system. Some details are shown below.

4.4.1 New holders designed for new install procedure

Since the latest install procedure involves hammering the scour post with a hydraulic pile driver, the holders were redesigned to withstand the install and more importantly protect the whiskers. Fig. 4.17 shows the new design for the seaweed like sensor and whisker sensor respectively. These holders were printed using a 3D printer.

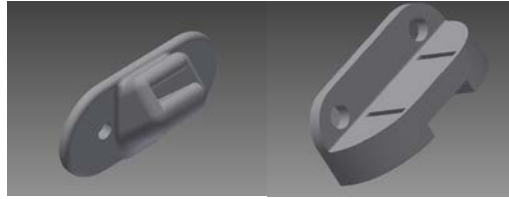


Fig. 4.17: CAD pgraded sensor holder design for the whisker and sea weed sensors

4.4.2 Construction of scour post

As mentioned previously, a new procedure was tried out for installing the scour posts. They were hammered into the riverbed using a pneumatic pile driver. For this, the post itself was redesigned to have a pointed base. Fig. 4.18 shows the pointed base which was cut using CNC and welded to help pounding the post into the ground.



Fig. 4.18: Pointed edge constructed using CNC and welded on to the base of scour sensor post.

The wires were cut to the required length and drawn into the post using mule tape. The hall sensors were soldered on the wires and then mounted on the holders as shown in Fig.

6a. six sea weed sensors and six whisker sensors were constructed and screwed into the post. The final post with the whisker and sea weed sensors in shown in Fig. 4.19.



Fig. 4.19: Scour post with the whisker and sea weed sensors mounted and wired up.

The wires running to the electrical box on the shore with the data acquisition system were attached to the wires from the 12 sensors using military grade water proof wire connectors. Small wedges were also welded on the post to protect the wire as it comes out from the window during installation. A all weather conduit was slipped on the wires running to the shore to protect them in the case of a storm. All electrical connections and sensors were waterproffed using silicone. Four such posts were constructed for install at the two sites.

4.4.3 Installation

The installation involved hammering the posts with the pointed edge in to the river bed using a pneumatic pile driver as shown in Fig. 20.



Fig. 4.20: Installing the scour post at Big Pipe creek.

The wires from the post were drawn to the electrical box on the shore where the DAQ and electrical systems will be. Chains will be wrapped around the conduit using hose clamps to keep it along the river bed.

4.5 Conversion to Autonomous Cellular Data Collection

In the final year of the project, wireless capabilities were added to the MD sites. This implementation project was undertaken in 2015, with the hardware has been installed in March and the system brought on line and debugged at all four Maryland sites in the over the summer (Fig. 4.21-Fig. 4.23). At the same time, revisions were made to software and hardware to improve system-level performance. System-level software design upgrades are being made to address a software glitch that has the UMD DAQ interrogating the sensors continuously instead of once an hour. Solar panels for the UMD DAQ were added to the Bennett Creek and Little Bennett sites in January, 2015, and to the Big Pipe site in March, 2015. This extended the battery life from 2 days to 4 with small low cost solar panels for continuous operation and indefinitely for daily operation (Fig. 4.22).

Cellular communications at these sites was initially hampered by use of metal enclosures for the base station. The addition of external cellular data antennas, one per site, is remedied this issue, but ruggedized PVC enclosures are likely better solutions for future installations so that the antenna can be protected inside of the enclosure.



Fig. 4.21: Installation at Little Bennett Creek showing power lines in close proximity to site.



Fig. 4.22: Installation of the cellular data collection device at Bennett Creek showing solar panels for the 6V batteries for the UMD DAQ



Fig. 4.23: Installation of the cellular device at Bacon Ridge Branch site.

4.5.1 Problems unique to wired system

A surprising artifact was discovered in the sensor output at three of the Maryland sites. Although the systems are all powered by batteries that are connected to grounding rods, 60-Hz noise in the signals were observed that were, at times, of the same order of magnitude as a wiggling whisker. These signals were believed to be associated with proximity to power lines. Analog, low-pass filters were designed and installed at all wired

sites to alleviate this issue. A similar issue was not observed at the fully-wireless sites in Michigan which did not utilize wires between the posts and the base station.

4.6 Bathymetric Surveys for 2013 & 2014

For the USDOT sponsored Automated Scour Detection project, the Michigan Tech Research Institute (MTRI) team, in conjunction with staff from the University of Maryland (UMD), conducted a bathymetric survey of the Bacon Ridge Branch River at MD450-Defense Highway near Annapolis, MD. This data collection was performed at this location during years 1 and 2 of the project. The intention of this second survey was to assess the changes in channel morphology between 2013 and 2014 that would be indicative of bridge scour issues that the scour posts would be able to monitor. In 2013, the survey was conducted in March and in May for 2014. Due to the tidal nature of the Bacon River, MTRI conducted water level surveys every 15 minutes to account for changes in water depth due to tidal influence. These surveys were conducted as close to high tide as feasible. The data provided by MTRI to UMD are normalized to represent river depth with respect to sea-level, as the height of the river is a reflection of sea-level; therefore as sea-level increases or decreases with respect to the tides so will the absolute depth values of the river. In this sense, these data provided by MTRI show the morphology of the Bacon River as close to high tide as was possible. This can impact in overall depth, but channel morphology is underlying concern of these experiments.

The experiments were conducted with Michigan Tech's BathyBoat and its new BathyBoat-II remote control survey vessel. During the 2013 collect, the original BathyBoat (seen in Fig. 4.24) was used to conduct the survey. This vessel has a minimum depth resolution of 4 inches with a minimum depth of 2 feet for collecting data.



Fig. 4.24: A photo of the original BathyBoat, which was used for the 2013 data collection.

During the 2014 data collection, MTRI deployed BathyBoat-II (Fig. 4.25). This system is equipped with a depth sounder which has a minimum depth resolution of 1/10 of a foot and a minimum data collection depth of 1 foot. This allows for more accurate depth measurements and must be considered when comparing the surveys. However, for the

purposes of determining channel morphology, these differences are not significant to the study.



Fig. 4.25: A photo of BathyBoat-II, which was used during the 2014 data collection.

The results of these two surveys show that the deepest part of the channel is located along the south-west edge of the river as it passes under the bridge in both 2013 and 2014. However, in 2014 a depression in the morphology has appeared just off the edge of the bridge on the south west side as seen in Fig. 4.26, and deepened the channel by approximately 2 – 2.5 feet.

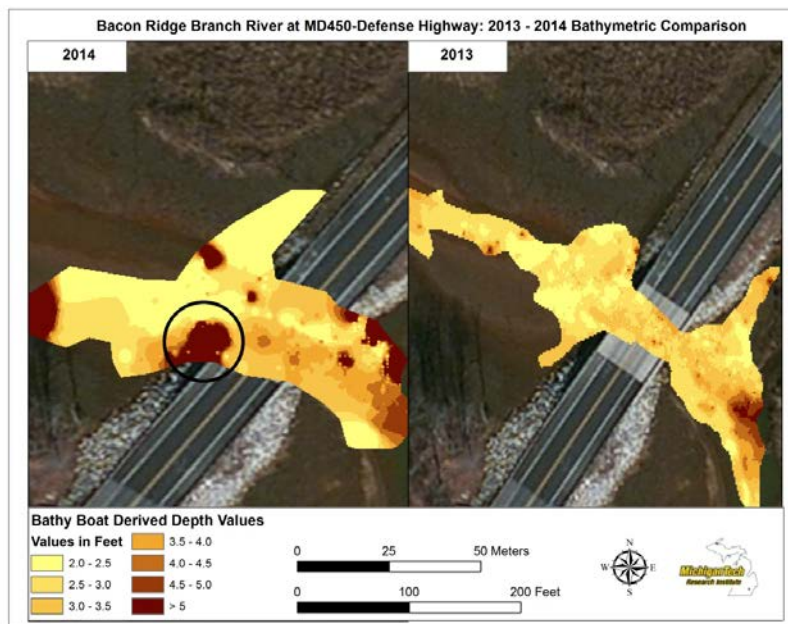


Fig. 4.26: Above are the two bathymetric profiles of the Bacon Ridge Branch River at MD-450. Between 2013 (on right) and 2014 (on left) the main channel that flows under the bridge has remained in the same relative position. However, a large depression (circled in black) just west of the south end of the bridge in the river channel has formed.

Bathymetric survey data collected in this portion of the study was used to confirm the scour detection results obtained from the post system. The tidal site at the crossing of the Bacon

Ridge Branch River by MD-450 was the one site studied where some minor scour was actually observed during the study.

5 Results of Laboratory Study

The laboratory study is a vital component of the scour detection experimental program providing a proof-of-concept study under controlled conditions. It will also allow the project team to identify the limits of the proposed technology under challenging conditions, specifically low-flow conditions where signals appear similar to static conditions. The signals recorded in the laboratory study will be vital for development of signal processing algorithms to be developed in Section 8. The laboratory study setup will also serve as the initial proving ground for the embedded data acquisition and processing components before they are tested in the field. The laboratory validation study will focus on quantifying the effects of both flow and scour rates on the performance of the system. Five levels of water depth as well as five levels of water velocity will be studied. In addition, performance in sand and silt conditions will be studied for sediments of varying size. Finally, a small-scale demonstration of the application of the smart scour-sensing posts for riverbank monitoring will be conducted in the scour flume located at Michigan Technological University (MTU).

To confirm the capability of the system a robust program of validation has been conducted to define the limits of the approach in the laboratory. The proof-of concept laboratory experiments were conducted to validate the ability of the system to monitor and measure scour and to check the ability of the network of wireless sensors to successfully process data. The results of the laboratory validation experiments have been presented here. The tests conducted were all clear water tests.

The laboratory experiment were conducted under controlled environment which allows a simulation of scour conditions at various water velocities and act as a test of the scour detection and monitoring system. Scour primarily affects the foundation, abutments and piers of the bridge. The effect of scour on abutments and piers was studied in the laboratory experiments. During the laboratory experiments, the water velocity varied to develop scour.

The laboratory experiments were performed in the Civil Engineering Hydrology Laboratory located at Michigan Technological University.

5.1 Objectives

Under two laboratory conditions, a flat river bed and a 45-degree river-bank, the proof-of-concept scour detection arrays were studied to meet the following objectives:

- Understand the role flow and scour rates play in the ability of the scour detection arrays to detect scour.
- Quantify which flow conditions create false indications based on low flow conditions.
- Evaluate new scour monitoring technology under study and identify improvements.
- Explore possible problems that might be encountered in field.
- Obtain a library of signals collected in a controlled environment to correlate outputs to transduce condition (*e.g.*, static vs dynamic, or nominal sensor condition vs fault condition).
- Calibrate thresholds for various transducer geometries to classify signals.

- Test autonomous data collection and interrogation systems for the field validation study and assess the scour prediction method.

5.2 Laboratory Facility

5.2.1 Flume (Water channel)

The water channel in the hydrodynamics lab is a rectangular, cement experimental tank. The inner walls were coated with epoxy spray to allow for a non-leaking tank. The dimensions of the flume were an inside width of 0.92m, a total height of 1.04m, and an inside length of 10.18m. It consisted of an inlet and outlet at the head and end of the tank, respectively. A pump was used to move the water from the outlet to the inlet through a 0.245m diameter pipe. The pipe had 27 1.588mm diameter holes facing in the downward position, which allow water to empty into the head tank. There was a wall that separated the inlet area and the main experimental tank. This internal wall was constructed of 20mm diameter PVC pipes, which were stacked parallel to allow for flow straightening into the main water channel.

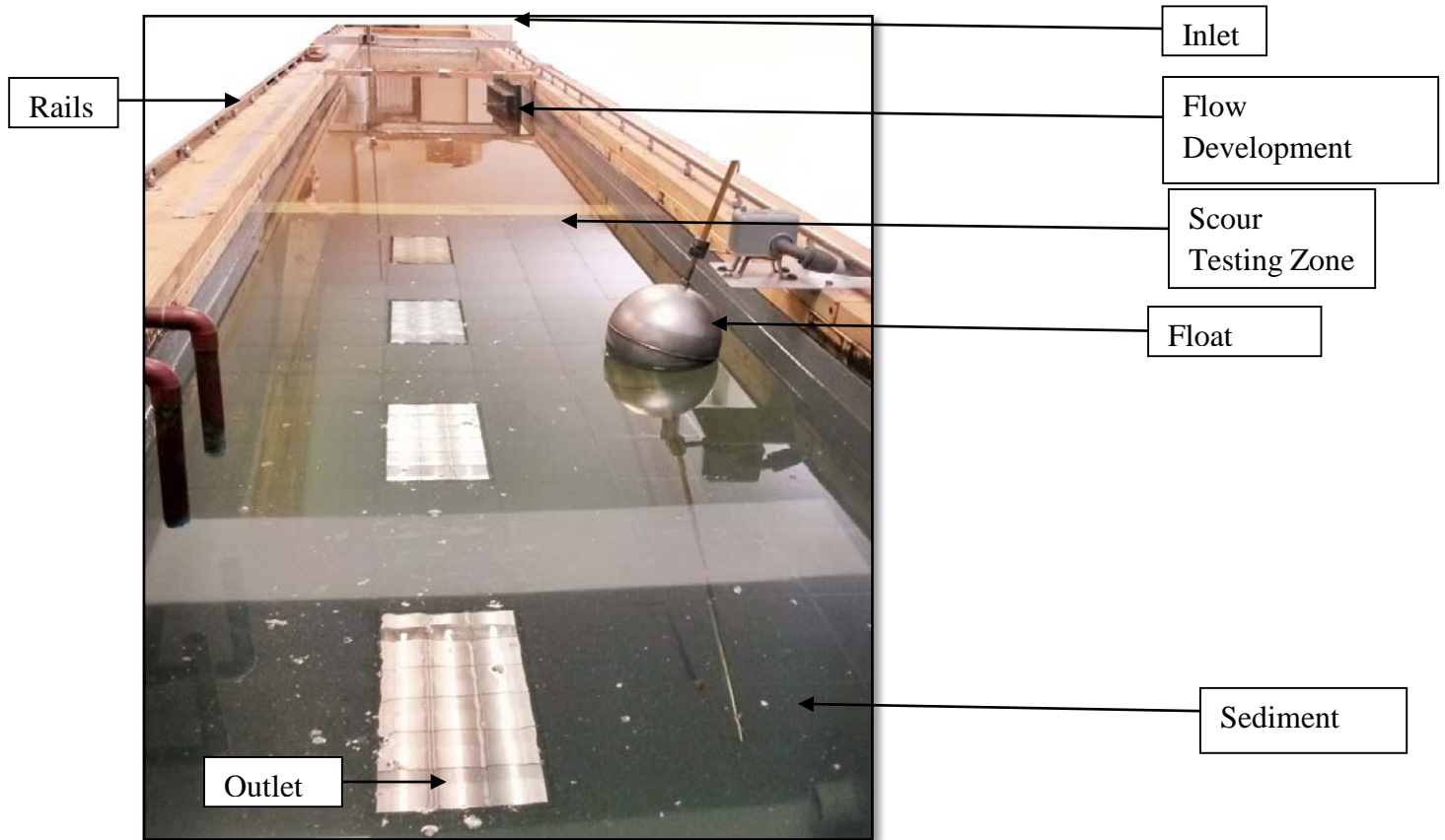


Fig. 5.1: Flume Structure

5.2.1.1 Water channel setup for first experiment

For the first case in the set of experiments, a flat bed was constructed following the flow straighteners section. This approach area was approximately 1m in height and 3m in length. This bed was made of plywood and had an epoxy varnish overlay for waterproofing

purposes. Soil was then placed on top of the flat bed. The next area was the scour section, which was filled with fine sand. The sand was filled from the bottom of the water channel, level with the soil in the preceding section. The bottom of the water channel was the cement floor of the laboratory. A wooden wall standing 630 mm tall from the flume floor was constructed near the end of the scour chamber for sediment trapping. The sand, in the scour chamber, was level with the soil in the flat bed section and ended at the wooden wall. The water height was made to be just above the top sensor of the pier.



Fig. 5.2: Flume setup for first experiment

5.2.1.2 Water channel setup for second experiment

For the second case in the set of experiments, the flat bed was removed. It was replaced with an angled embankment bed that was positioned 45 degrees from floor of the flume. The flow straighteners were repositioned to accommodate for the embankment slant. The approach area had dimensions of 3m length and 0.5m height. It was constructed of plywood and had a coarse sand paper overlay. The scour section was filled with the same fine sand from the first case. The sand was angled at a 45 degree position, which lined up with the bed. This exposed a portion of the flume floor from the angled bed section through the scour section. The wooden standing wall was removed and the scour chamber tapered off before it reached the sediment trap area.



Fig. 5.3: Flume setup for second experiment

5.2.2 Scour experiment structure

5.2.2.1 Model Pier and Abutment

To conduct the proof-of concept laboratory experiment a pier and an abutment were assembled using PVC board and pipes for the laboratory test. The pier was made using a 4 inch diameter Poly vinyl chloride (PVC) pipe attached to a box made up of rigid form of PVC board. Also a simple abutment was constructed using PVC boards and 2 inch PVC pipe was used make piles. Waterproof glue and quick setting super glue was used to hold the assembly together.

The dimensions of the pier and abutment were to scale with the flume being used for the experiment. The models were made to closely match a similar structure in the field. The total height of the pier was 2 ft 10 inch and it was made to be 4 inch wide and the abutment was approximately 2 ft 10 inches in height and 2 ft wide. Both the pier and abutment were coated with waterproofing silicon and was spray painted white to make it waterproof and weather proof. The transducers were attached to the pier and abutment assembly itself for the experiment. Holes that fit the sensors were drilled into the abutment and pier using a drill and sensors were mounted on the models. The hole was then coated using silicon for waterproofing. Four whisker type transducers each was mounted on both pier and abutment models. The transducers were spaced 6 inches from each other. Fig. 5.4 shows the model pier and abutment used for the laboratory experiment.



Fig. 5.4: Pier and Abutment

5.2.2.2 Posts

For the river bank experiment two simple posts, one with bio inspired whisker type sensors and other with airfoil sensors were made. PVC strips two feet in length and one inch in width were used as posts. The sensors were mounted on the posts using waterproof glue. Three sensors each were mounted 3 inches apart in each post. Fig. 5.5 shows an example of the post used.

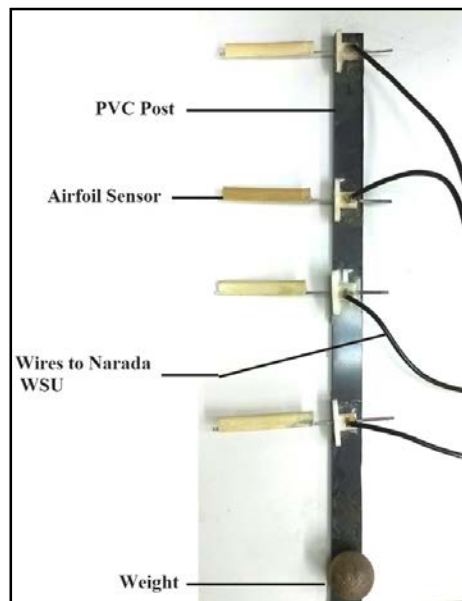


Fig. 5.5: Sample Airfoil posts

5.3 Proposed Scour Detection System

For the purpose of lab validation tests two Narada WSU were used. The transducers were mounted on the model pier and abutment and PVC posts. The sensors were connected to each Narada WSU using wire setup. Power was provided to the Narada's using an AA battery pack. In the test the Narada wireless sensors was setup to send the data to a laptop computer in the first case and to a single board computer in the second case for analysis. While this function is not strictly necessary for wireless systems with full embedded data processing abilities, it is necessary to validate the functionality of the sensors.

5.4 Equipment for scour monitoring and detection

5.4.1 Transducers

In the proof-of concept laboratory tests two different sensors were used. The sensors used in the laboratory study are 1) Bio-inspired magnetostrictive whisker sensors and 2) Magnetostrictive Airfoil sensors.

5.4.1.1 Bio-inspired magnetostrictive whisker sensors

The whisker shaped sensors are inspired by the whiskers of marine animals which provide the marine animals with important sensory information of the environment around them. The whisker sensors are made of Galfenol wire, which is an alloy of iron and gallium. Galfenol is magnetostrictive in nature and has corrosion properties that are similar to those of steel, and four times less that iron. The whisker sensor consists of five main components 1) Galfenol whisker 2) GMR sensor 3) clamping fixture 4) Small permanent magnet and 5) Low power operational amplifier. Fig. 5.6 shows an example of whisker sensor.

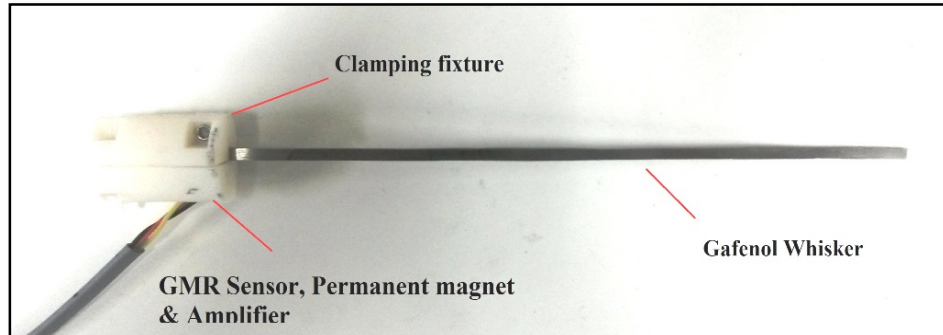


Fig. 5.6: Whisker Sensor

5.4.1.2 Magnetostrictive Airfoil sensors

The Airfoil sensors are an improved version of whisker inspired magnetostrictive Galfenol sensors. Airfoil sensors work on the exact same concept as the bio-inspired whisker flow sensors. However, the airfoil sensors are much more robust compared to the whisker inspired sensors. A wax layer in a shape of airfoil was added in the sensors to improve its sensitivity Fig. 5.7 shows an example of airfoil sensor.

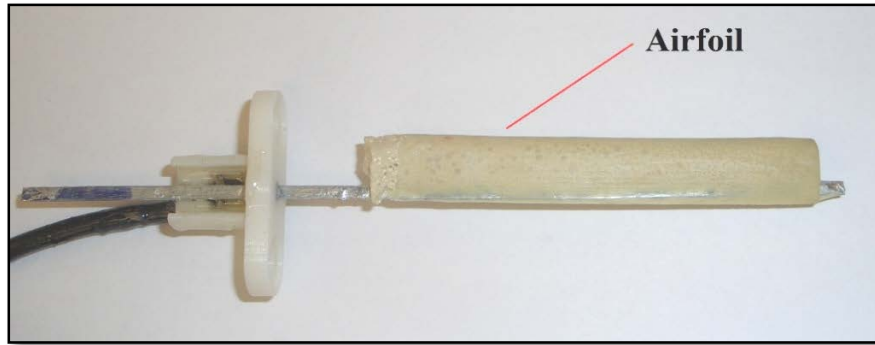


Fig. 5.7: Airfoil Sensor

5.4.1.3 Wireless sensing unit

Low power *Narada* wireless sensing unit was used in the laboratory study as the wireless sensing interface. The *Narada* WSU is developed by Swartz *et al* (2005) and is produced by Civionics Inc.

5.4.1.3.1 Narada Wireless sensing unit

The *Narada* (Fig. 5.8) is a low-power wireless sensor node designed explicitly for the monitoring of civil infrastructure systems and has been successfully used in many types of structures in the past. It has been designed for applications requiring high resolution data collection, and/or real-time control (Civionics). The *Narada* consists of ADS8341 16-bit sensing interface to digitize and sample analog transducer signals with four analog input channels that can read analog signals ranging from 0 to 5Volts. The computational core of *Narada* is 8-bit ATmega128 microcontrollers that is responsible for managing sensor operation and perform analysis, including the storage of sensor data. The ATmega128 is an 8 bit, low power microcontroller that has 128 kB of flash memory to for temporary data storage, and 4 kB of electrically erasable programmable read only memory (EEPROM). It also features IEEE 802.15.4 compliant wireless modem, the Chipcon CC2420 that adopts the 2.4 GHz IEEE 802.15.4 radio standard, which acts as a communications interface and serves as WSU's link to the world. The *Narada* wireless sensing unit contains an inbuilt actuation interface to allow the sensor to command actuators. The actuation interface consists of a Texas Instruments DAC7612 2 channel 12-bit DAC capable of outputting analog signals from 0 to 4.1 V with a resolution of 1 mV.

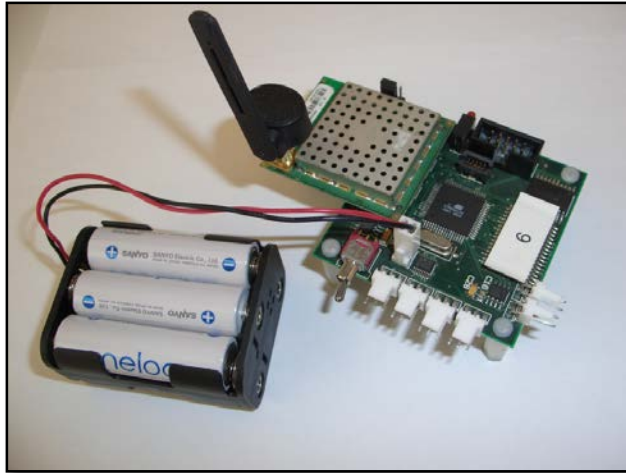


Fig. 5.8: Narada WSU with battery pack

5.4.1.4 Base Station

The base station aggregates the data from multiple wireless sensing units in use and it creates a decision file in accordance to the data received from the wireless sensing units. The base station assembly used for the laboratory experiment composed of Narada Base Station, centralized PC laptop or Single Board computer (SBC), and a power supply.

5.4.1.4.1 Narada Base Station

The Narada Base Station (Fig. 5.9) is produced by Civionics Inc. The Narada Base station is a wireless data acquisition hub built around the Atmel ATmega128 microcontroller. The ATmega128 is an 8 bit, low power microcontroller. The Narada Base station connects to the PC through an available USB port and can facilitate data collection, real-time control, and network maintenance tasks (Civionics).



Fig. 5.9: Narada Base Station

5.4.1.5 Centralized PC Laptop / Single Board Computer

A normal laptop was attached to the Narada base station using a USB port to for the laboratory experiment. A single board computer was also utilized for the river bank experiment. The single board computer used for this study is PPM-LX800-G manufactured by WinSystems Linux (Ubuntu 11.10) operating system, shown in Fig. 5.10.

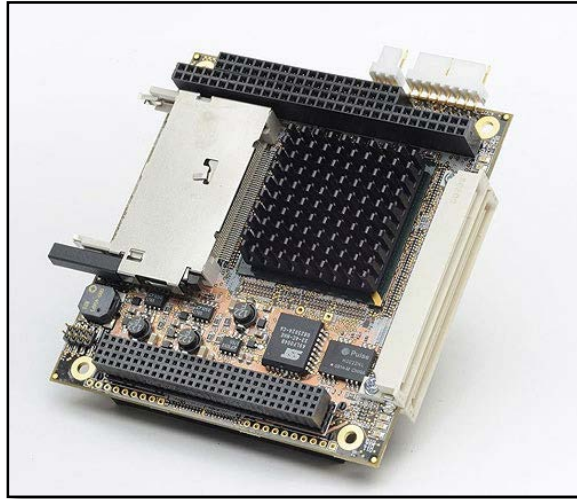


Fig. 5.10: Single Board Computer

5.5 Scour Measurement (Hydrology)

Scour was measured using a point gage. Before the initial pump speed, the bed elevation was measured as 77.3 cm. This measurement was a baseline for calculating all scour depths.

Change in pressure (Δh , measured in ft) for each pump speed was recorded from the manometer. In order to convert pump speed to channel flow, Q (cfs), the following equation was used:

$$Q = 0.203\sqrt{\Delta h}$$

5.6 Experimental Setup

5.6.1 Pier and abutment experiment

The first case, the flat bed was filled with a layer of soil. There were three divisions of soil types laid on the flat bed. The first section was about 1m in length and was filled with gravel about 25.4mm deep. This gravel section transitioned into a gravel/sand mixture of about 25.4mm deep and 1m in length. The final transition was filled with fine sand to about 25.4mm deep and spilling into the scour sector. The sand had a d_{50} of 0.56mm. The same sand was filled to this height in the scour section of the flume. Placed in the sand, was a replica of a bridge pier and abutment. These models were scaled 1/30th of the size of a bridge pier and abutment. The pier was made of a 30mm PVC tube and was placed perpendicular to the flow and channel bed. It had a height of 0.3m above the sand bed. The abutment was placed in contact with the east wall of the flume and the pier was placed 1 ft away from the west wall of the flume, shown in Fig. 5.11. The distance between the abutment and pier was 1.6 ft. The height of the abutment above the sand bed was 0.3m. It

had a width of 20 mm and a length of 40 mm. The width of the abutment faced the oncoming flow, while the length of the abutment was parallel to flow. For laboratory testing purpose, to make the installation easy, the bio inspired whisker type sensors were mounted on the model abutment and pier itself for scour detection and monitoring. Four sensors each was mounted on both pier and abutment models. For the purpose of lab validation tests two Narada WSU were used. The transducers that were mounted on the model pier and abutment were connected to each Narada WSU. Power was provided to the Narada's using an AA battery pack. In this test the Narada wireless sensors was setup to send the data to a laptop computer for analysis.



Fig. 5.11: Flume setup for Pier and abutment experiment

5.6.2 River bank experiment

The second case, two posts were used. The flume was setup to match a river bank for this experiment. The flow development zone which was a wooden structure from the previous setup was removed and replaced by an inclined wooden structure to create a riverbank. Fine and clean sand was used to create a river bank on one side of the flume. The posts were then buried in the river bank so that the sensors were aligned perpendicular to the flow of water (Fig. 5.12). To make the posts stable, weights were attached to the ends of the posts. The transducer on the top of the post was left unburied, the bottom two transducers were fully buried in the sand and one of the transducer was partially buried when placed in the flume. For the purpose of lab validation tests two Narada WSU were used. The transducers that were mounted on the posts were connected to the Narada WSU. Power was provided to the Narada's using AA battery pack. In this test the similar to the previous setup the Narada wireless sensors was setup to send the data to a laptop computer for analysis.



Fig. 5.12: River bank experiment

5.6.3 Experimental Procedure

In an effort to understand the impacts of flow and scour on the ability of the detection sensor to detect scour, a model of a bridge pier and abutment were installed in a laboratory flume. In both laboratory set-ups, the proof-of-concept sensors were tested and associated scour was measured.

In order to generate a database of signals to be used for classification (static versus dynamic signals) multiple pump speeds were used. Pump speeds started at 9.06 Hz, and were increased in 1.0 increment, up to a maximum pump speed of 30 Hz.

Scour was measured for each pump speed at multiple time intervals. Once equilibrium was reached, scour was measured and recorded as “worst scour” for each pump speed. Equilibrium is defined as less than 1% change in scour over a 3-hour period. The worst scour location, either upstream or downstream of each structure, was also documented.

The data was collected periodically for the entire duration of the experiment using two Narada sensor units powered by battery pack for detecting scour. The data collected was processed to determine the dynamic and static states of the sensors.

The sand used for the experiment had sediment of mean size, d_{50} , of 0.56mm (0.0018ft) and geometric standard deviation = σ_{sed} , $(d_{84}/d_{16})^{1/2} = 1.25$.

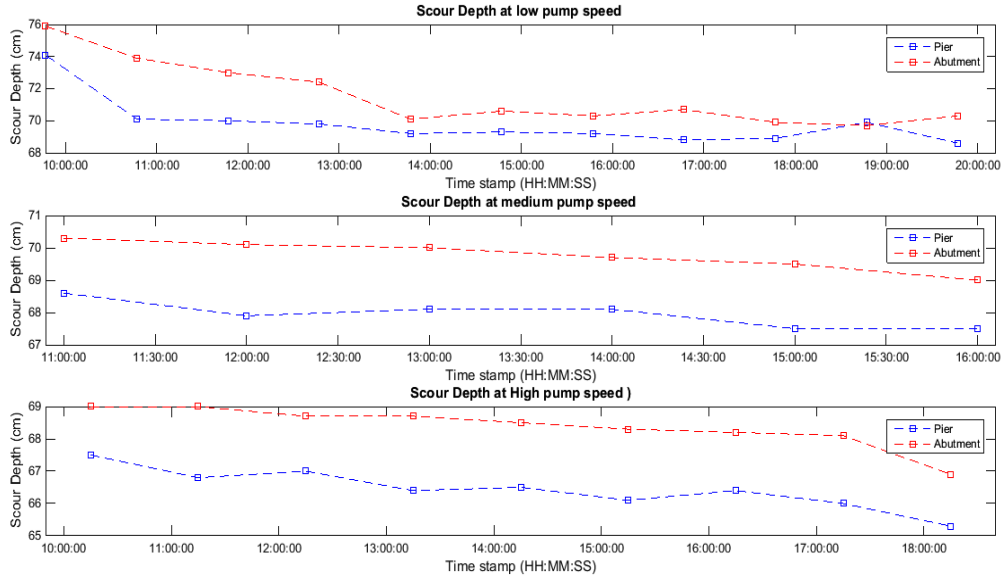


Fig. 5.13: Scour hole developed

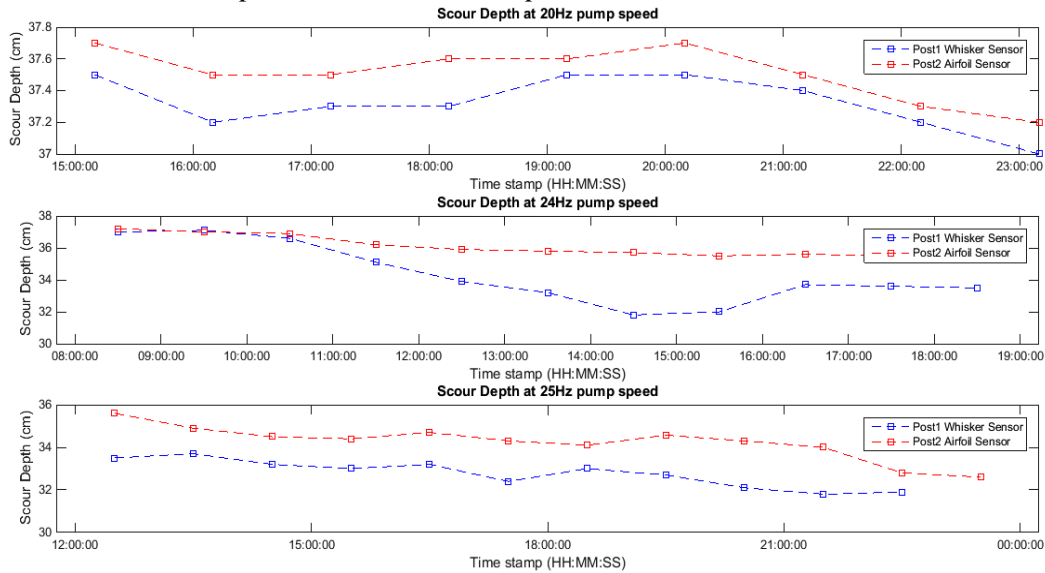
The following plots show the depth of scour developed during various velocities during the experiment. The first plot shows the depth of scour hole generated during the

experiment using model pier and abutment. The next figure shows the plot of depth versus time for the river bank experiment.

5.6.3.1 Scour Depth Plot Pier and abutment experiment



5.6.3.2 Scour Depth Plot River bank experiment



5.7 Results

Figure through shows time domain plot of sensors when they are buried (static) and unburied (dynamic).

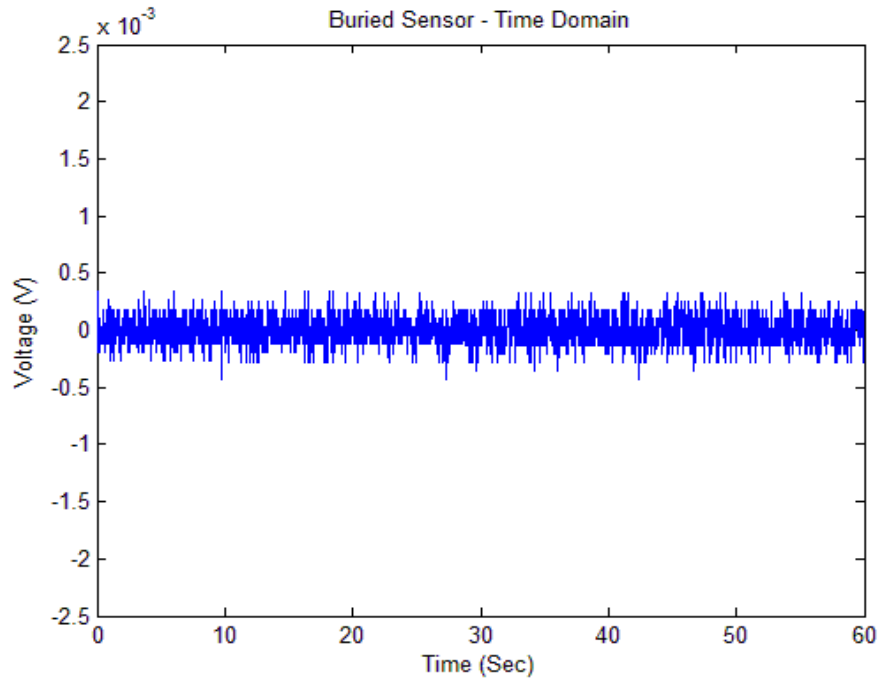


Fig. 5.14: Time domain plot of Buried Sensor (Static State)

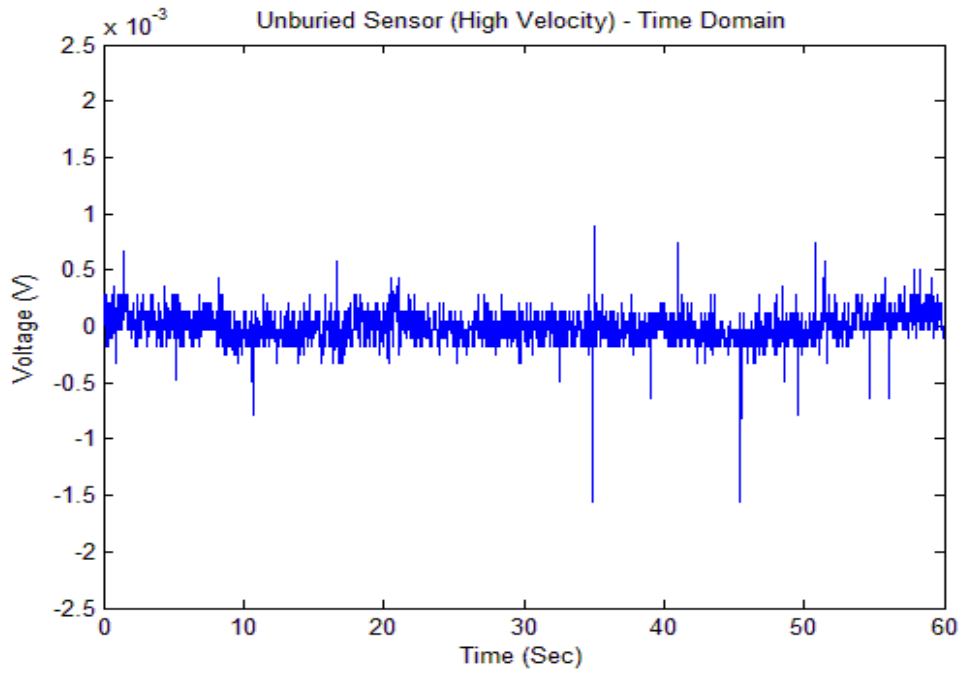


Fig. 5.15: Time domain plot of Unburied Sensor (Dynamic State)

5.7.1 Data collection analysis of laboratory experiment: model pier and abutment

In this laboratory experiment the data were collected the monitoring system every hour and transmitted to the server which in this case was a laptop. Scour hole developed was measured at regular intervals. The plots below show the time domain plot of the data.

Test Parameters:

Sampling frequency (Hz) = 100 Hz

Sampling time (sec) = 30 Seconds

Samples per polling cycle = 3000 samples

No of Units = 2

Unit ID (s) = 77 WSU (Whisker) (Abutment)

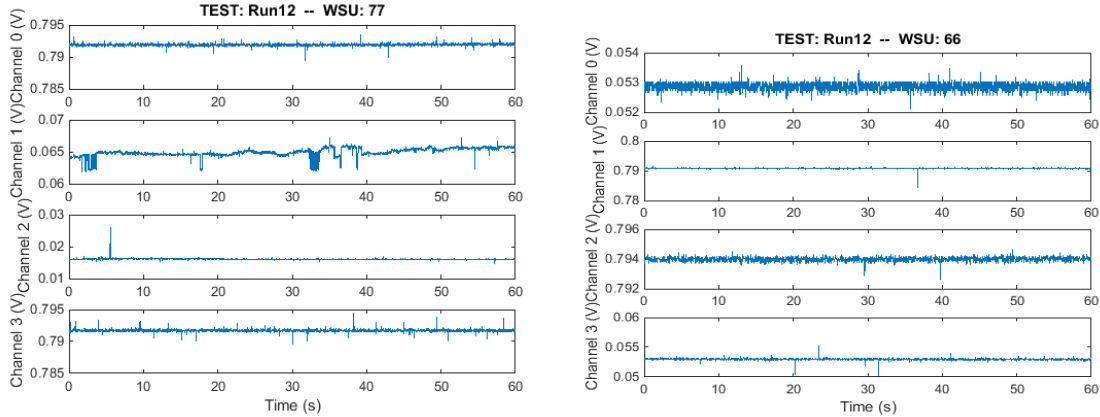
Channel(s) LEGACY_CH0, LEGACY_CH1, LEGACY_CH2, LEGACY_CH2

Unit ID (s) = 66 WSU (Whisker) (Pier)

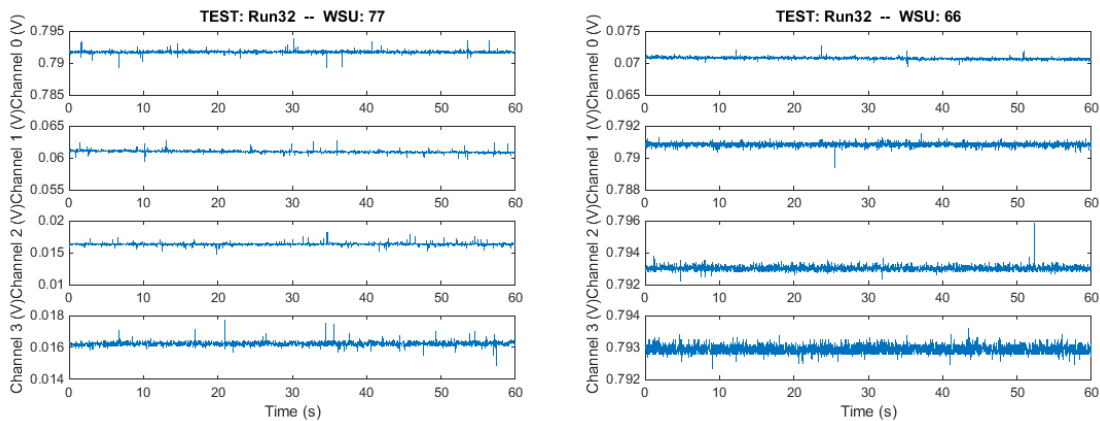
Channel(s) LEGACY_CH0, LEGACY_CH1, LEGACY_CH2, LEGACY_CH2

Sample time histories are shown below.

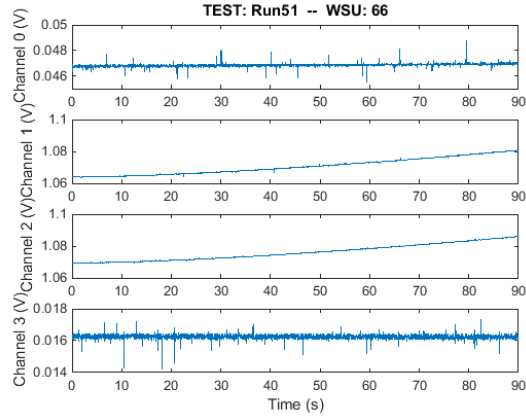
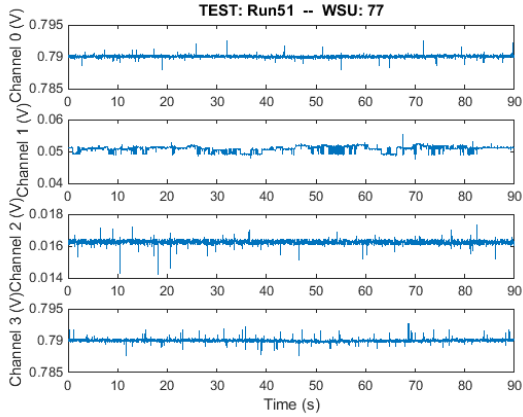
Time domain plot at low water velocity (Time stamp 12:03:08):



Time domain plot at medium water velocity (Time stamp 13:29:12):



Time domain plot at high water velocity (Time stamp 15:09:28):



In some cases, minor mean drift was observed on one or more channels in the outputs from the Hall sensors. In these cases it becomes clear that detrending algorithms will be necessary as part of the autonomous data interrogation algorithms.

5.7.2 Data collection analysis of laboratory experiment: model post

In the laboratory experiment the data were collected the monitoring system every hour and transmitted to the server which in this case was the Single board computer. Scour hole developed. The plots below show the time domain plot during different velocities.

Sampling frequency (Hz) = 50 Hz

Sampling time (sec) = 60 Seconds

Samples per polling cycle = 3000 samples

No of Units = 2

Unit ID (s) = WSU 7 Post 1 (Whisker)

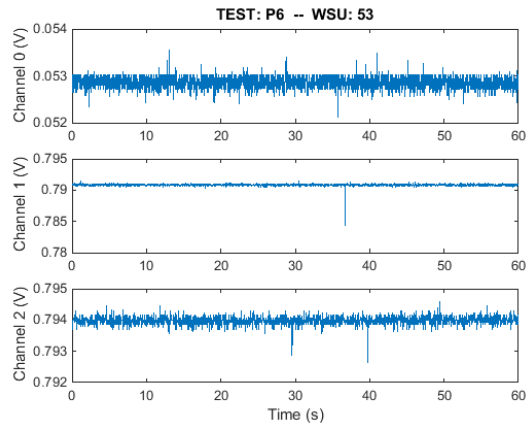
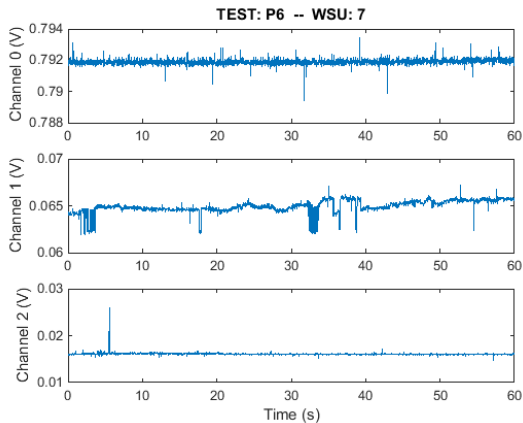
Channel(s) LEGACY_CH0, LEGACY_CH1, LEGACY_CH2

Unit ID (s) = WSU 53 (Airfoil)

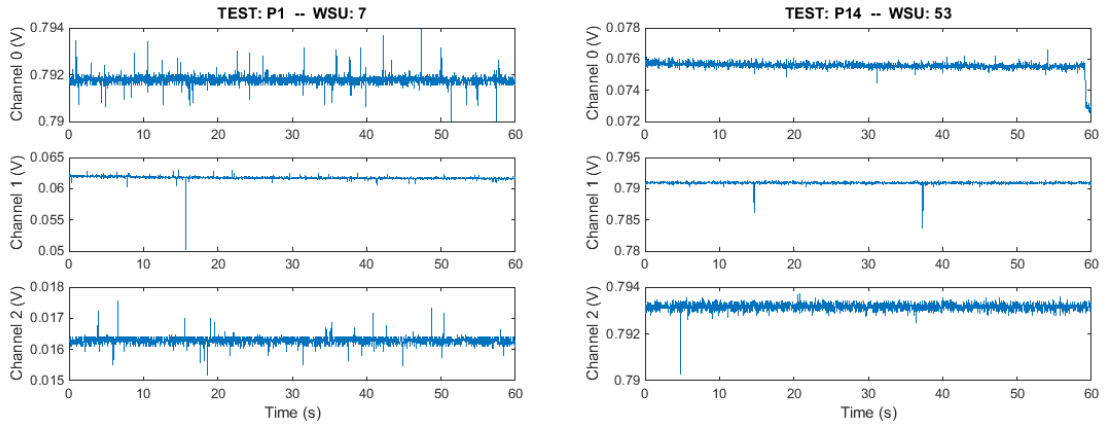
Channel(s) LEGACY_CH0, LEGACY_CH1, LEGACY_CH2

Sample time histories are shown below.

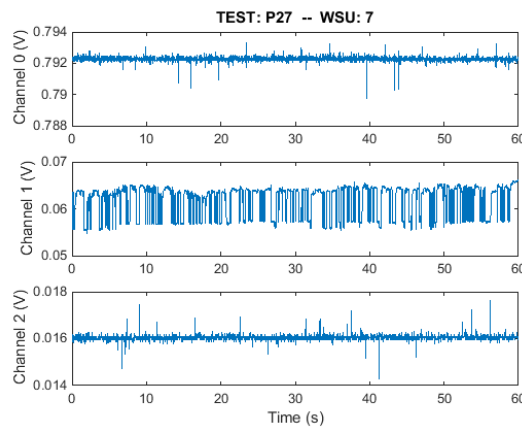
Time domain plot at low water velocity (Time stamp 15:03:32):



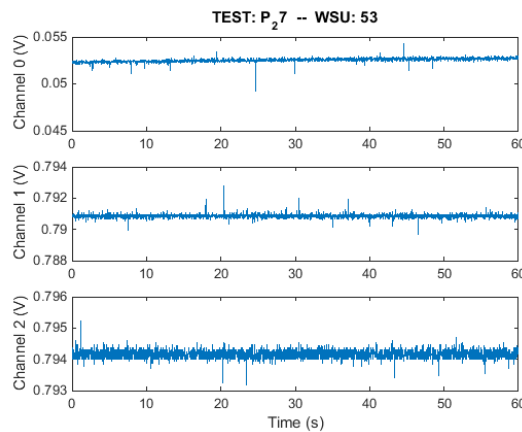
Time domain plot at medium water velocity (Time stamp 14:01:25):



Time domain plot at medium water velocity (Time stamp 18:06:52):



Here, on Channel 1, a sensor fault condition (poor connectivity of the sensor to the data acquisition device) was observed. This signal, and others like it will be useful to establish a library of fault signals for later classification algorithm development.



The plot below shows the success rate of the sensors (whisker and airfoil type) in correctly stating the state of the sensors at different velocities of water in the flume.

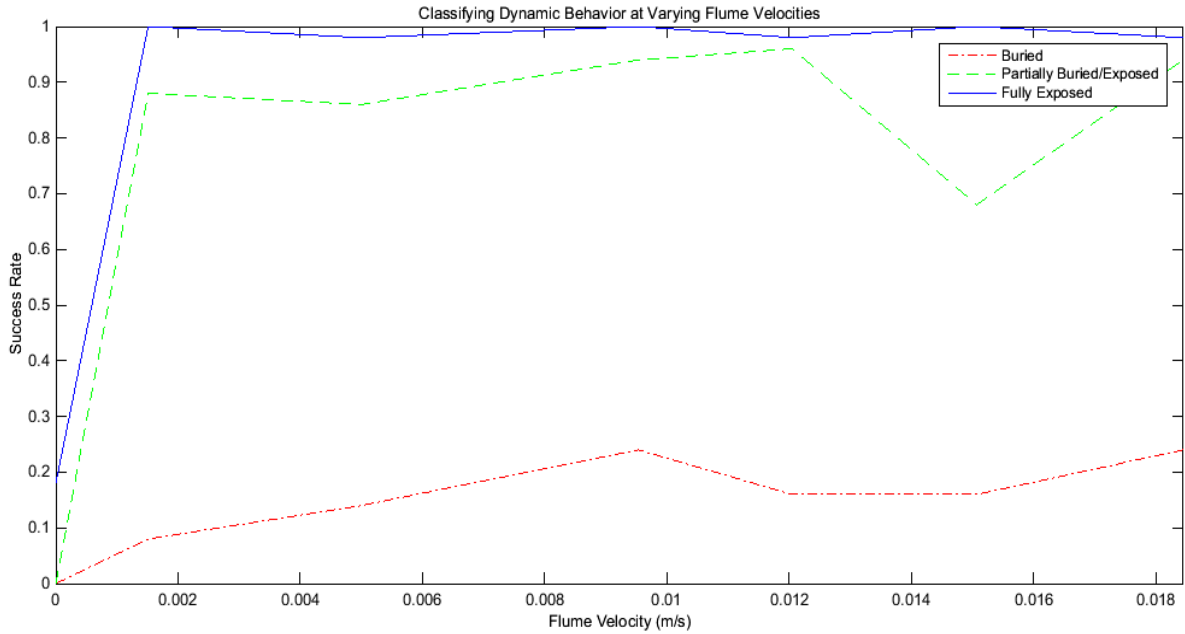


Fig. 5.16: Success rates of sensors

5.8 Conclusions

The proof-of-concept experiments were performed in the laboratory to validate the ability of automated scour detection and monitoring system that is based on bio-inspired magnetostrictive flow sensing sensors to successfully monitor scour. The laboratory results demonstrated that distinction between static sensor and a dynamic signal can be made, and with the knowledge of the depth of the sensor scour can be measured and monitored up to the spatial resolution of the transducer sensor locations. The laboratory tests established the automated characteristic of the system and displayed the ability of the system to give a warning of impending bridge failure successfully. The ability of the system under study to automatically capture and log peak scour events was shown. Laboratory tests also yielded a useful library of signals characterizing dynamic water-borne sensor data for the various transducer geometries used in the study. This data will be used in later phases of the study to develop interrogation algorithms that will autonomously classify the condition of the transducer and identify the presence or absence of scour.

6 Embedded System Design

This report details the embedded hardware developed for autonomous remote sensing of bridge scour using magnetostrictive scour sensing posts. Data aggradation from multiple posts on-site as well as transmission of data to the remote bridge owner are the two major tasks that this hardware must be capable of completing. On-board data computation reduces power consumption in the field as the results from engineering algorithms are transmitted in lieu of raw data. Hardware needed for sensor posts as well as for cellular-enabled base stations is detailed.

Outputs:

- Autonomous, wireless scour sensing posts.
- Solar powers, cellular-enabled base station units.

In this study, a low-power wireless sensor network constructed from the *Narada* wireless sensing unit is used to create a wireless monitoring system with enhanced longevity in the field. The power source for the system is provided via solar energy. The system under study deploys and tests an embedded array of sensors located near bridge foundations, at varying heights and determines the sediment depth and profile around the waterway in real time. The hardware of the system consists of bio-inspired magnetostrictive flow sensors that detect water flow by bending. A wireless sensing unit, Narada WSU that converts analog voltage output signals from sensor into digital signal, collects and analyzes data, communicates with the remote base station and relays the analyzed data. A base station system which includes a Narada Base Station, single board computer, cellular data link and power source, that aggregates the data collected from multiple units, creates a decision file and sends scour alerts to relevant authorities using a cellular link.

6.1 Sensors

The magnetostrictive flow sensors utilized in this study are developed at University of Maryland. Different ruggedness tests and various methods of sensor protection have been carried out at University of Maryland. During the course of this study three different sensors have been used: 1) whisker-inspired sensors; 2) airfoil sensors; and 3) seaweed sensors.

6.1.1 Whisker inspired magnetostrictive Galfenol sensors

The whisker shaped sensors are inspired by the whiskers of marine animals. Whiskers provide the marine animals with important sensory information about the world around them. The configuration of the whisker sensor is very simple and easy to assemble. It consists of five main components: 1) Galfenol whisker 2) GMR sensor 3) clamping fixture 4) Small permanent magnet and 5) Low power operational amplifier. Fig. 6.1 shows a typical flow sensing components.

The whisker-inspired flow sensors are constructed using a magnetostrictive Galfenol wire. Magnetostrictive materials have the ability to transducer or convert magnetic energy to mechanical energy and vice versa. Galfenol is an alloy of iron and gallium which has corrosion properties that are similar to those of steel, and four times less that iron.

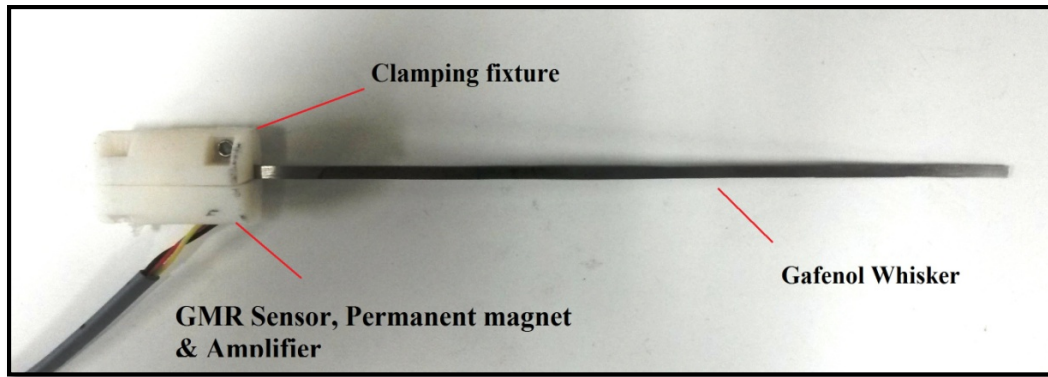


Fig. 6.1: Bio-inspired magnetostrictive whisker sensor

One end of a Galfenol whisker is fixed and the other end is free to deflect under fluid flow-induced drag forces (Fig. 6.2). The bending causes stress near the fixed end of the whisker which produces local change in the orientation of magnetic domain, which is followed by a global change in the magnetic flux density in the whisker. A giant magnetoresistance (GMR) sensor at the fixed end of whisker senses this change of magnetic field and converts it into electrical signal which is amplified, and transmitted. The GMR sensor is soldered to a printed circuit board and includes a Burr Brown INA118 instrumentation amplifier. A permanent magnet is in contact with the whisker to align magnetic domains along the whisker when it is not deformed. Different strength magnets can be used as long as a proper magnetic field strength is achieved at the root of the whisker to ensure internal magnetic dipole rotation in response to movement of the whisker without saturating the GMR sensor.

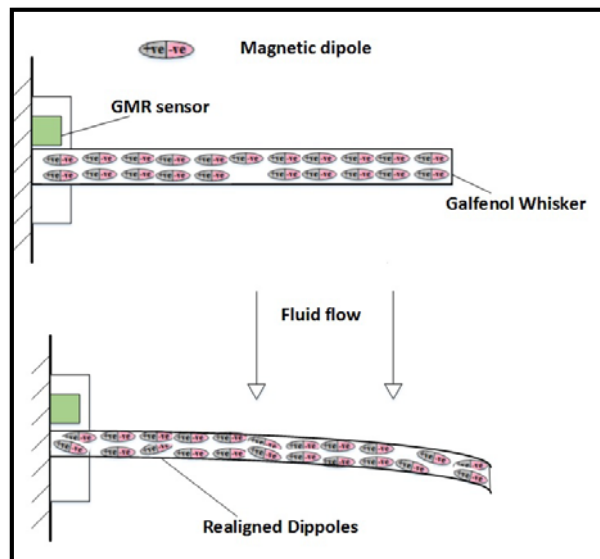


Fig. 6.2: Working principle of magnetostrictive sensor

6.1.1.1 Airfoil magnetostrictive Galfenol Sensors

The Airfoil sensors are an improved version of whisker inspired magnetostrictive Galfenol sensors. Airfoil sensors work on the exact same concept as the bio-inspired whisker flow sensors. However, the airfoil sensors are much more robust compared to the whisker inspired sensors. A wax layer in a shape of airfoil was added in the sensors to improve its sensitivity (Fig. 6.3).

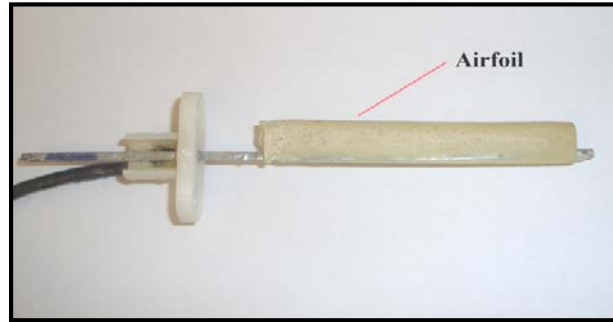


Fig. 6.3: Airfoil-type sensor

6.1.1.2 Magnetic Seaweed Sensor

Seaweed type sensors are the latest sensor that has been developed after the airfoil type sensors. The seaweed sensors have undergone quite a few changes compared to its predecessor. The airfoil and galfenol whisker have been replaced by a strip of thin fabric material. The strip has a small magnet attached to it. The strip deflects under fluid flow, causing change in the magnetic field. The GMR sensor at the fixed end of the strip, inside the clamping fixture detects this change of magnetic field and converts it into electrical signal. A seaweed-type sensor is depicted in Fig. 6.4.

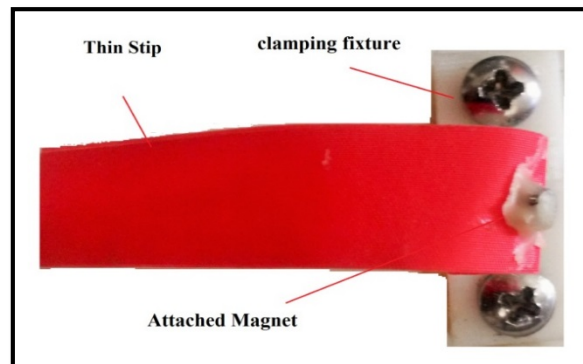


Fig. 6.4: Seaweed-type sensor

6.2 Wireless sensing unit for scour sensing posts

For a wireless network design to excel, specific hardware requirements must be satisfied to tackle the inbuilt challenges of wireless network operations. In order for a wireless sensing unit to perform to its full capacity it must have low power consumption, low latency, and the ability to quickly process data and execute control algorithms. For wireless sensor nodes to communicate with one another a digital wireless radio is required and as the output from most sensors is analog, the signal at some point must be converted into

digital signal domain in order to be transmitted. Furthermore, the tasks performed by the sensing node such as sampling computations, communications require time-specific coordination. To full fill these requirements wireless sensing unit must contain the following modules: 1) sensing interface; 2) communication interface; 3) computational core; and 4) actuation interface. The wireless sensing interface used in this research is Narada wireless sensing unit (Fig. 6.5) and are produced by Civionics Inc.

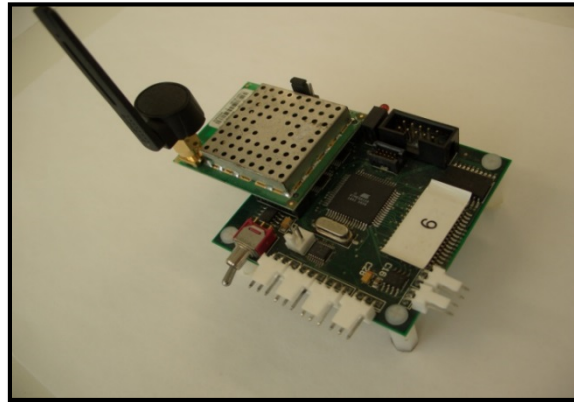


Fig. 6.5: Narada WSU

The Narada is a low-power wireless sensor node designed explicitly for the monitoring of civil infrastructure systems and has been successfully used in many types of structures in the past including buildings, bridges, wind turbine towers, and naval vessels. It has been designed for applications requiring high resolution data collection, and/or real-time control.

The Narada features ADS8341 16-bit digitalization of analog sensor data with four analog input channels that can read analog signals ranging from 0 to 5Volts. The core of the wireless sensor is an 8-bit ATmega128 microcontroller that is responsible for the overall node operation including the storage of sensor data. The ATmega128 is an 8 bit, low power microcontroller that has 128 kB of flash memory to store data and embedded algorithms, and 4 kB of electrically erasable programmable read only memory (EEPROM). The computational core of the Narada consists of the AT mega128 augmented with 128 kB of external static random access memory (SRAM) for temporary data storage. The maximum number of sampling points that can be saved in the core is limited by the node's 128kB static random access memory (SRAM) bank. The Narada features an IEEE 802.15.4 compliant wireless modem, the Chipcon CC2420 that adopts the 2.4 GHz IEEE 802.15.4 radio standard (Zigbee). The transceiver is designed with a power amplifier (Fig. 6.6) to boost the communication power of the node of long-range communication (i.e., 700 m line-of-sight). The Narada utilizes low-power wireless signal network the Zigbee to communicate with local base stations. However, every sensor board has to be able to reach the base station in order to transfer data, limiting the distance between the base station and the sensor that is farthest away.

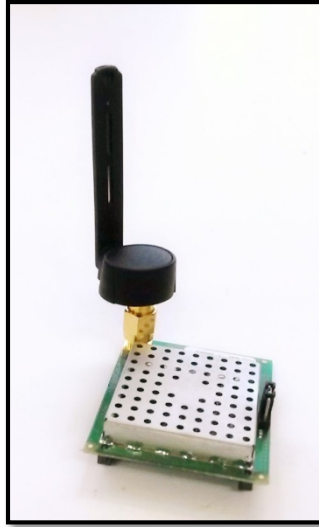


Fig. 6.6: Antenna and radio daughter board

In the Narada WSU any type of sensor can be attached and external sensors on the Narada system allows easy removal in case of the sensors are damaged or faulty by any reason. However, the drawback of Narada is that it has inflexible power management schemes and relatively slow floating-point calculations emulated its fixed point microcontroller.

The Narada wireless sensing unit contains an inbuilt actuation interface. The actuation interface allows the network to engage in active sensing and to be applied to a wireless feedback control application. The actuation interface consists of a Texas Instruments DAC7612 2 channel 12-bit DAC capable of outputting analog signals from 0 to 4.1 V with a resolution of 1mV.

Table 6.1: Technical Specification of Narada WSU

Dimensions	69 mm x 72mm x 12mm	CPU	
Base station to PC interface	RS-232,USB	Processor	Atmel ATmega 128
Voltage Actuation		FLASH	128 kB
Output Channels	2	EEPROM	4 KB
DIGITAL TO Analog Conversion	12-bit resolution	SRAM	4 KB
Maximum output Current	15 mA	External SRAM	128 kB
RADIO		Power Consumption	
Transceiver	TI CC2420	Current draw in sleep mode	10 mA
Frequency Band	2.4000 - 2.4835 GHz	Current draw in active mode	30 mA
Data Rate	250 kb/s	Current draw in Rx/Tx mode	52 mA
Range (line of sight)	500-600m	Input Voltage	6.0-9.0 V

Data Acquisition			
Input Channels	4 single ended/2 differential	DC Sensor Excitation	+5 V DC
Analog to Digital Conversion	16 bit resolution	Real time data throughput	1500 sample/sec
Data Storage Capacity	128 kB	Maximum Sampling Rate	10000 samples/sec

6.2.1 Assembled smart scour sensing posts

The smart scour-sensing posts developed are made of 13 feet long PVC pipe (steel is also an option). The bottom 1 foot of the posts was filled with concrete so that the posts could be easily driven into the ground near abutments or placed using an auger. Four transducer elements with 3 feet spacing to each other were mounted on the posts. Polycase waterproof enclosures made of polycarbonate and (YH-080604 YH Series Hinged Waterproof NEMA Electrical Enclosures) of dimensions 8.59 x 6.59 x 5.11 in. containing an embedded data collection and interrogation electronics, power manager and a long-lived battery pack packaged were mounted on top of the post using mounting flange assembly. The tops of these posts are designed to be located in air to facilitate wireless operation. Low-power components and use of sleep mode was employed to extend the battery life. Fig. 6.7 depicts the electronics in the protective enclosure and Fig. 6.8 shows a packaged smart scour-sensing post prepared for field installation.

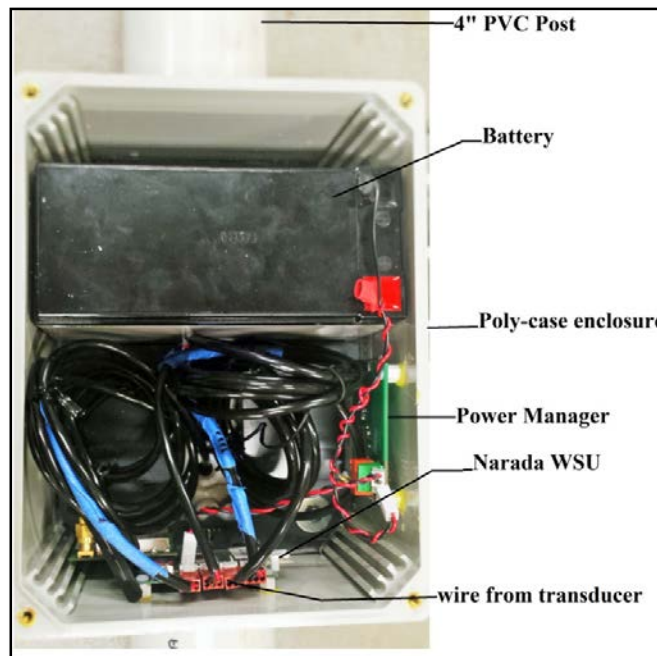


Fig. 6.7: Post electronics packaged in Polycase enclosure



Fig. 6.8: Packaged smart scour-sensing post

6.3 Base Station

The base station aggregates the data from multiple on-site posts and it creates a decision file in accordance to the data received from the wireless sensing units. The base station then relays the file to relevant authorities using a cellular data link to aid them to take suitable required action.

The base station is composed of Narada Base Station, Single Board computer (SBC), cellular data link and a power supply for the setup.

6.3.1 Single Board Computer

The Single board computer used for this research is an industrial platform that can safely operate in harsh field. The PPM-LX800-G manufactured by WinSystems (Figure 10). The PPM-LX800-G is a highly integrated, PC/104-Plus single board computer (SBC) designed for embedded, space limited, low power applications. The PPM-LX800-G is well suited for rugged applications requiring excellent processor performance in an embedded PC design. Its low power dissipation permits fan less operation from -40° to $+85^{\circ}\text{C}$ [WinSystems].

The server consists of a low-power single board computer (SBC) that operates Linux (Ubuntu 11.10).

Table 6.2: Technical Specifications of SBC (WinSystems)

Processor	LX800 @ 0.9W with 500MHz system clock
Memory	256KB of L2 cache Up to 1GB with a 200-pin SDRAM in a SODIMM connector
Network Interface	One 10/100 Mbps using the Intel 82551ER LAN
Storage	One Compact Flash socket supports Type I or II devices
Power	+5V required, 1.2A typical

6.3.2 Cellular Data Link

A 3G cellular modem is included in the server for the communication of data to and from the server. The cellular data link used is Pantech 4G LTE USB Modem UML290 is utilized as the cellular data link (Fig. 6.9). The UML290 is designed with manufacturer designed power management and system overhead reduction functions to take advantage of the USB interface to reduce power consumption. It contains an internal antenna which is designed to optimize data transfer rate and sensitivity to network signals”. The UML290 has typical download speeds of up to 5 to 12 Mbps in mobile broadband coverage area. The UML290 comes equipped with a fold-away, 180 degree rotating USB connector. The UML290 is also well-suited for use with Linux with minimal driver installation effort required by the user.



Fig. 6.9: UML 290

Table 6.3: Technical Specifications UML 290

Broadband	4G LTE Mobile Broadband and Mobile Broadband (Rev. A) capable
Memory	Qualcomm MDM9600
Network bands	CDMA 1xEV-DO Rev. A/Rev. 0: 800/1900 MHz, LTE CDMA (700MHz)
Antenna	External Antenna Connector

6.3.3 Narada Base Station

The Narada base station (Fig. 6.10) is an IEEE802.15.4 data transmission device that connects to a PC via USB and serves as the base station’s low-power link to the on-site posts. The Narada Base Station is produced by Civionics Inc. The Narada Base station is a wireless data acquisition hub built around the Atmel ATmega128 microcontroller. The ATmega128 is an 8 bit, low power microcontroller. The Narada Base station connects to the PC through an available USB port and can facilitate data collection, real-time control, and network maintenance tasks (Civionics).



Fig. 6.10: Narada Base Station

Table 6.4: Narada Base Station Technical Specifications: (Civionics)

Dimensions	3.0" x 2.0" x 1.5"
Base station to PC interface	RS-232,USB
CPU	
Processor	Atmel ATmega128
	FLASH 128 kB
	EEPROM 4 kB
	SRAM 4 kB
	External SRAM 128 kB
	External Clock Speed 8 MHz
RADIO	Transceiver TI CC2420
Frequency Band	2.4000 - 2.4835 GHz
Data Rate	250 kb/s
Range (line of sight)	600m

6.3.4 Assembled Base Station

Polycase waterproof enclosures (YH-161407 YH Series Hinged Waterproof NEMA Electrical Enclosures) of dimensions 16.59 x 14.59 x 8.24 in. was used for the base station which included a Narada base station, Single board computer, a wireless communication interface, Power manager and a battery pack. The base-station units were fitted with solar panels for battery recharging. Fig. 6.11 shows the base station assembly and Fig. 6.12 shows the solar panel that was used to recharge the base station battery.

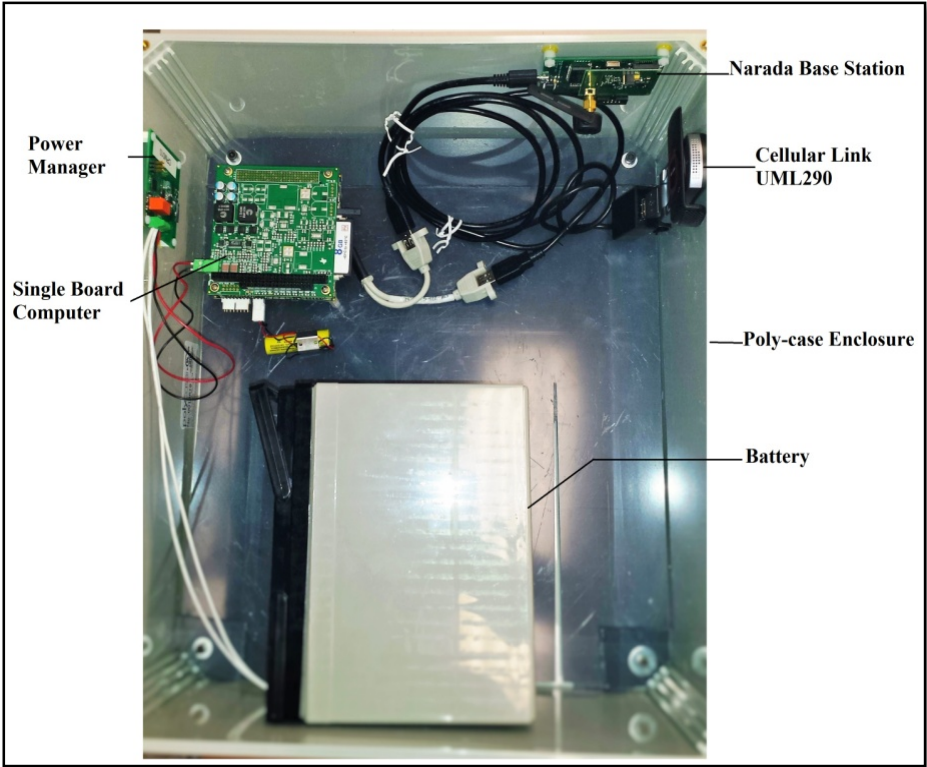


Fig. 6.11: Base station electronics in protective enclosure



Fig. 6.12: Assembled based station with solar panel installed in the field

7 Scour Sensor Design – Corrosion Protection and Fluid

Since Galfenol is largely an iron alloy, corrosion protection measures are vital to ensure long-term system performance. This section discusses the sensitivity and corrosion properties of Galfenol whiskers with alternative corrosion protection measures were augmented and studied and compared to alternatives (*e.g.*, Alfenol). The ability to engineer aerodynamic instabilities into the whisker shape, with the goal of increasing the range of fluid velocities under which dynamic signals are returned, was also studied. The behavior of these improved whisker geometries was evaluated under a range of flow conditions. Finally, a novel magnetic sea weed sensor type was developed for use in very low-flow conditions. In addition, unexpected breakage of the Alfenol whiskers were observed early during the project. The cause of this breakage was examined and corrected.

Output(s):

- Improved corrosion properties for the whiskers.
- Improved fluid interaction for the whiskers in low flows.
- Magnetic sea weed sensors were developed for very low-flow conditions.

In this phase, whisker sensors were optimized for scour detection purposes in the underwater environment. Material and geometric studies were conducted to maximize corrosion resistance, ruggedness, and sensitivity of the sensors. Alternatives to magnetostrictive materials were also considered, including a magnetic sea weed sensor designed to still return signals even in very low flow conditions when the sensor itself is not trapped in sediment. Transducers were characterized in both wet and dry conditions.

7.1 Development of Magnetostrictive Transducers

Initial flow sensors were based on designs for aerospace applications based on Galfenol, an iron-gallium (Fe-Ga) alloy with high magnetostrictive coupling. The Maryland team demonstrated that iron-aluminum (Fe-Al, Alfenol) whiskers have more desirable mechanical properties with only a modest reduction in output sensitivity (still ~100 mV output for high speed flows) and thus have moved to fabrication and calibration of Fe-Al whiskers in addition to Galfenol. As such, a Galvanization process was developed and implemented for both Galfenol and Alfenol whiskers for corrosion protection.

Iron-rich Fe-Al alloys (Alfenol) are a promising structural material in view of their alternative properties such as low cost, good wear resistance and good corrosion resistance, alternative for Fe-Ga alloys (Galfenol). The crystal structure and magnetostriction trends of Fe-Al alloys, up to ~20 at.% Al, are similar with those of Fe-Ga alloys. Recently, Clark et al. (A. E. Clark, *et al.*, *J. Appl. Phys.* **103**, 07B310, 2008) have made updates to the magnitudes of $(3/2)\lambda_{100}$ in Fe-Al alloys reported by Hall in 1959, with data showing magnetostriction values approaching a half of that in Fe-Ga. In polycrystalline Fe-Al, a fair magnetostriction of 112 ppm was obtained via rolling and annealing processes produced (Z. N. Bulycheva *et al.*, *Phys.Met. Metallogr.* **19**, 147, 1965), slightly higher than that of as-cast and annealed samples ($\lambda_{||, \perp}$ =99 ppm) (N. Mehmood, *et al.*, *J. Magn. Magn. Mater.* **322**, 1609, 2010). The team has developed abnormal grain growth (AGG) of (011) grain in Fe₈₀Al₂₀ with varying contents of niobium carbide particles that are used to inhibit normal grain growth. AGG behaviors in 0.75%NbC- and 1.0%NbC-added Fe₈₀Al₂₀ rolled

sheet are shown to depend strongly on annealing temperature (1000-1300°C) in samples annealed for 5h (Fig. 7.1), where the annealing protocols for developing textured Galfenol whisker was employed to Alfenol. There is no AGG in the 0.75%NbC-added $Fe_{80}Al_{20}$ samples annealed at temperatures lower than 1200°C, showing small grain size of $\sim 20\ \mu m$ and low magnetostriction values of $\sim 40\ ppm$. A large single Goss grain has begun abnormal growth in the sample annealed at 1200°C, partly consuming the sample, while the sample annealed at 1250°C, was consumed by an abnormally grown Goss grain which was accompanied with $\lambda_{||-\perp}=132\ ppm$. Of particular interest is that the magnetostriction response along $\langle 100 \rangle$ in Fig. 7.2, denoted as “C”, shows 160 ppm, approaching to $\sim 92\%$ of the single crystal $(3/2)\lambda_{100}=174\ ppm$ at 19.5 at.%Al. This high magnetostrictions along $\langle 100 \rangle$ orientation were also observed in the 1250°C- and 1300°C-annealed sample with 0.75%NbC in Figure 1(c)-(d). On the other hand, the grain growth is retarded at a temperature of 1200°C in 1.0%NbC-added samples as shown in Fig. 7.1 (e)-(g). This is because grain boundary pinning force by NbC particles increases with increasing NbC content. Annealing at high temperatures of 1250 and 1300°C produced large (011) grains with sharp $\langle 100 \rangle$ orientation in Fig. 7.1(f), exhibiting a maximum magnetostriction of $\lambda_{||-\perp}=162\ ppm$. So we used the 1.0%NbC-added $Fe_{80}Al_{20}$ alloy material and applied the annealing protocol for preparing textured whiskers.

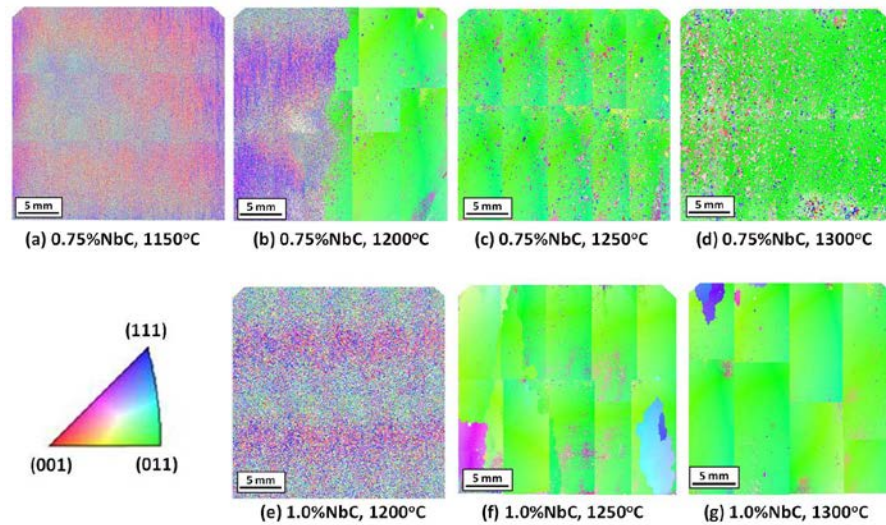


Fig. 7.1: EBSD-scanned images of 0.75%NbC- and 1.0%NbC-added $Fe_{80}Al_{20}$ rolled samples annealed at 1150-1300°C for 5h, where a sample dimension is 25.4 mm x 25.4 mm x 0.45 mm.

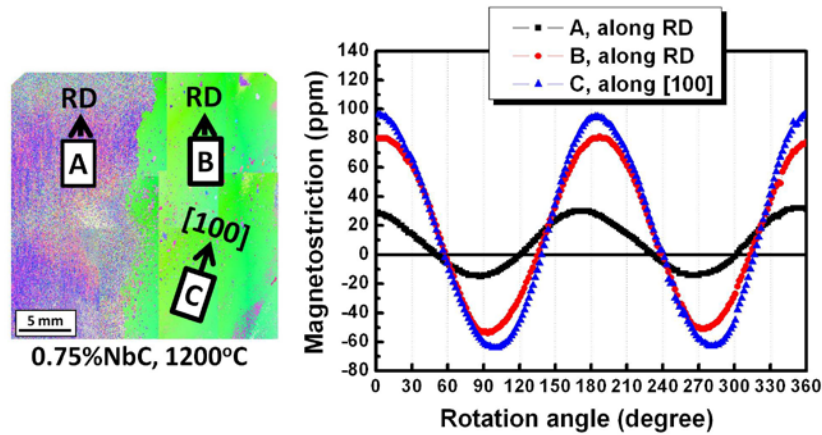


Fig. 7.2: Observed magnetostriction along the rolling direction and $\langle 100 \rangle$ orientation in both regions of the 0.75%NbC-added Fe80Al20 sample annealed at 1200°C.

Zinc metal has a good corrosion protection property for use in iron and iron-based alloys as a protective coating in most environments, especially in water. The team tried to coat zinc on the surface of whiskers using hot-dip galvanizing method with 99.99%Zn pellets. A large number of zinc-coated whiskers were prepared for flow sensing post as shown in Fig. 7.3, where the whisker dimensions for Alfenol and Galfenol are 152.4 mm (L) \times 2 mm (W) \times 0.35 mm (t) and 152.4 mm (L) \times 2 mm (W) \times 0.45 mm (t), respectively.



Fig. 7.3: A photo of zinc-coated whiskers of Alfenol and Galfenol.

The $\langle 100 \rangle$ orientations on the (011) matrix grain for each sample annealed for 24h are tilted from ideal $\langle 100 \rangle$ orientation parallel to rolling direction (RD). Annealing for 24h in Fig. 7.4 (a) was accompanied by magnetostriction values of 143 and 170 ppm along the RD and $\langle 100 \rangle$ orientation, respectively. To calculate the total magnetostriction, $(3/2)\lambda_s$, generated on the (011) grain matrix along RD, we simplified the anisotropic magnetostriction equation for cubic single crystal presented by Lee [1], so that the direction cosines of the saturation magnetization and strain measurement directions are same. Each direction cosine is defined by $\alpha_1 (\cos \omega)$, $\alpha_2 (\cos(90^\circ - \omega))$, and $\alpha_3 = 0 (\cos 90^\circ)$, where ω is a deviation angle from RD to $\langle 100 \rangle$. The simplified equation for total magnetostriction can be expressed as

$$\left(\frac{3}{2}\right)\lambda_s = \left(\frac{3}{2}\right)\left[\frac{3}{2}\lambda_{100}\left(\alpha_1^4 + \alpha_2^4 - \frac{1}{3}\right) + 3\lambda_{111}\left(\alpha_1^2 + \alpha_2^2\right)\right]$$

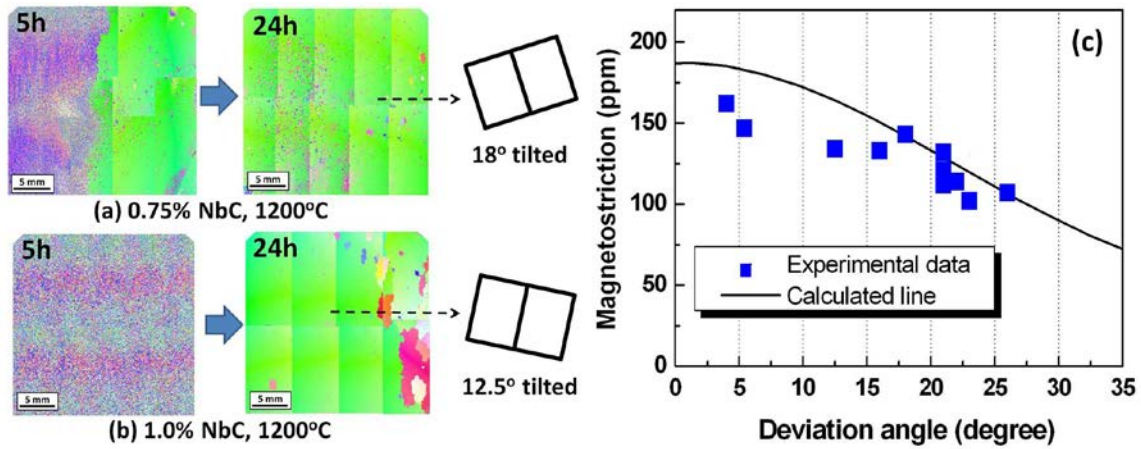


Fig. 7.4: (a) and (b): EBSD-scanned images of NbC-added Fe₈₀Al₂₀ rolled sheets annealed at 1200°C for 5 and 24h, respectively, where a sample dimension is 25.4 mm × 25.4 mm × 0.45 mm. (c): Plots of the both of measured and calculated data on magnetostriction which were obtained from single-grain-oriented Alfenol samples.

where the magnetostriction constants to be experimentally identified are $(3/2)\lambda_{100}=174$ ppm and $(3/2)\lambda_{111}=4.5$ ppm at 19.5 at.% Al. The calculated $(3/2)\lambda_s$ of 187.5 ppm along the $\langle 100 \rangle$ is a maximum value to be generated if the $\langle 100 \rangle$ orientation is perfectly aligned along RD in the Goss-oriented Fe₈₀Al₂₀ alloy. It is slightly greater than $(3/2)\lambda_{100}$ because of the incorporation of small number of positive λ_{111} grains. The $\langle 100 \rangle$ orientations on the (011) grain are mainly aligned within the range of 16-26° from the RD as shown in Fig. 7.4 (c). This is larger than the typical deviation angles of less than 15° which were observed in Goss-oriented Fe-Ga and silicon steels. The reason for the deviation in orientation between the RD and $\langle 100 \rangle$ is not well understood yet. We will investigate the deviation on orientation alignment, which may associate with the microstructures of the deformed and primarily recrystallized conditions, and develop the $\langle 100 \rangle$ orientation along RD to maximize the magnetostriction.

Magnetostrictive Fe-based alloy materials, e.g. Fe-Al (Alfenol) and Fe-Ga (Galfenol) alloys, exhibit good roll-ability, allowing use of thermo-mechanical deformation processes to be used in producing thin sheets and foil forms of the alloy. The thin sheet magnetostrictive materials are flexible yet have a high elastic modulus, and thus appear to provide a viable candidate for design of flexible flow sensors that are inspired by the vibrissa (whisker) sensors found on the face of many mammals (cats, rats, sea lions, etc.). The bending-induced stress in response to fluid flow over the whisker would couple with the alloy magnetoelastic properties to produce local changes in magnetization proportional to the local changes in stress so as to achieve the minimum energy state. In the case of positive magnetostrictive materials such as Alfenol and Galfenol alloys, the magnetic domains will align along the tensile stress direction, while they will rotate to the direction perpendicular to the direction of a compressive stress. Thus, the magnetostrictive whisker sensor must be able to withstand the range of tensile and compressive stress loadings caused as the whisker bends.

For Alfenol, the peak magnetostriction value of ~184 ppm along $\langle 100 \rangle$ orientation in single crystal Alfenol alloys at ~20 at.% Al approaches half that of Galfenol alloys with ~20 at.% Ga, while their magnetoelastic coupling coefficients are similar in magnitude. Aluminum is also a cost-effective element, which is less than 1% of gallium cost. The team developed textured Alfenol thin sheets of different thicknesses, ranging from 0.06 to 0.5 mm, and cut them into whiskers to demonstrate the magnetoelastic response from bending stress. Firstly, was tested 190-mm long whiskers with the thickness of 0.35 and 0.5 mm, where the rolling and annealing processes used to develop highly textured thin sheets of NbC-added Alfenol alloy with Al content of 20 at.%. Fig. 7.5 shows the whisker sensor configuration and net voltage change as a function of applied force by bending. The assembly is very simple, consisting of Hall-effect sensor and biasing permanent magnet that were placed on the one end of whisker and were covered by plastic holder that was clamped to a rigid fixture. Bending forces were applied by adding weight at the other end of whisker. The net voltage changes in the Hall-effect sensor were proportional to the applied tip force for the 0.35-mm thick whisker. The output of 200 mV in the 2-mm wide whisker sensor was saturated at a tip force of 0.411 N. The saturation force trend is consistent with this value being half that of 4-mm wide whisker sensor (which extrapolation of data suggests will saturate at ~0.8 N), as the wider whisker has twice the area moment of inertia and hence twice the bending stiffness of the 2-mm wide whisker sensor. A different trend was observed for the 0.5-mm thick whisker sensor, which has a peak output of 97 mV for a tip load of 0.143 N. With this sensor, the springback to the original position was somewhat incomplete when the 0.143 N load was removed, suggesting plastic deformation. The remaining strain/stress imposed in loading the whisker lead to work hardening of the material and ultimately to fracture of the whisker. The fractograph of 0.5-mm thick whisker is shown in Fig. 7.6. To understand the fracture, we calculated the stress applied to whisker. The bend radius (R) is defined as the radius of curvature on the concave side of the bend shown in the top illustration of Fig. 7.6. The strain (or stress) increases with decreasing the radius (R). Fig. 7.6 shows the plots of maximum stresses versus R at the bend region is proportional to the whisker thickness. Considering the yield and ultimate tensile strengths of 450 and 500 MPa reported in Fe-18at.%Al, respectively, whiskers with $t=0.35$ and 0.5 mm will both be over-stressed beyond the yield strength at a radius of curvature of between 0.01-0.02 m. From this analysis, the whisker thickness should be reduced to below 0.20 mm to preserve the elasticity and flexibility of whisker if a 54° bend angle is expected to be exceeded. As a result, the team made 0.06, 0.1, and 0.2-mm thick Alfenol thin sheets. The yield and tensile strengths in 0.1-mm thick sheet before annealing are enhanced to 824 and 1125 MPa, respectively (Fig. 7.7). Tensile tests of the textured thin sheets with varying thickness will be carried out for comparison with the as-rolled sheets. Annealing for developing texture with $\{011\}\langle 100 \rangle$ orientation was conducted on samples with the thickness of 0.06, 0.1, 0.2, 0.35 and 0.5 mm at a temperature of 1250°C for 7 and 12 h, where a dimension of all samples was 25.4 mm x 25.4 mm. Magnetostriction data are plotted in Fig. 7.8 to provide an indication of the extent of texture development for a given anneal protocol. Low magnetostriction values of ~30-40 ppm in the as-rolled samples (*i.e.*, prior to the texture development anneals) for the each thickness are fairly similar as expected. Subsequent annealing of the as-rolled samples led to magnetostriction values of up to ~158 ppm, which approaches ~85% of the magnetostrictive performance of single crystal Alfenol. This result

indicates the occurrence of abnormal grain growth of (011) grains as shown in Fig. 7.9. The whole scanned-EBSD (electron backscatter diffraction) images were obtained from the both samples with $t=0.2$ and 0.5 mm, where the samples were annealed 1250°C for 12 h. Large single (011) grains were fully grown, covering $\sim 80\text{-}90\%$ of sample surface.

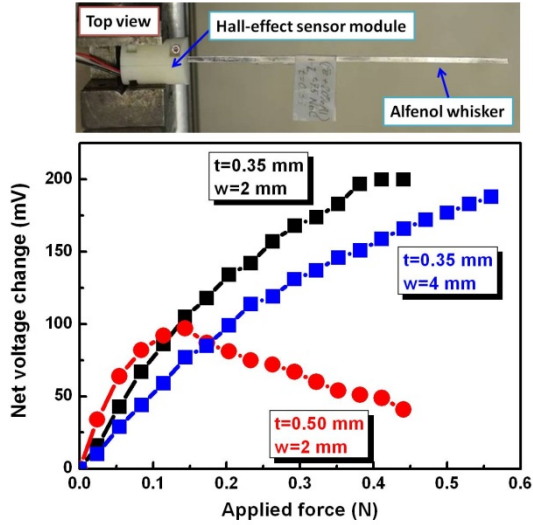


Fig. 7.5: Flow sensor configuration with hall-effect sensor (upper figure) and net voltage change as a function of applied force at the free end of textured Alfenol whisker (lower figure).

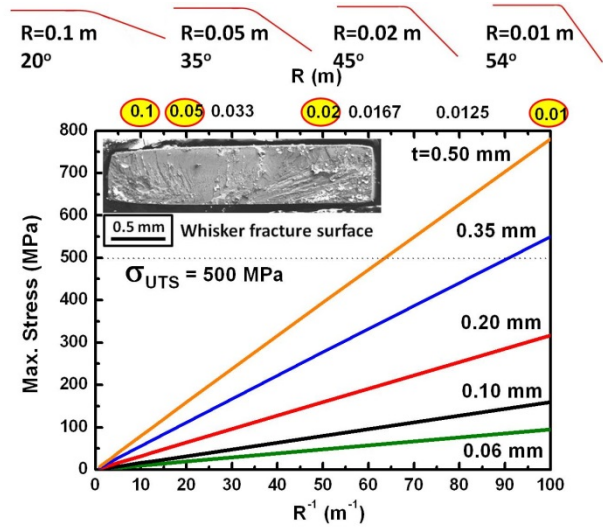


Fig. 7.6: Maximum applied stresses at the bending region of top whisker as a function of bend radius (R) and fracture surface of 0.5-mm thick whisker (inserted figure).

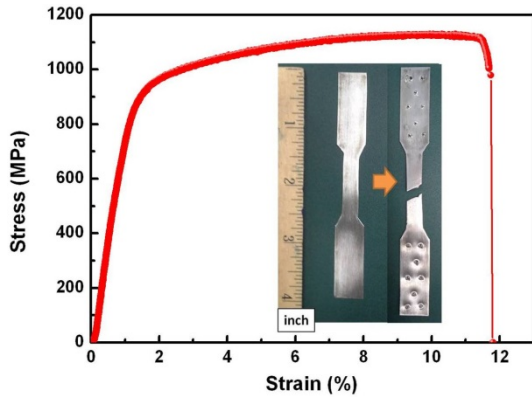


Fig. 7.7: Stress and strain response of 0.1-mm thick rolled sheet of Alfenol before annealing.

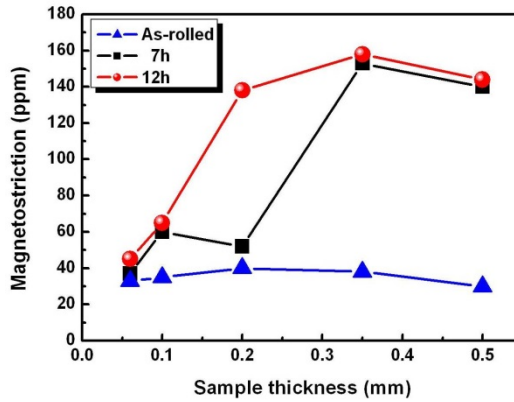


Fig. 7.8: Magnetostriction data as a function of the sheet thickness in as-rolled and annealed Alfenol sheet samples at 1250°C for 7 and 12 h under a sulfur atmosphere.

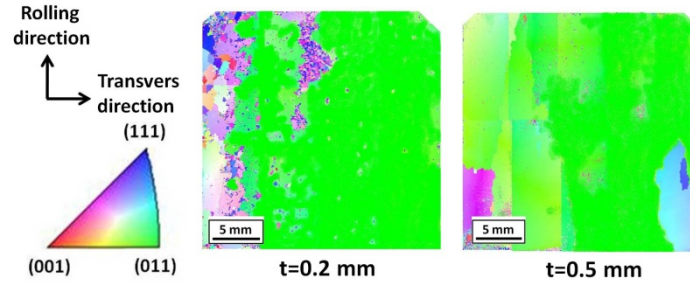


Fig. 7.9: EBSD scan images of the annealed Alfenol thin sheets with the thickness of 0.2 and 0.5 mm at 1250°C for 12 h.

Progress was also made towards understanding the variation in the performance of these whiskers of varying dimension. Different widths and thicknesses were tested to understand the influence of flux leakage on the signal and to interpret the micromagnetic behavior exhibited by magnetostrictive Fe-Al. 5 samples were tested with three of the whiskers having the same width and three of them having the same thickness as shown in Table 7.1.

Table 7.1 Whisker samples of different dimensions that were tested

a) Varying width

Sample	Width	Thickness
Whisker 1 (RED)	2 mm	0.20 mm
Whisker 2 (BLUE)	4 mm	0.20 mm
Whisker 3 (BLACK)	6 mm	0.20 mm

b) Varying thickness

Sample	Width	Thickness
Whisker 2 (BLUE)	4 mm	0.20 mm
Whisker 4 (PINK)	4 mm	0.35 mm
Whisker 5 (AQUA)	4 mm	0.50 mm

The whiskers were all deflected to the same extent at the tip using a servo motor and the results from varying width and varying thicknesses were as shown in Fig. 7.1 (a) and (b).

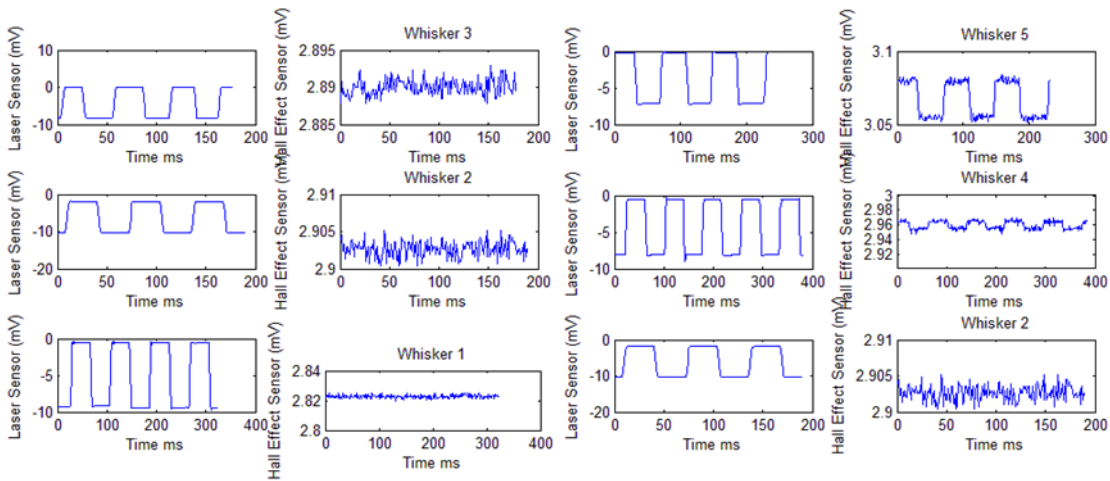


Fig. 7.10: Comparison of data from the laser displacement sensor and the Hall-effect sensor output for tip deflection of whiskers of (left) varying width and (right) varying thickness.

Fig. 7.11 shows the change in the magnetic state experienced by the whiskers for varying widths, thicknesses and cross sectional areas.

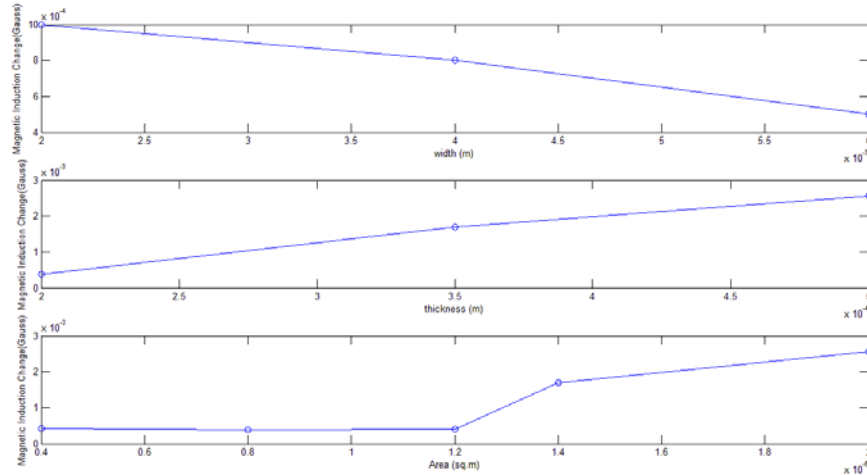


Fig. 7.11 Change in magnetic induction for varying (a) widths, (b) thicknesses and (c) cross sectional area.

Conclusions from these experiments:

- Thicker whisker soaks up flux from the bias magnet better.
- Wider sample also soaks up flux better but extent is lower as compared to thickness variation.
 - Suggests that there is very high flux leakage in thin, very high aspect ratio samples.
 - Flexibility decreases drastically as we increase thickness and onset of plastic deformation is easier in a thicker sample.
- Response reduces with increasing width in the edge configuration of holder.
- Response increases with increasing thickness in the edge configuration of holder.
 - Suggests that face configuration might work the best.
- A critical value for cross section area exists where high response is observed beyond which any increase in cross section area does not affect response much more.

The effect of bias magnet location on the response of Alfenol whiskers was also studied. The objective of these experiments was to find out the extent to which the magnetic state of the whisker changes in the three mutually perpendicular directions when a bias magnet was moved farther and farther away from the clamping point. This experiment would also help in determining ideal bias magnet placement for the three Hall-effect sensors measuring along the length (HE3), width (HE2) and thickness (HE1) of the whiskers. The whiskers were deflected at the tip using servo motor in these experiments as well. The summary of the response (change in magnetic state) recorded in the three mutually perpendicular directions for the different bias magnet locations is shown in Fig. 7.12.

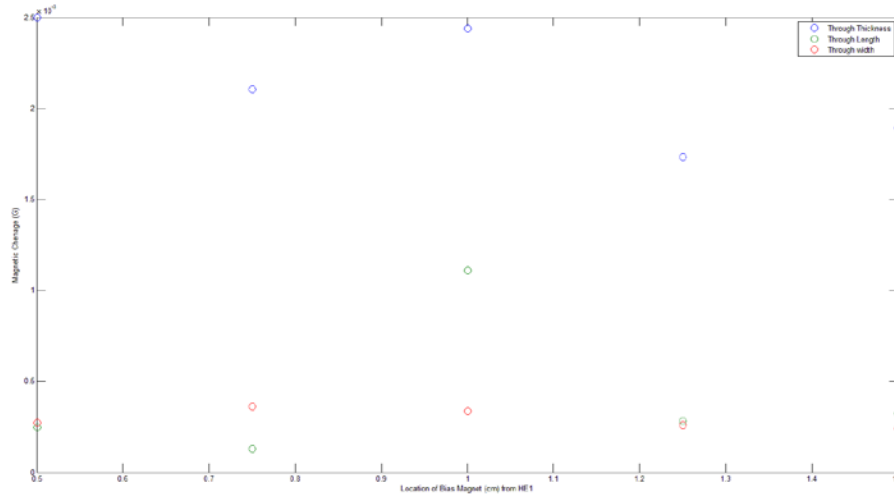


Fig. 7.12 Variation in the magnetic state change recorded by the three Hall effect sensors measuring in the three mutually perpendicular directions for different bias magnet locations from the clamping point.

Conclusions from these experiments:

- HE 2 – measuring along the width of the whisker does not see much change for any bias configuration.
- HE 3 – measuring along the length of the whisker picks up a response which peaks at bias magnet location 1cm behind the HE sensors.
- HE 1 – measuring across the thickness shows better response than both HE2 and HE3 for all bias magnet locations.
- This data was acquired in the face configuration which should show higher output as suggested by previous results.
- Adding up data from HE 1 and HE3 might give us better signal to noise ration.
- These results help in understanding the micromagnetic behavior to applied bending stress for various bias locations.

7.1.1.1 Tensile tests of Alfenol whisker materials with varying thickness

Tensile tests of Alfenol thin sheets were conducted in a MTS 858 Mini Bionix 25kN servo-hydraulic load frame at a rate of 0.0025 mm/s. The strain was monitored with a gage length of 25 mm. The test specimens were prepared according to ASTM A370-12a (Standard Test Methods and Definitions for Mechanical Testing). In order to obtain actual data on tensile properties in 20%Alfenol with varying thickness, we have made 0.06, 0.1, 0.2, 0.35, 0.5-mm thick Alfenol thin sheets. Tensile tests of the thin sheets for each thickness were carried out for verifying the predictions made based on the data shown in previous report on the maximum applied stresses as functions of bend radius and whisker thickness. Both values of yield strength (YS) and ultimate tensile strength (UTS) in the as-rolled samples were much higher than those of the annealed ones, shown in Fig. 7.13. This is because of severe plastic deformation as much as ~95% reduction in thickness, resulting in introducing stored energy by elastic strains and lattice defects. And the magnitudes of UTS for all annealed samples of 20%Alfenol are higher than those of 18%Alfenol (UTS=500 MPa) over all.

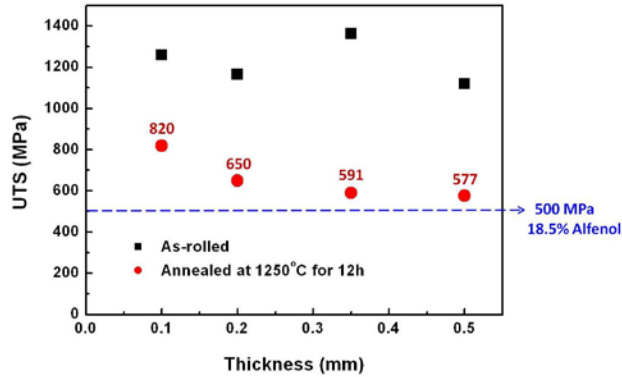


Fig. 7.13: Tensile properties of as-rolled and annealed 20%Alfenol sheets with varying thickness via tensile test to fracture.

7.1.1.2 Relationship between mechanical properties and microstructure in Alfenol

Tensile tests were carried out for the 0.35 mm-thin sheets of 20%Alfenol (Alfenol with 20 at% Al) with different microstructures. Values of yield strength (YS) and ultimate tensile strength (UTS) in the as-rolled sample, shown in Fig. 14, were much higher than those of the annealed samples. This is because of severe plastic deformation, of as much as ~95% reduction in thickness, introduced elastic strains and stored energy. In the case of both annealed samples, YS is similar, with levels of ~600-650 MPa, while there are big differences in UTS and elongation. This can be well explained by Hall-Petch strengthening in which strengthening materials arises with changes in average grain size. Grain boundaries act as pinning points, impeding further dislocation propagation. Since the lattice structure of adjacent grains differs in orientation, more energy is required for a dislocation to change directions and move into the adjacent grain. Impeding this dislocation movement will hinder the onset of plasticity and hence increase the yield strength of the material as the grain size decreases. As shown in EBSD images of Fig. 7.14, the primary recrystallized sample have quite small grain size and random orientation, while the textured sample has a huge green (011) grain and several small island grains. In addition to UTS, the elongation might be affected by shear stress applied along the direction perpendicular to tensile direction. For the textured sample, it was observed that the fracture surface was parallel to a $\langle 110 \rangle$ orientation that is perpendicular to the tensile load direction.

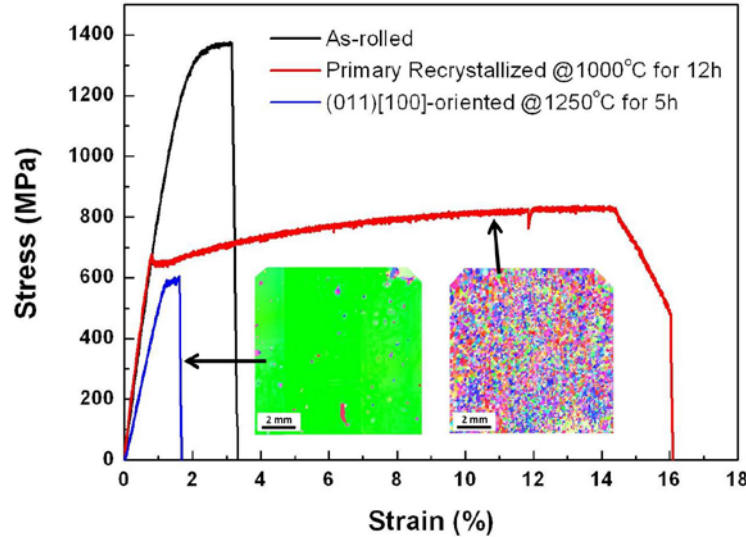


Fig. 7.14: Stress-strain curves of 20%Alfenol alloy sheets with different annealing protocols to form different microstructures.

The additions of carbon and boron in Alfenol steel will be studied to gain insights into enhancement of strength by more than enhancement that arises as a result of the formation of secondary hard phases such as cementite (Fe_3C) and iron borides (Fe_2B). Also, C (0.05-0.5%) and B (0.1-2.0%) will introduce solid solution strengthening and grain boundary cohesion that will be considered. Each ingot of material will be prepared by induction melting techniques and they will be rolled through thermo-mechanical processing to thicknesses in the range of 0.20-0.5 mm. A series of subsequent annealing under a sulfur atmosphere using 0.5-5.0% H_2S in argon will be conducted on the rolled samples at temperatures of 1000-1300°C for 1-24 h. All samples will be rapidly quenched in water from a temperature of 800°C after annealing. It is believed that the quenching process preserves the disordered α -iron structure matrix and forms a secondary hard phase at room temperature.

7.1.2 Fracture mode of Alfenol whiskers

The team has observed the fracture surfaces of whiskers that were broken when in post. Fig. 7.15 shows the fractographs of two Alfenol whiskers with galvanizing zinc coating and binary Galfenol alloy as a comparison. The Alfenol whiskers in Fig. 7.15 (a) and (b) exhibit a transgranular fracture, with ductility. And those are in stark contrast with a fractograph of binary Galfenol shown in Fig. 7.15 (c), showing an intergranular fracture mode with brittleness.

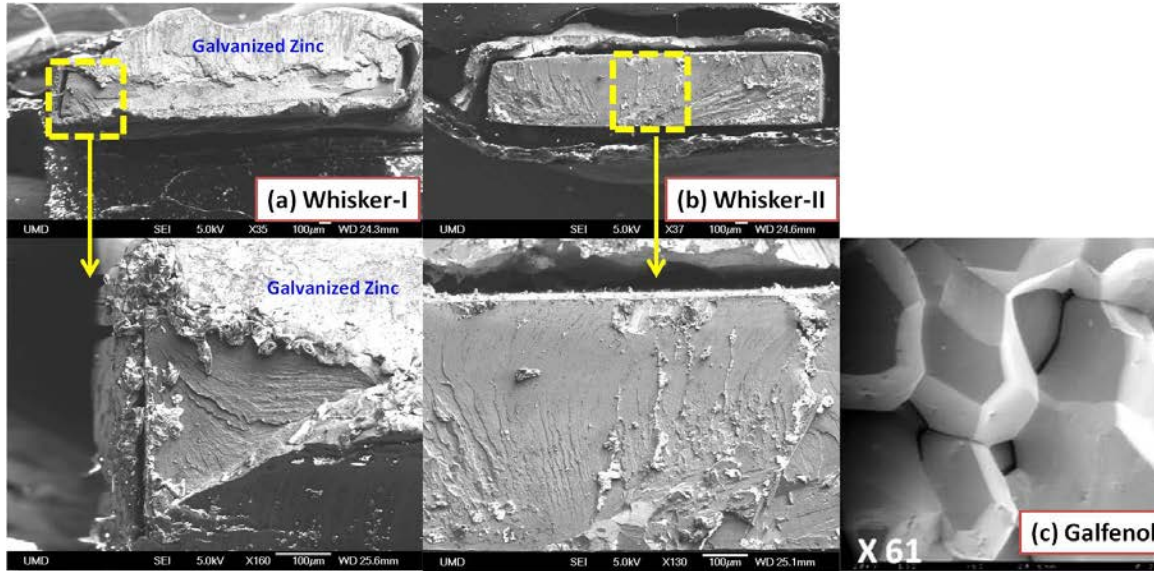


Fig. 7.15: Scanning electron microscopy fractographs of Alfenol whiskers and binary Galfenol ($\text{Fe}_{81}\text{Ga}_{19}$) alloy as a comparison.

The team has determined that two issues combined to cause these unexpected failures and have made improvements to eliminate this issue. First, thinner cross sections used to increase the sensitivity of the whisker have led to significantly higher stresses in the whisker sensor. Secondly, there was an issue with the size hole that was cut into the face of the post for the whisker to protrude from. In order to help hold the whiskers in place within the posts, these holes in the faces of the posts were made slightly smaller than the whisker itself. The stresses caused by this confinement, lead to fracture of the whiskers. Future designs will use thicker whisker sensors and oversized holes to reduce these stresses and prevent breakage.

7.1.2.1 Galvanizing Zn coating on Alfenol whiskers

The galvanizing Zn coating on whisker sensors is to prevent corrosion under water and to enhance hardness for providing abrasive resistance due to contacting soil and gravel when scour occurs. Zinc has been the most widely used for protecting ferrous materials, which is reliable and inexpensive in corrosion protection. New embedding technique of nano-sized alumina particles in the Zn layer during electroplating were employed to improve hardness property of Zn layer on Alfenol whisker materials. Alumina (Al_2O_3) was chosen based on its high tensile strength and other advantageous material properties. This process allows the alumina to be caught in the zinc matrix during electroplating at the current density of 0.14-0.42 A/inch² for 10-40 min., where the solution contains the alumina amounts of 10 and 50 grams, respectively. The results are updated for hardness test results of alumina-embedded Zn layer as shown in Fig. 7.16. It shows the enhancement of ~30-40% in hardness overall thickness. The great increases of hardness at the thickness thinner than 7 µm are due to being affected by substrate, where the micro-tip of hardness test penetrated the zinc layer and indented substrate during testing.

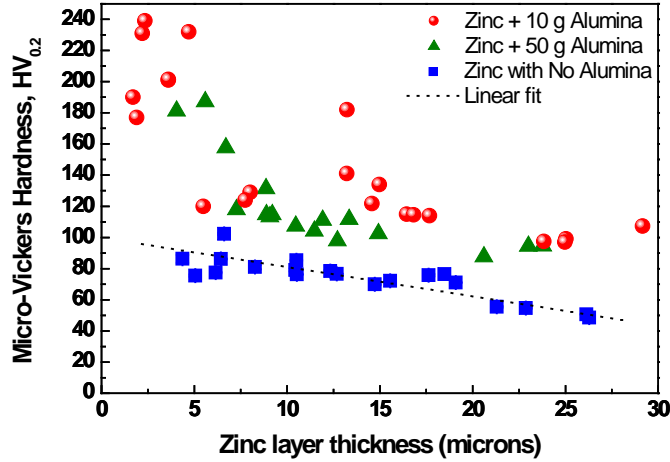


Fig. 7.16: Microvickers hardness test of electroplated zinc layers and alumina particle embedded zinc layers as a function of the thickness that depends on the plating condition.

7.1.2.2 *Microstructure analysis of Alumina-particle-embedded electroplated Zinc Layer*
 Results on micro-hardness tests of alumina-embedded Zn electroplated layer were presented in the previous section. It indicated that the enhancement of ~30-40% in hardness overall thickness for both 10 and 50 gram alumina solutions of zinc galvanizing coating. There is no significant difference in the hardness between the samples prepared by 10 and 50 gram alumina solutions, respectively. Their microstructure were, thus, examined for the both using a scanning electron microscopy (SEM) and a transmission electron microscopy (TEM) with energy-dispersive X-ray spectroscopy (EDS).

Fig. 7.17 shows morphologies and elemental mapping of aluminum (red color) and zinc (green color), respectively. The both samples prepared by 10 and 50 gram alumina containing solutions have a needle-like-structure with some small clusters of ~1-5 μm in diameter. They were identified as an agglomerate of alumina particles by EDS elemental mapping technique. And the needle-like structure is mainly composed of electroplated zinc. It was confirmed by TEM study as shown in Fig. 7.18. The agglomerate of alumina particles (79%) was mixed with zinc (21%). From these results, it is considered that the agglomerate of alumina particles plays an important role in the enhancement of hardness property in the zinc layer.

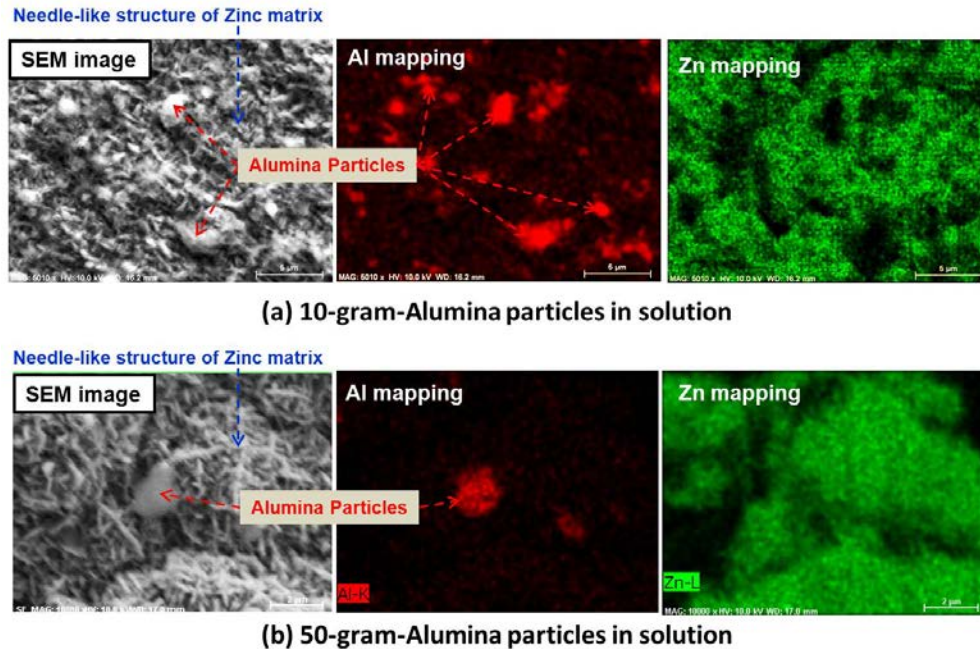


Fig. 7.17: SEM images and elemental mapping of aluminum (red color) and zinc (green color), respectively, for the both samples prepared by 10 and 50 gram alumina containing zinc electroplating solutions

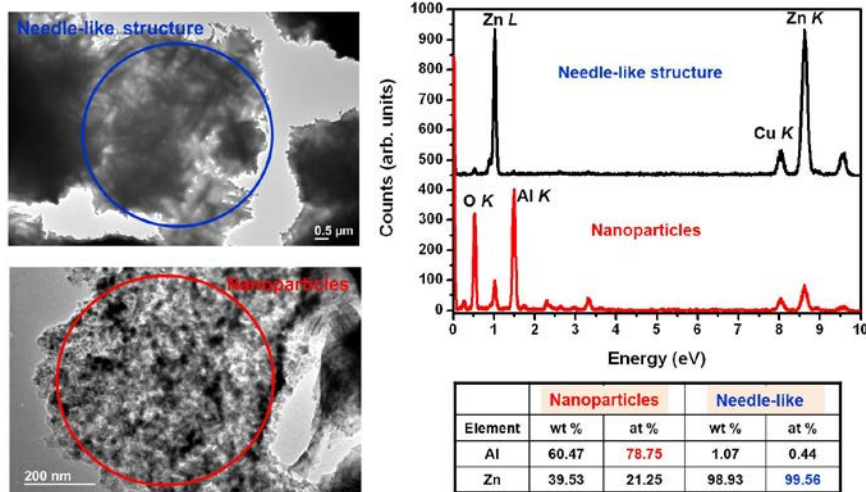


Fig. 7.18: TEM images and EDS composition analysis of the sample prepared by 50 gram alumina containing zinc electroplating solution.

7.1.3 Increasing response from Galfenol whiskers

Magneto-Optic Kerr Effect (MOKE) microscopy on the Galfenol whiskers was performed to understand the evolution of magnetic domains when the whisker is bent as shown in Fig. 7.19. The change in the magnetic domain orientation upon application of bending stress is picked up by the Hall Effect sensor which puts out a voltage that gets recorded in our

sensor. The bias magnet used in our sensor fixes the initial magnetic state of the whisker and change occurs from this point.

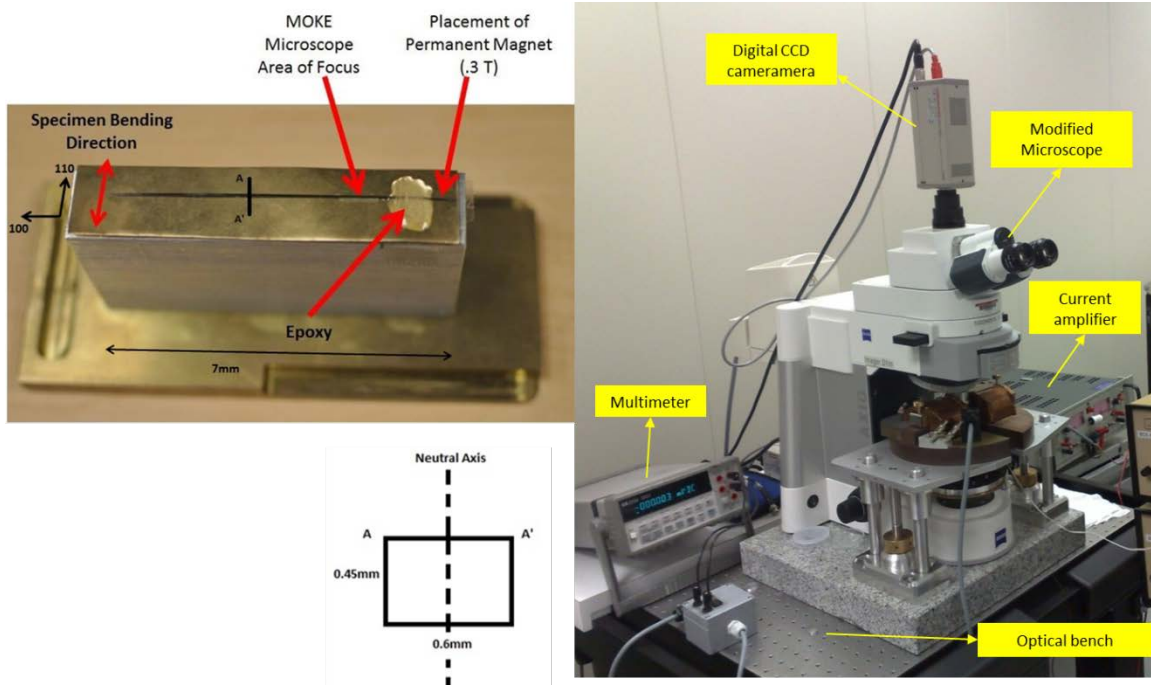


Fig. 7.19: MOKE microscopy of Galfenol whisker

Until the team were able to generate the MOKE images, we had assumed that the bias magnet that was being used was strong enough and that the initial state had all the magnetic domains oriented along the length of the whisker. Hence, when there was bending, the domains would rotate from this initial state to being anti-parallel and perpendicular to the long axis of the whisker in the region under compression. The domains would grow along the length of the whisker in regions that were under tension when the whisker was bent.

But the MOKE images that were captured told a different story. The bias magnet that was being used did not saturate the sample. Instead, we start at a state where the magnetic domains are oriented anti-parallel along the length of the whisker as shown in Fig. 7.20. The region that goes into compression has the magnetic domains break down into smaller domains that are anti-parallel and perpendicular to the length of the whisker. The magnetic domains continued to be anti-parallel in regions that were close to the neutral axis.

MOKE Images

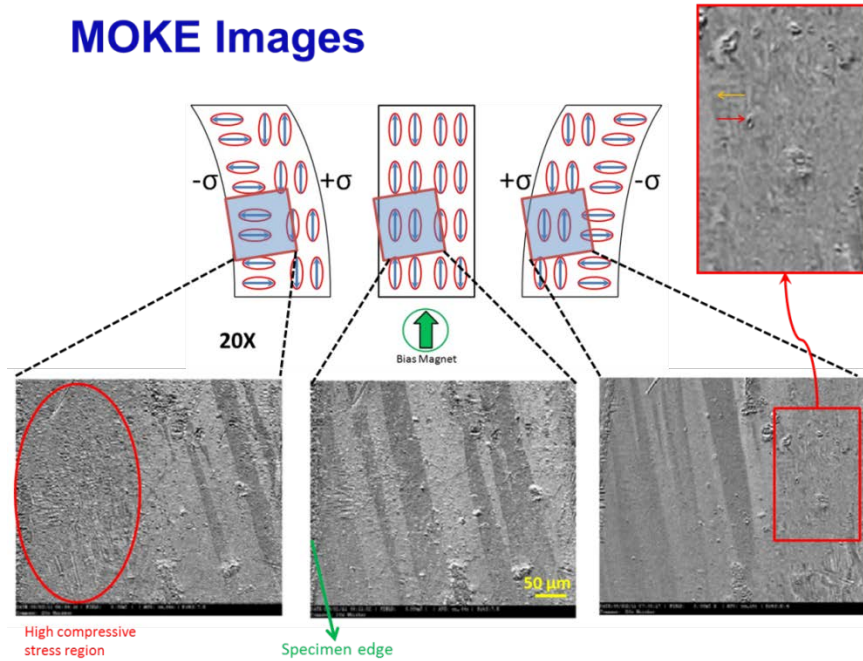


Fig. 7.20: MOKE images on bending Galferol whisker.

This had been predicted by a magneto-mechanical coupled COMSOL model as shown in Fig. 7.21, but was not understood completely without the help of pictures from the MOKE microscope. The results from these simulations are shown in Fig. 7.22. The whisker in the model is clamped at 2 cm on the x-axis and various tip loads were applied along the z direction as shown. The stress distribution along the length of the whisker and the change in the magnetic flux density were plotted. The solid lines correspond to an upward force and the dashed lines correspond to a downward force.

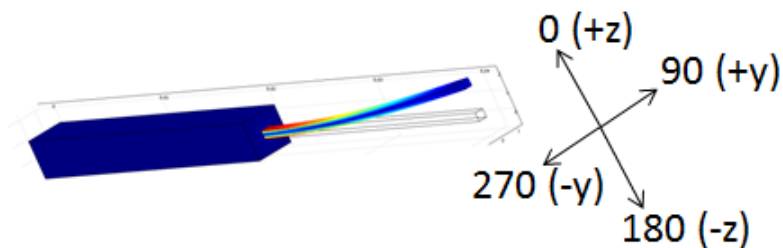


Fig. 7.21 Magneto-elastic model in COMSOL.

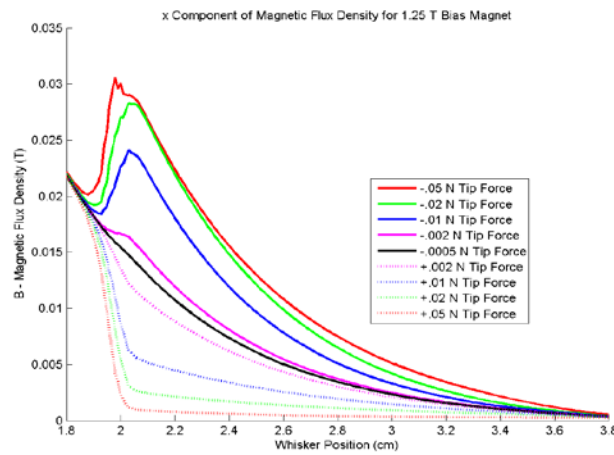
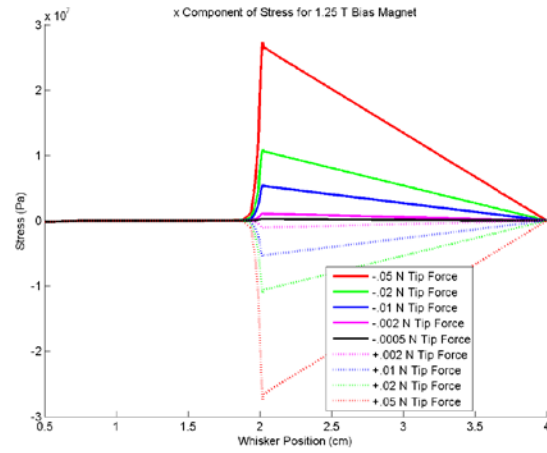


Fig. 7.22: Results from COMSOL simulation showing stress distribution and flux density along the x-direction for various tip loads.

With the initial holder that uses just one Hall effect sensor, we are measuring the magnetic change that occurs only in the region of compressive stress. This magnetization change is shown with a green arrow in Fig. 7.23.

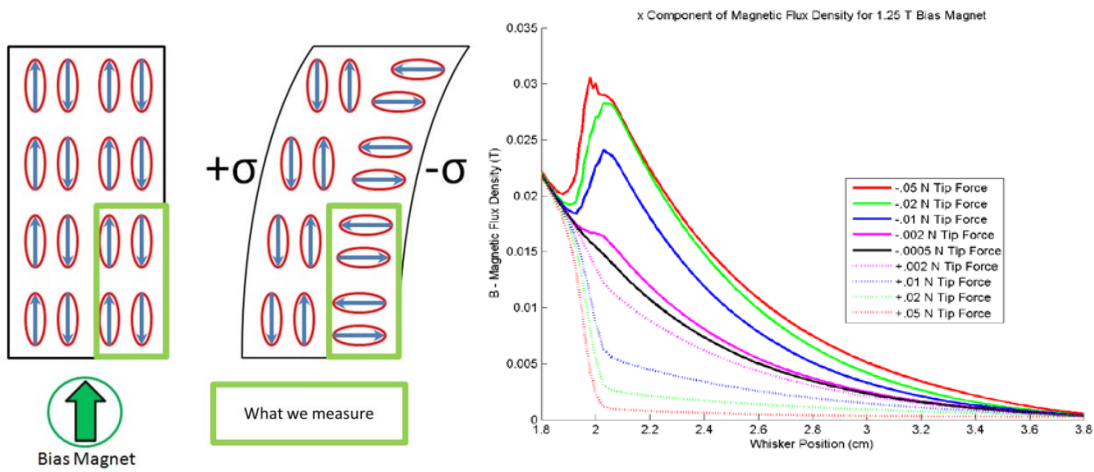


Fig. 7.23: Magnetic domain cartoon depiction magnetic change that is recorded by the Hall Effect sensor in the current holder setup.

One way to increase the signal that we are seeing in the setup is to include an additional Hall Effect sensor to record the increase in the orientation of the domains in the region under tensile stress, indicated with a purple arrow in Fig. 7.24, and adding it up to the signal. Future work may implement this and to build up a circuit to add the signals that would give improved signal to noise ratio.

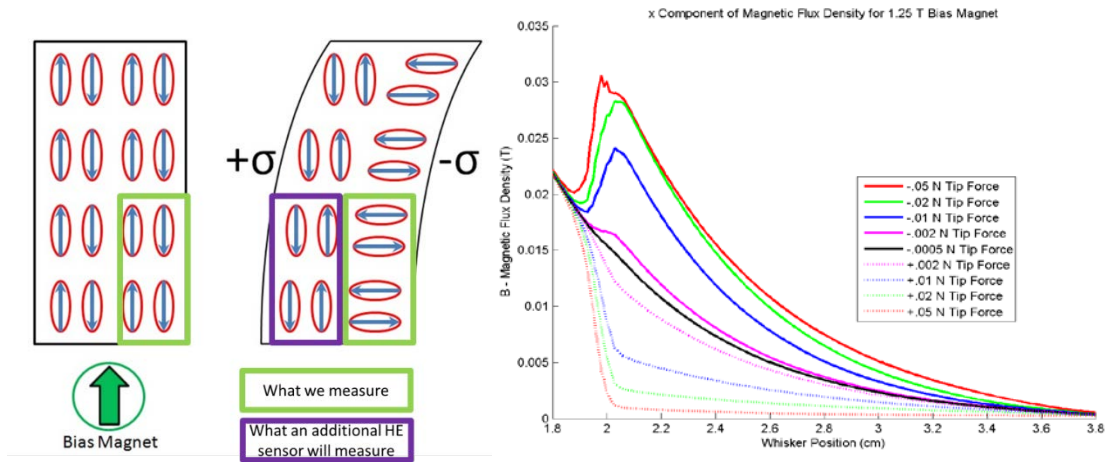


Fig. 7.24: Magnetic domain cartoon depiction magnetic change that is recorded by 2 Hall Effect sensor in the proposed holder setup.

COMSOL simulations to understand the initial state in the whisker from the permanent magnet have shown that biasing to saturation occurs in a very small region and that as we go further away from the bias magnet, we would get anti-parallel domains oriented along the length of the whisker as shown in the MOKE images. Since the permanent magnet is located behind the clamping point of the whisker, the region experiencing high stress does not start at a completely saturated state. The results from these simulations are shown in Fig. 7.25.

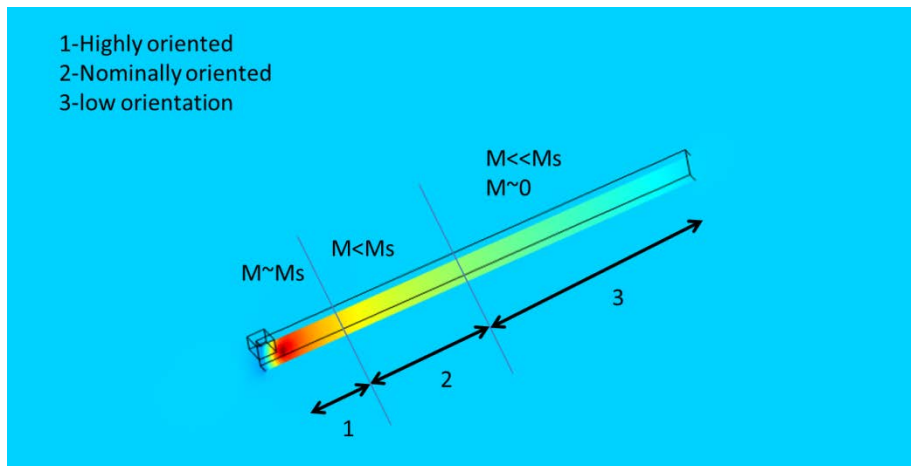


Fig. 7.25: Magnetization along the length of the whisker.

Using a strong magnet to obtain a highly oriented starting state at the point of clamping was also explored. This is shown in Fig. 7.26 with a motive to find the magnetization value at which complete saturation is lost. Fig. 7.27 shows results from a 0.3T bias magnet that is moved to different locations on the whisker.

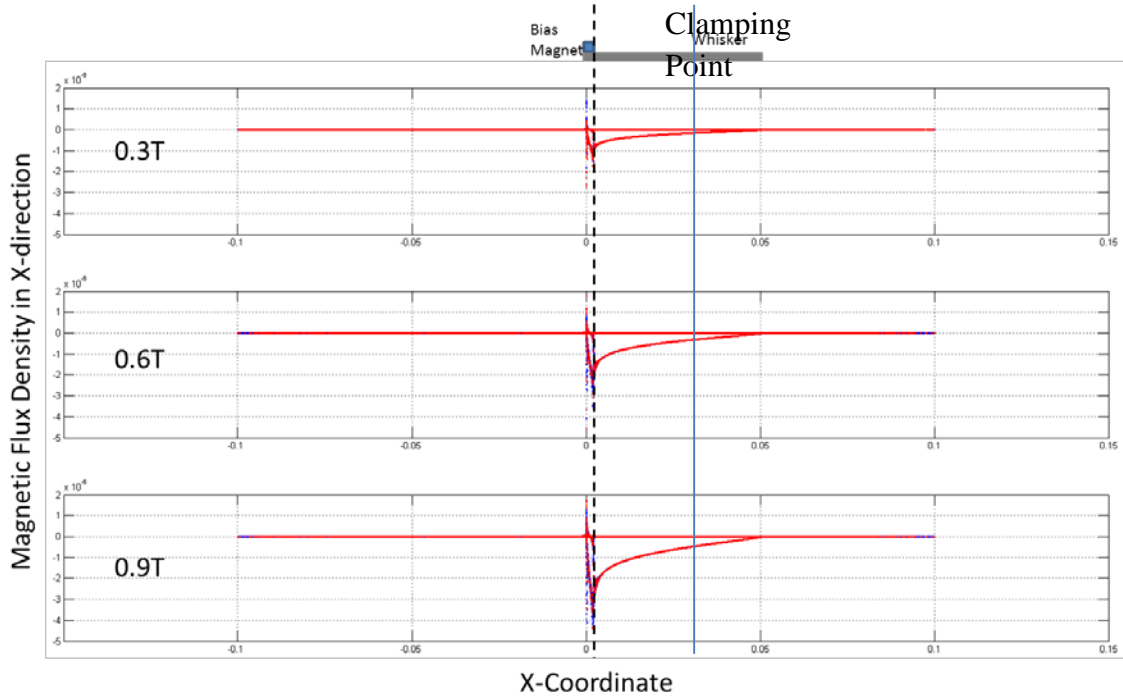


Fig. 7.26: Results of magnetization at the point of clamping for different bias magnets.

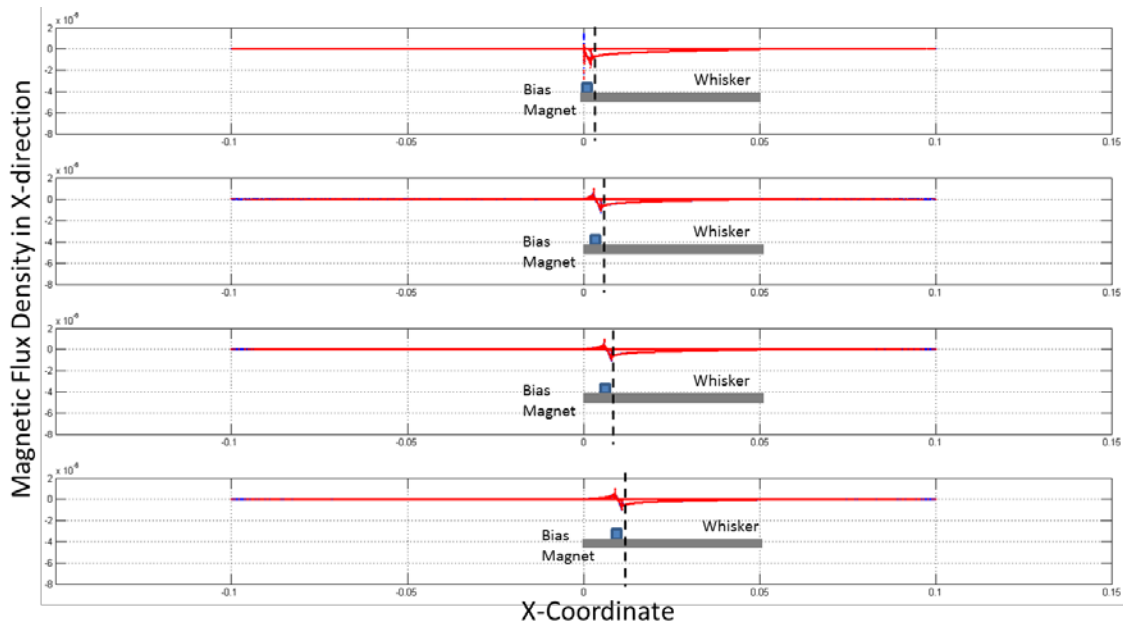


Fig. 7.27: Results of magnetization along the length of the whisker for different magnet locations for the 0.3T bias magnet.

7.1.3.1 Galfenol thickness effect on magnetostriction and grain growth

Extending an investigation on the influence of sheet thickness on abnormal grain growth and texture development to Galfenol rolled sheets beyond the results on 20% Alfenol. In order to test the effect in 19% Galfenol with varying thickness, we have made 0.2, 0.35, and 0.5-mm thick Galfenol thin sheets. Subsequent annealing was conducted at temperatures of 1200-1250°C under a sulfur atmosphere. The magnetostriction values were plotted in Fig. 7.28. Low magnetostriction values of ~25-45 ppm in the as-rolled samples for the each thickness are fairly similar. The 1200°C-annealing of 0.35- and 0.50-mm thick samples led to magnetostriction values of ~250 and ~279 ppm, respectively, whereas the data of 0.20-mm thick samples is consistent with that of the as-rolled sheet. This is due to the enhanced pinning sites by NbC particles, which inhibit grain growth. To overcome the pinning, the temperature was elevated to 1250°C, which probably imparts more thermal energy to grain boundaries for grain growth. The magnetostriction of 0.20-mm samples annealed at 1250°C was linearly increased to 135 ppm. It is lower than those of the thicker samples. The discrepancy results from the different behavior on abnormal grain growth with different orientation, as shown in Fig. 7.29. The both 0.35- and 0.50-mm thick samples show conventional Goss grains with $\langle 100 \rangle$ orientation, but the 0.20-mm thick sample has $\{131\}\langle 237 \rangle$ orientation along the rolling direction, deviated from the $\langle 100 \rangle$ as much as 40 degrees. The orientation component was observed at the sub-grain area that was formed in the as-rolled structure before abnormal grain growth. It might be successive to final texture. Tensile tests of the textured Galfenol sheets will be conducted for comparing the mechanical properties to those of Alfenol.

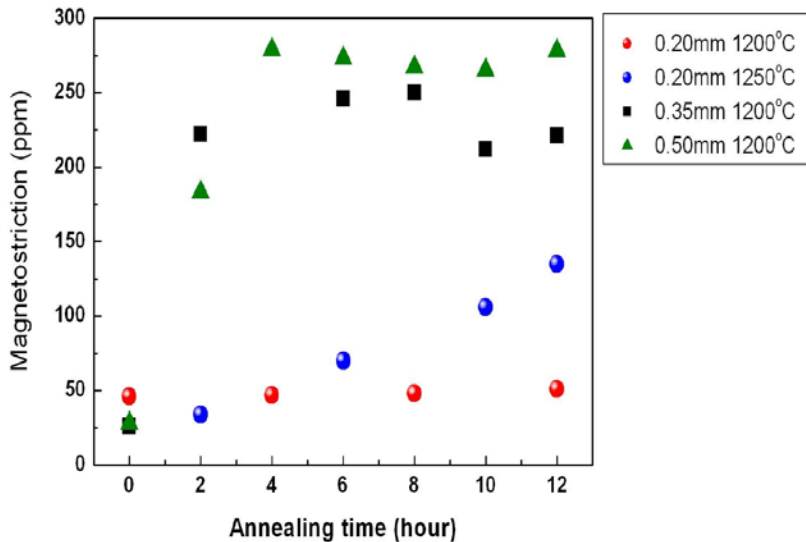


Fig. 7.28: Magnetostriction data of as-rolled and annealed 19%Galfenol sheets with varying thickness as a function of annealing time.

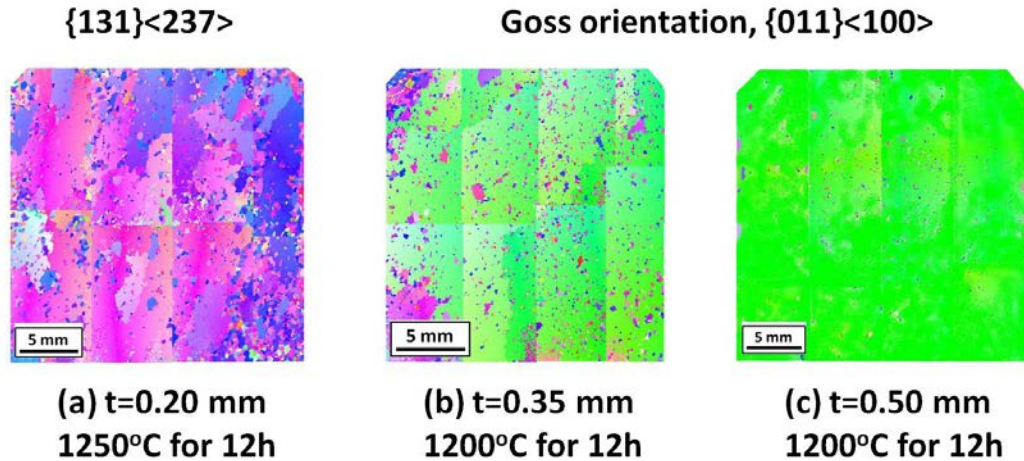


Fig. 7.29: EBSD scan images for each thickness sample annealed for 12h, where the sample size is 25.4 mm x 25.4 mm.

7.2 Slow/Steady Flow and Seaweed Transducer Geometry

To overcome concerns involving the induction of whisker vibrations in slow/steadily flowing water, an unstable airfoil design, displayed in Fig. 7.30, was envisioned, providing the promising results. After some testing, it was determined that the optimal configuration of this airfoil is a NACA 0050 with a ¼-in chord (a symmetrical airfoil with 50% camber). The airfoil runs along the entire length of the whisker, as increased vibrations are observed with increased airfoil length. Due to this favorable characteristic obtained from having longer airfoils, we decided to install the whiskers into the post at a 45 degree angle. This allows for the use of longer whiskers while still allowing them fit inside a hollow stem auger. The 45 degree angle was tested in a flume and determined not to have a negative effect on the performance of the whisker.



Fig. 7.30: Unstable airfoil whisker design.

Upon visiting the first installation site, a tidal bridge in Maryland, it became apparent that even with the strong vibrations present in the whisker at speeds as low as 0.12 m/s, a sensor to measure slower currents was needed. The water at the site seemed slower moving than most streams or rivers, possibly due to the dependence on tidal flow. The proposed solution was to create a near neutrally buoyant sensor that would move with the slightest alteration in flow velocity. This need led to the design of the “seaweed” sensor (Fig. 7.31).

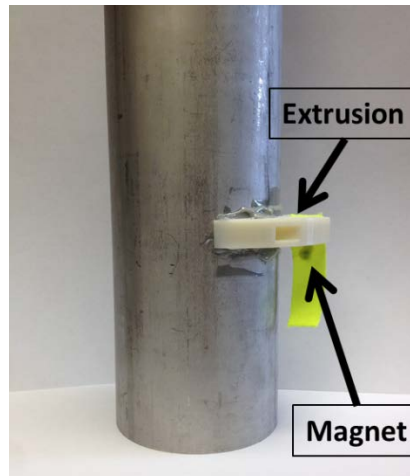


Fig. 7.31: Seaweed sensor.

The seaweed sensor consists of a piece of fabric dangling from a small extrusion protruding out of the post. Located in the extrusion is a hall sensor with the ability to read a magnet attached to the fabric a few millimeters below. Upon testing in the flume, the setup has the ability to measure extremely small flow variations, including those at the test site. The seaweed morphology proved to be sensitive and robust, and was incorporated into the field demonstrations in both Maryland and Michigan.

8 Signal Processing for Scour Detection

This report details the signal processing approach taken to detect flow at whisker sensors for autonomous remote sensing of bridge scour using magnetostrictive scour sensing posts. Static flow indicates a sensor buried in sediment while dynamic flow signals indicate a lack of sediment and potential scour. Autonomous algorithms to detect these conditions are required to free the bridge owner from data interrogation duties allowing them to focus on bridge management instead. A number of approaches are investigated, but a frequency-domain approach is ultimately selected for signal detection to increase sensitivity, reduce computational effort, as well as reduce the false alarms caused by sensor failure and noise.

Outputs:

- Autonomous embedded algorithm for bed detection.

This report presents the implementation details of the river bed detection algorithm, showing how it has been executed. The riverbed detection algorithm analyzes the raw sensor data from each buried whisker transducer and classifies the output as corresponding to either static, dynamic, or some sensor fault behavior. Those sensors that are static are assumed to be buried in sediment while those that are dynamic are considered to be above the riverbed or located in a scour hole. In this effort, simple algorithms that give good sensitivity even in low-flow conditions are preferred in order to allow for more reliable autonomous operation as well as reduce the computation effort required to classify the data (which will save battery energy within the post). The algorithm must also have minimal memory requirements to allow it to be executed, embedded in resource-constrained, low-

power wireless sensor units (WSUs) that form the computational core of the smart scour-sensing posts developed for this study. Direct data interrogation within the post will eliminate the need to communicate copious amounts of raw data wirelessly at bridge sites improving network and system resilience and reducing energy consumption. In addition to the low-power WSUs, the algorithm will be implemented on single board computers (SBCs) at some sites where wireless operation is not an objective. In these implementations, energy and computational resources are less limited.

8.1 Objectives for autonomous detection algorithm

The design of the algorithm had several objectives:

- Simplicity
- Minimal memory utilization
- Fast execution time
- High sensitivity
- Repeatability
- Error detection

8.2 Platforms

The project will use both low-power WSUs as well as more capable SBCs as data acquisition and processing platforms. The WSUs employed are Narada wireless sensing and control devices with 8-bit fixed-point microcontrollers and a scant 128kB of SRAM provided for data storage. Narada wireless sensor node comes with a custom written embedded operating system. The operating system simplifies the process of the wireless sensor for the user and serves as an intermediary software layer between hardware and software written for data interrogation. Within the custom operating system, additional engineering algorithms for data interrogation may be used with a number of algorithms already developed in an existing library. Some of the algorithms that were utilized for this project included computation of basic statistical measures, the fast Fourier transform (FFT), as well as least-squares approximations of time-series models for input/output data (*e.g.*, AR, ARX, ARMA, *etc.*).

To support additional platforms (and for debugging purposes), these algorithms were ported to Linux as well as Windows. Since, for implementation in the SBCs selected for this study, the Linux operating system (Ubuntu 11.10) is being utilized, the final integrated detection algorithm was ported to Linux.

8.3 Operation

In this study, a central based station (composed primarily of a SBC) was used to coordinate the activities of the wireless monitoring system and to serve as storage of network measurement data of the system. To initialize the Narada WSUs and execute the riverbank detection algorithm, three server setup files are used. The first file `default_settings.dat` is a text file containing DAQ parameters is created by the user, processed by an executable server program running on the PC, and wirelessly transmitted to the network over Narada IEEE802.15.4 receiver board connected to the SBC USB port. This file `default_settings.dat` allows the user to modify the IEEE802.15.4 network settings defined for the wireless sensor network including the communication channel, personal area

network (PAN) ID, and the server node ID. A second file, called DAQ_settings.dat, is used to set data acquisition parameters including the sampling frequency, total sampling time for a test, the number and ID of the WSUs participating in a test, and the WSU data channels to be used. A final setup file, analysis_settings.dat, is defined to establish the thresholds to apply to each sensor channel that help the algorithm to differentiate between static and dynamic signals (these thresholds will vary according to the transducer used).

The base station initiates data acquisition from all WSUs within the local network at the beginning of a scour detection cycle. WSUs within scour posts collect and store time history data from all transducers on the posts. At the end of the test, the base station ensures that the test has completed and then requests that the WSUs perform data processing on their locally collected data including finding basic statistical measures as well as frequency-domain analysis using an FFT and rudimentary digital filtering. The results of these algorithms are reported to the base station which then classifies each signal according to the rules defined in the setup file. The results from each channel are then uploaded via cellular data modem to a central server to be presented to the user. An overview of this process is shown in Fig. 8.1. Additional details of the individual steps are provided in subsequent sections of this report.

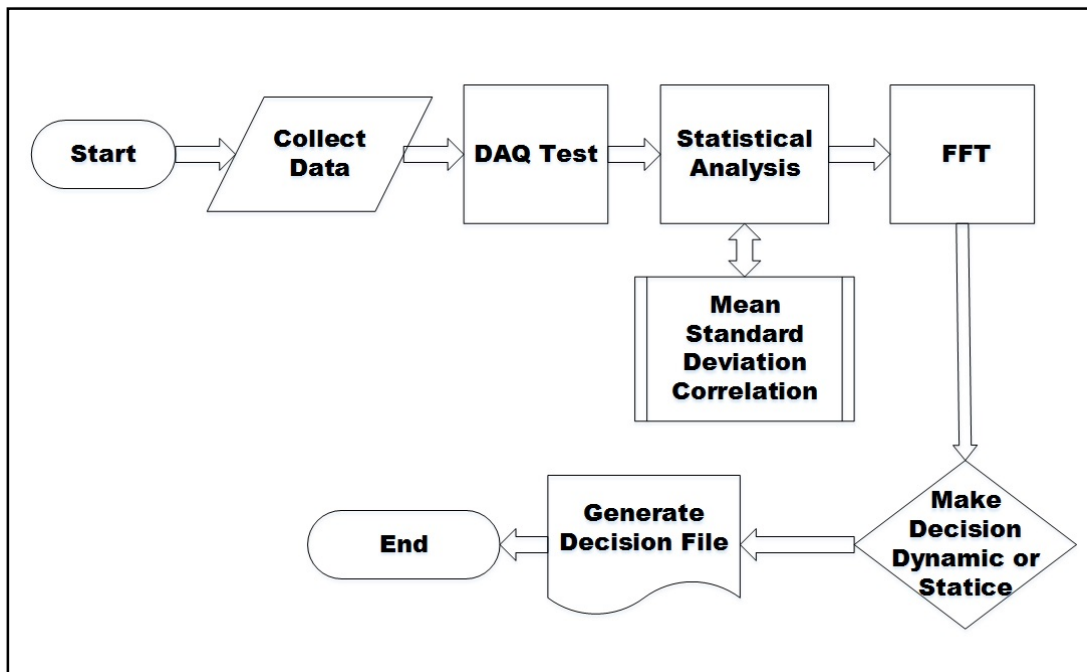


Fig. 8.1: Basic Algorithm Steps

8.3.1 Data acquisition (DAQ)

Data acquisition (DAQ) module written for the embedded operating system provides the Narada wireless sensing unit with the ability to collect and store data or of real-time continuous data streaming to a server, the former being most useful in this application. The DAQ collects data from the node analog-to-digital converter (ADC) and stores it in SRAM. Data processing activities take place within the sensor node and only processed results are reported to the base station. Bridge managers may make a request from the remote

visualization client to view raw sensor data from the sensors in upcoming detection cycles. In this case, the base station will request raw data from the WSUs as well, collecting it and uploading it to the remote server via cellular data link.

8.3.2 Statistical computation

Statistical modules have been added to allow the Narada to perform statistical analysis of the data collected. The algorithm is written so that the Narada can calculate the mean, standard deviation, correlation and the cross correlation between the sensors. Normal or Gaussian distribution is used to calculate the mean, standard deviation, correlation and the cross correlation. These measures (particularly standard deviation) can be compared to a threshold to determine whether the transducer is measuring static or dynamic signals. In addition, cross correlation measurements can be helpful in identifying cross-talk and other indications of faulty sensor channels.

Calculate the mean for all channels (for n samples):

$$\mu_x = \left(\frac{1}{n}\right) \sum_{i=1}^n X_i$$

Calculate the Gaussian standard deviation for all channels:

$$Var = \left(\frac{1}{n-1}\right) \sum_{i=1}^n (X_i)^2$$

$$\sigma = \sqrt{\text{Variance}}$$

Calculate covariance between all channels:

$$cov(X, Y) = \frac{\sum_{i=1}^n (X_i - \mu_x)(Y_i - \mu_y)}{n-1}$$

Calculate correlation coefficients:

$$r_{X,Y} = \frac{cov(X, Y)}{\sigma_x \sigma_y}$$

8.3.3 Fast Fourier transform and frequency-domain analysis

The fast Fourier transform (FFT) modules have been written for the embedded operating system to provide Narada with the capability to perform frequency-domain analysis of the data. The FFT previously included has been altered to make it able to compute FFT for channels ranging from one to four. It also calculates the magnitude and phase angle of the FFT which is used to define the static/dynamic signal threshold. To conserve memory within the WSU, only the lower half of the FFT is stored in memory (*i.e.*, those values below the Nyquist frequency) owing to the lack of independent information contained in

the remaining portion of the FFT results. For dynamic signal detection, only low-frequency values of the FFT are owing to the limited bandwidth of the fluid-coupled transducer output. Laboratory studies revealed that frequencies above 10 Hz generally did not contain signals corresponding to the vibrations of the whisker sensors in their submerged state. Rudimentary digital filtering of the signal above 10Hz was performed and the sum of the remaining FFT magnitude is used as the primary indicator of the presence of dynamic signals with large sums indicating dynamic behavior. High levels of signals in frequencies above 10 Hz and poor signal-to-noise ratios measure in the frequency domain were used as indicators of sensor faults.

8.3.4 Decision file and application of thresholds

A decision file ALGOTEST in “csv” format is created by the base station at the end of every scour monitoring test. The file informs the end user the time test was conducted, the unit numbers of the sensing units, used and the states of each transducer. Table 8.1 shows the states defined. The decision on whether the sensor is dynamic or static is made after comparing the mean, standard deviation and the magnitude of the frequency-domain analysis to a certain pre-assigned. These thresholds were determined for each transducer type after carefully studying the data collected in the laboratory tests. Decision integer is assigned to each sensor which informs the user about the state of the sensor. Fig. 8.2 shows an example of the decision file created. In addition, sensor fault states including excessive noise and inconclusive (intermediary) flow states are also defined.

Table 8.1: Decision states

Decision Integers	State
0	Static State
2	Dilatory State
3	Transitional State
4	Dynamic State
5	Noise

	A	B	C	D	E
1	time	sensing_uchannel	state		
2	2014/07/02T09:29:01	WSU03	4	4	
3	2014/07/02T09:29:01	WSU03	1	0	
4	2014/07/02T09:29:01	WSU03	2	0	
5	2014/07/02T09:29:01	WSU03	3	2	
6	2014/07/02T09:29:01	WSU66	0	3	
7	2014/07/02T09:29:01	WSU66	1	3	
8	2014/07/02T09:29:01	WSU66	2	2	
9	2014/07/02T09:29:01	WSU66	3	4	
10					

Fig. 8.2: Decision File

This data is uploaded to the remote decision support client to be interpreted and presented to the end user. A summary of the entire test algorithm is depicted in Fig. 8.3.

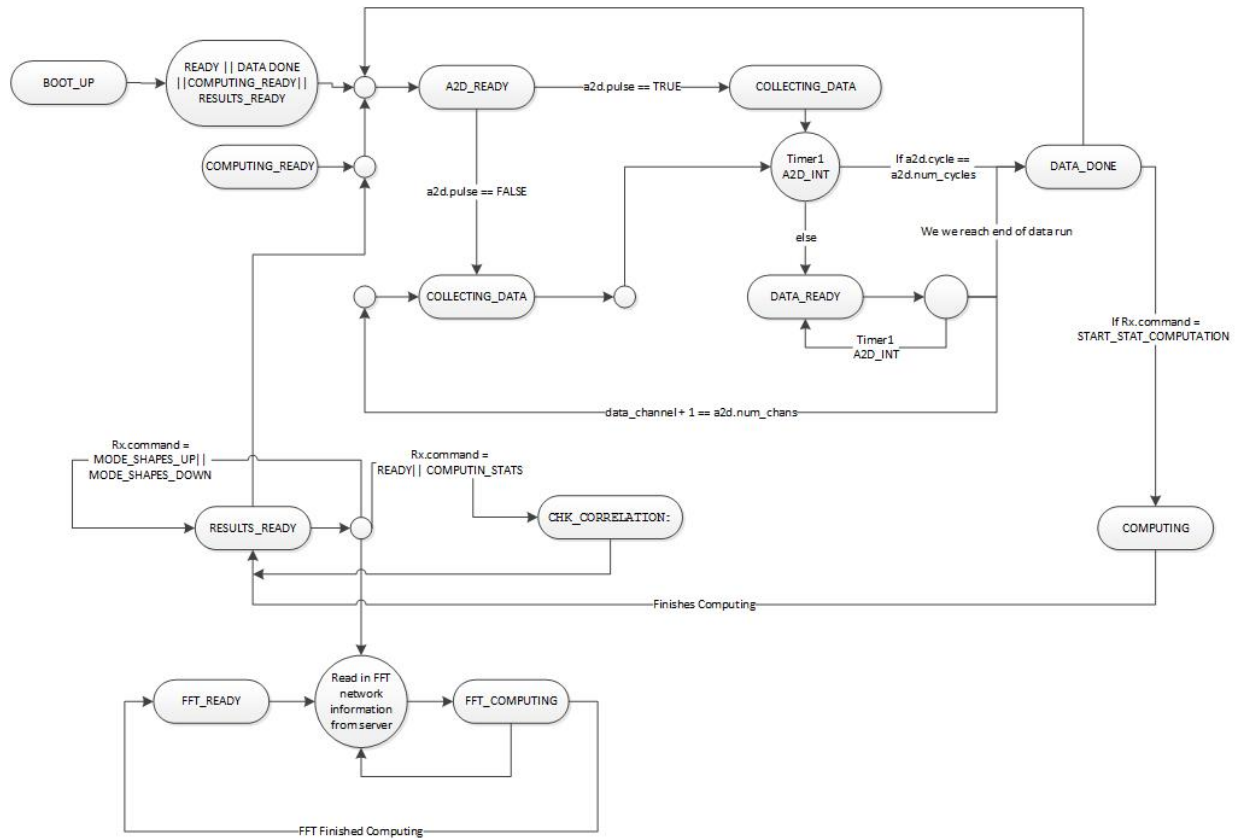


Fig. 8.3: Flow chart depicting Narada WSU algorithm in scour sensing post

9 Decision Support Engine for Scour Monitoring

The DSS work was also completed to display conditional data for the sensor posts located at all 6 field sites (2 in Michigan and 4 in Maryland). Historical scour states are viewable and user-defined alerts are supported. Locations of instrumented bridges are displayed for the user and details for each bridge can be inspected by clicking on individual bridges. Bridges with alerts are highlighted in different colors from bridges showing nominal conditions. Because only limited data with only limited observed sensor states were available from field instrumentation sites, two additional bridges using representative data were also added to the DSS client to demonstrate its functionality (seen in red above). Detail views for each bridge show the information and time history results for each whisker associated with each post at the bridge site. Based on sponsor feedback, post and channel location data was incorporated to improve usability.

The Bridge Scour Decision Support System (DSS) is a web-based application for desktop and laptop computers intended to serve as a single portal for managing information about the condition of one or more bridges affected by scour. While the demonstration Bridge Scour DSS web application is intended only for desktop and laptop computers, it will work to a limited extent on tablet devices since it is a web based application. The Bridge Scour DSS would allow users to view the scour status of the bridge inventory at a high level, to see the detailed scour status of any individual bridge including historical data, and to schedule alerts for when scour conditions at one or more bridges change.

The Bridge Scour DSS web application features prominently a map display through which the spatial context of the bridge inventory is made explicitly visible. Once a bridge and the scour feed is integrated, users can configure alerts for each sensor post. Alerts include a severity rating and compound with other alerts from the same bridge to produce a severity rating for each bridge. The DSS maintains a list of bridges based both on the number and severity rating of bridges, allowing managers to quickly assess which bridges are most in need of attention.

The commercial potential of the Bridge Scour DSS is based on its ability to integrate established bridge condition and inventory information with a new technique for automatically and remotely monitoring the scour condition of bridges over waterways. The web application was developed only with open-source software that is licensed for commercial applications. The final product is intended to be an end-to-end system that can be deployed on any web server with a connection to a suitable database and will provide tools for data managers to connect their systems to existing real-time streams from embedded scour sensors.

9.1 DSS Server

The DSS Server is the software that stores and manages the data received from the sensor post feeds. It is composed of a database, in this case PostgreSQL, and the web server infrastructure: Apache web server and Django web framework.

Django framework acts as an interpreter for web requests received by Apache, determining what data in the database should be manipulated and what if any information Apache should return to the client. This framework is tightly coupled with the database since the

database schema is actually defined within the Django models list and appropriate database tables are automatically generated. This ensures compatibility between the database and the web requests it must handle.

The DSS data model starts with bridges, in this case the NBI inventory data. Each NBI bridge can have one or more sensors which have one or more channels. This corresponds to the scour monitor post setup for which a single board computer controls multiple scour whiskers. The sensor represents the managing computer while each channel is an individual whisker. When data from the whiskers is loaded, it is stored as observations linked to these specific channels. Incoming observations may also trigger alerts: alerts are defined using the alert registry which encapsulates the conditions of the alert (ex. Whisker below normal stream-bed level is active). Each alert instance references the alert registry, which in turn references the severity rating.

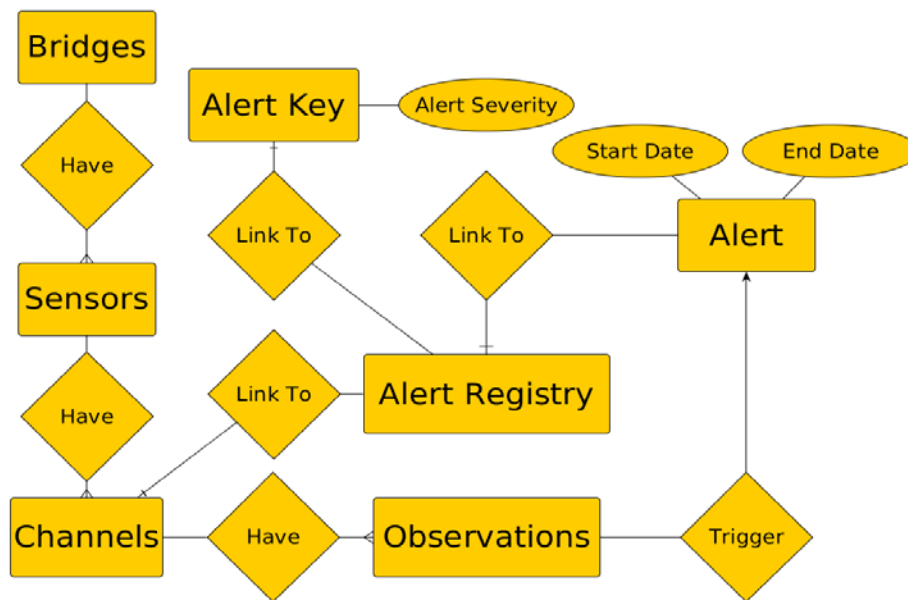


Fig. 9.1: DSS Data Model

9.2 DSS Client Process

Using the available data models, Django works with 'Views' to negotiate web requests and generate responses. Each View is associated with a base URL which is called when Apache receives a request. The View then processes the remaining URL to extract specific parameters passed in such as database query parameters or form fields. Once the URL parsing is complete the View can then do any data retrieval and processing necessary to formulate a response. For example, one of the DSS View's accepts an ID for an NBI bridge and returns all of the NBI data for that bridge. If the bridge ID is excluded from the URL, then a list of all the NBI bridges is returned instead.

The DSS Server also contains a suite of tools to help administrators set up and maintain the database. These are mostly data loaders, scripts that load data such as NBI bridge information or observations from scour sensors, but also utilities that assist in configuration

such as generating sensor and channel database entries for new scour posts or to generate the alerts from observations that are being loaded.

9.3 DSS Client Software

The DSS Client is a web application built on ExtJS 4.2 JavaScript framework and Google Maps API V3. ExtJS provides user interface capability to JavaScript along with the the capability to interact with database web API's. In this case, the web API is simply the DSS Server, which provides the client with the appropriate information to populate the Client user interface. Google Maps provides web mapping capability with which the bridge information is summarized geographically, while other ExtJS based pages provide more detailed information and administrative functionality.

The main page of the DSS is the Map view. This page incorporates the Google Map to display bridges geographically. By default this is the page that is loaded and it will display instrumented bridges regardless of alert status. Each bridge is displayed with a circular marker, which is color coded as green for no alert status, and red for bridges with alerts. Which bridges are displayed is configurable through the bottom right portion of the control panel, including the ability to display all of the NBI bridges available in the database as white bridge markers. Each of the bridge markers is clickable and will update the top portion of the control panel with summary details about the bridge, including bridge ID, description of the bridges location, number of alerts, and total alert severity accrued by any active alert states. Active alerts are also listed for quick viewing. The tools menu may be used to view top ten lists of bridge severity. The search bar between Tools and View can be used to look up a specific bridge using its bridge ID, or to peruse the list of bridges in general. This listing is also includes the number of alerts and the severity of alerts. Once a bridge has been identified, using the view button will pan and zoom the map to the bridges location.

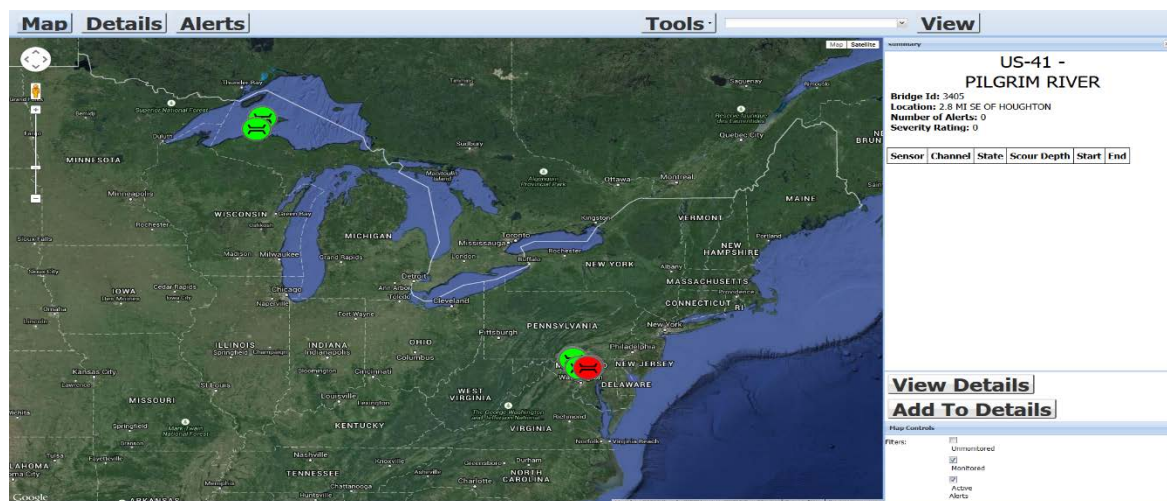


Fig. 9.2: DSS Client Map View

Once a bridge or set of bridges of interest has been identified, the user will undoubtedly be interested in more information about the state of those bridges, for this there is the Details view. The easiest method is to click on a bridge of interest and then either the “View Details” button, or the “Add To Details” button. Each of these will add the current bridge

to the Details view, but the View Details also switches over to that view while the other remains in map view, allowing the user to queue up multiple bridges of interest. Alternatively, the user can click on the Details button on the top panel to switch to that view, and then use the tools menu or search bar and view buttons to pull up bridge details.

The details view itself has a tab for each bridge that has been pulled up, each tab contains a set of charts as well as a full list of all active or inactive alerts for that bridge. The chart section has the ability to view graphs of sensor states for all of the sensors and channel on that bridge, allowing the user to examine the bridge condition in exacting detail. The severity rating chart shows the instantaneous severity rating of the bridge over time, allowing the user to easily identify time periods in which alerts were triggered and ended. The alerts history table lists all of the alerts that pertain to the bridge, including which sensor/channel, the sensor state, the alert state, depth, severity, status, and start/end dates. The table is both filterable and sortable through the column headers allowing the user to search for relevant information. Active alerts can also be selected and dismissed through this table when a user has reviewed the alerts and no longer considers them relevant to current management decisions (the alerts remain in the database as inactive, preserving the history).



Fig. 9.3: Sensor State chart from the Details View

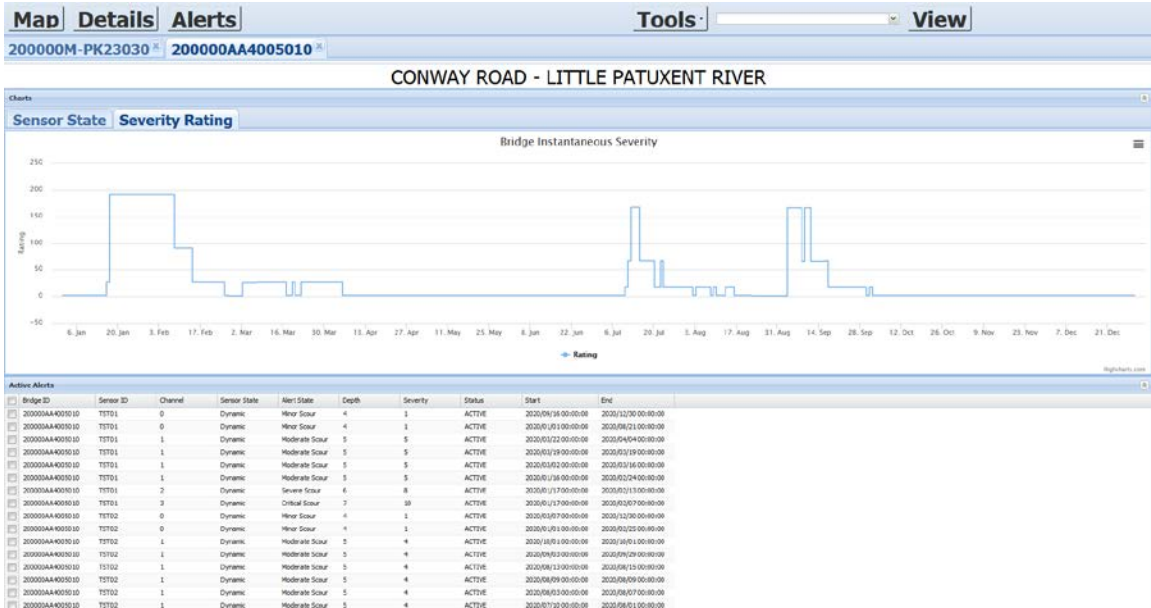


Fig. 9.4: Severity Rating Chart and Alerts Table for Details View

The final DSS view is the Alerts View, which allows the user to review, add, or delete alerts. The primary component of this view is a table listing all alert configurations for bridges/sensors/channels. Like the alert history table in the Details View, this table can be filtered and sorted using the column headers to search for relevant information. The tools and search bar can also be used to immediately filter for a specific bridge. The control panel on the right has options for creating and deleting alert configurations. The new alert option contains drop-downs that are filtered based on the information being entered, including sensor state, scour severity, and the alert key (descriptive text labeling the configuration). For example once the bridge ID is selected, the only available sensor IDs are those for that bridge and so on. Each of the drop-downs accept text entry and will dynamically further the list even further based on what has been typed so far. The delete alert function simply accepts an alert configuration ID and then deletes it after confirming the user's intentions. It is important to note that adding new alert configurations does not generate alert instances for past observations, preserving the existing history. Deleting alert configurations on the other hand will affect past history since that configuration is no longer available for reference.

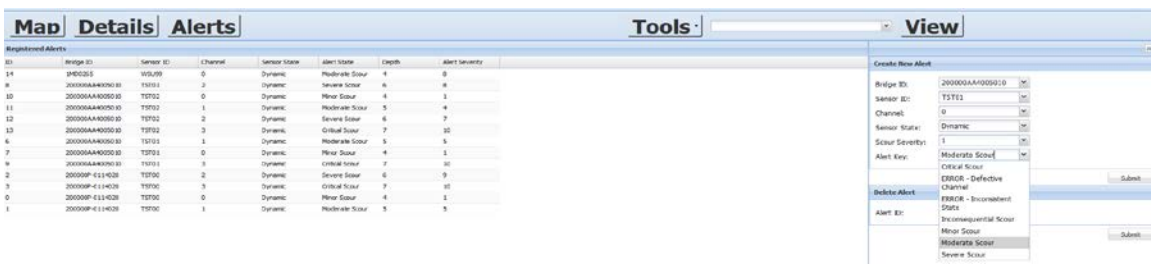


Fig. 9.5: DSS Alert View

Registered Alerts							
ID	Bridge ID	Sensor ID	Channel	Sensor State	Alert State	Depth	Alert Severity
0	200000P-0114020	Sort Ascending		Dynamic	Minor Scour	4	1
1	200000P-0114020	Sort Descending		Dynamic	Moderate Scour	5	5
2	200000P-0114020	Columns		Dynamic	Severe Scour	6	9
3	200000P-0114020	Filters	200000P-0114020	Dynamic	Critical Scour	7	10

Fig. 9.6: Filtering alert configuration table using column headers

9.4 Conclusions

By combining commercially licensable open source software, the BridgeScour Decision Support System represents a server to client software package for distributing scour information to bridge managers. The server software handles the receipt and maintenance of scour measurements then delivers these to the web client software for expedient analysis on a variety of platform including mobile devices such as tablets. The client software presents the user with a geospatial overview of the bridges and includes tools to quickly locate scour critical bridges and to view detailed information about sensor states, scour severity, and alert status over time. Together these tools provide managers with the information they need to make prompt decisions regarding critical scour situations.

10 Field Validation of Magnetostrictive Scour Monitoring

This section discusses the wireless scour-sensing post assemblies described in Section 6 and autonomous algorithms developed in Section 8 were field tested. In addition to the four field sites used for the year 1, Section 4 field campaigns in Maryland utilizing wired posts, 2 additional sites were identified in Michigan for deployment of wireless scour-sensing posts for pier and abutment monitoring. Data from the whisker sensors was collected using *Narada* wireless sensing nodes, transmitted to a local base station via low-power wireless local-area network (LAN), and sent remotely to the decision support system (DSS) database via cellular data network. Installation at the two sites was achieved using auger-hole installation. Significant effort was required to ensure reliable operation of the field system, particularly in ensuring synchronization of the posts and base station on site.

10.1 Installation Plan

Installation of the field sites, discussed in this section, was performed during the week of October 13, 2014. Permits for this work were obtained and advanced notices issued. A crew from Michigan Department of Transportation (MDOT) will traveled to the Upper Peninsula to assist with this installation. Details of the 2 sites are given below.

10.1.1 MI Bridge Number 1 – US41 crossing of the Pilgrim River City of Houghton, Houghton County

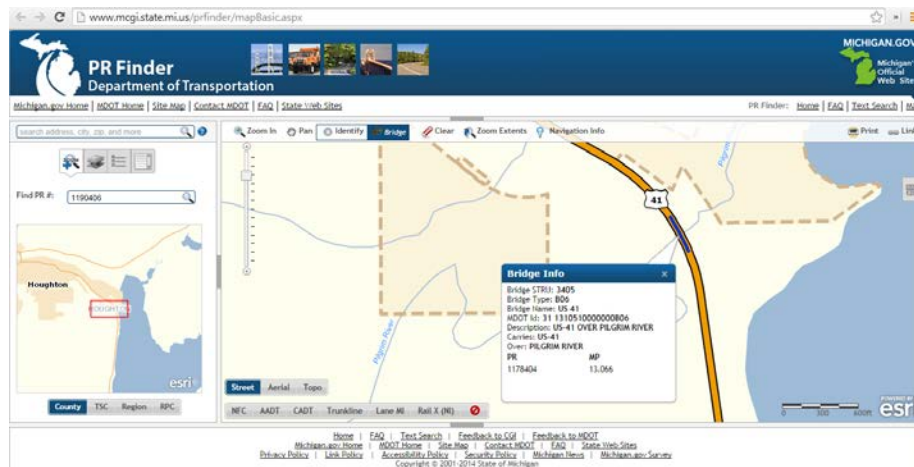


Fig. 10.1: MI Bridge 1 location.

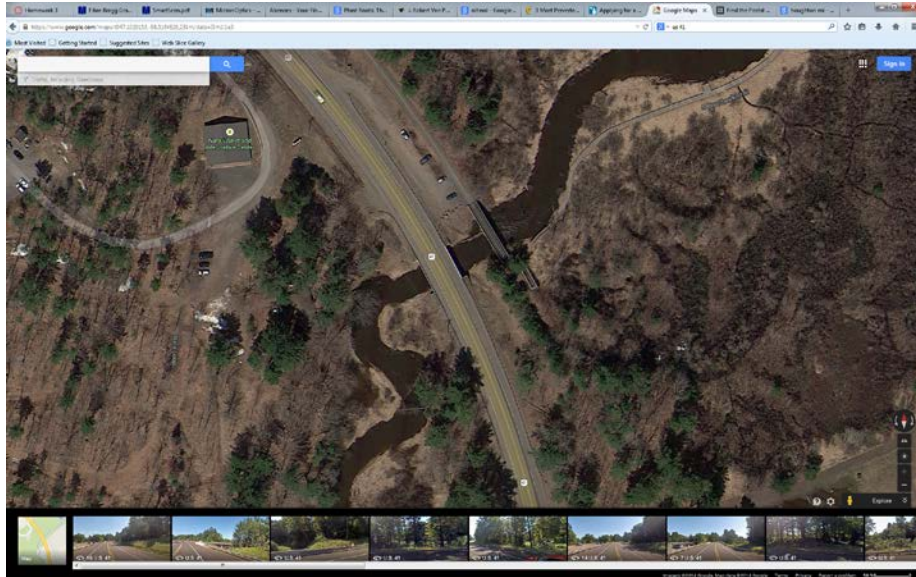


Fig. 10.2: Bridge 1 satellite image.

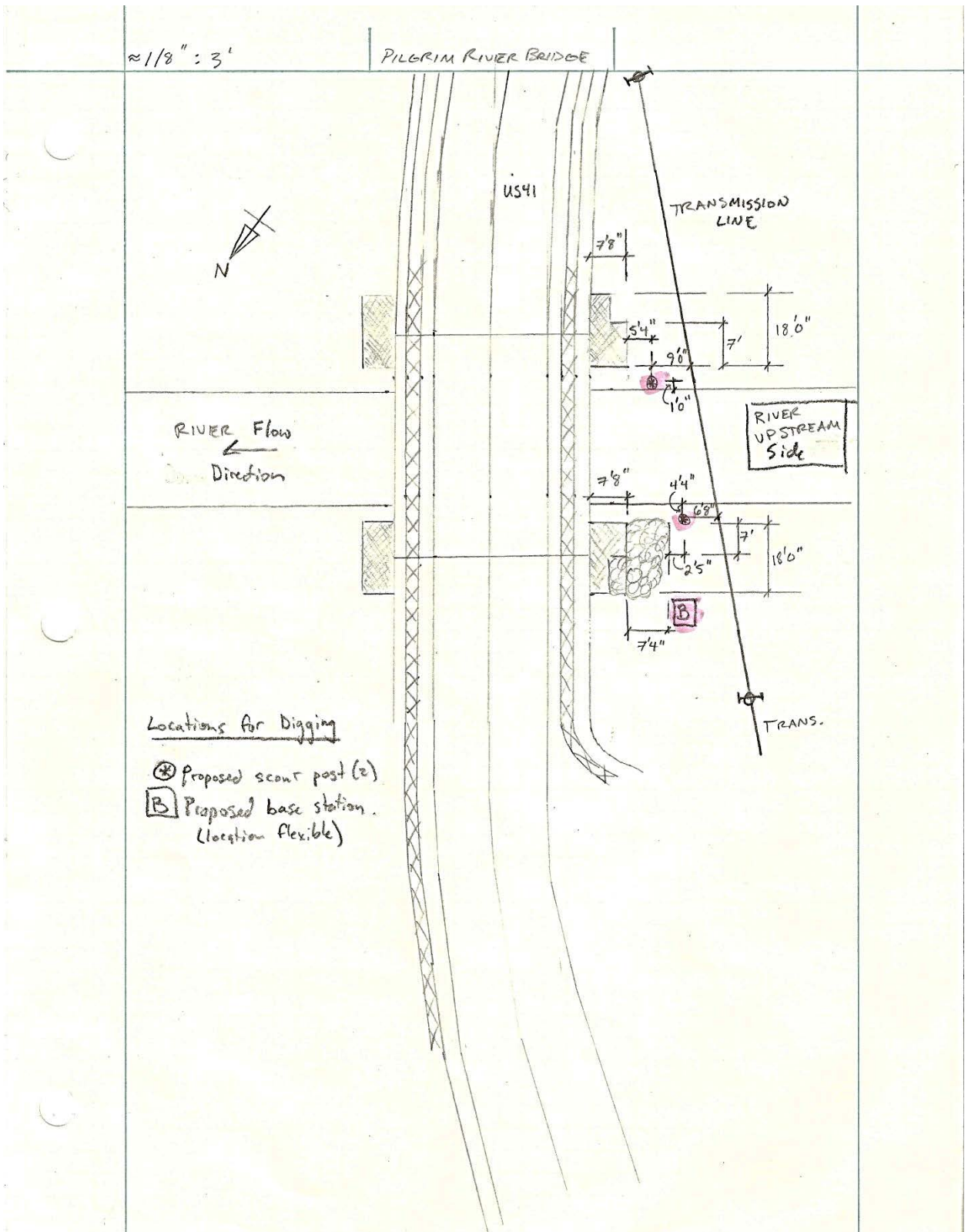


Fig. 10.3: Bridge 1 installation schematic.



Fig. 10.4: View of working (West) side of Bridge 1 looking South.



Fig. 10.5: Alternate view of West (working) side of bridge 1 (looking South) including overhead transmission wires



Fig. 10.6: West side of North abutment (post location 1)



Fig. 10.7: West side of North abutment (post location 1)



Fig. 10.8: West side of South abutment (post location 2)



Fig. 10.9: West side of South abutment (post location 2)

10.1.2 Bridge Number 2 – M38 crossing of the Sturgeon River
 Village of Baraga, Baraga County

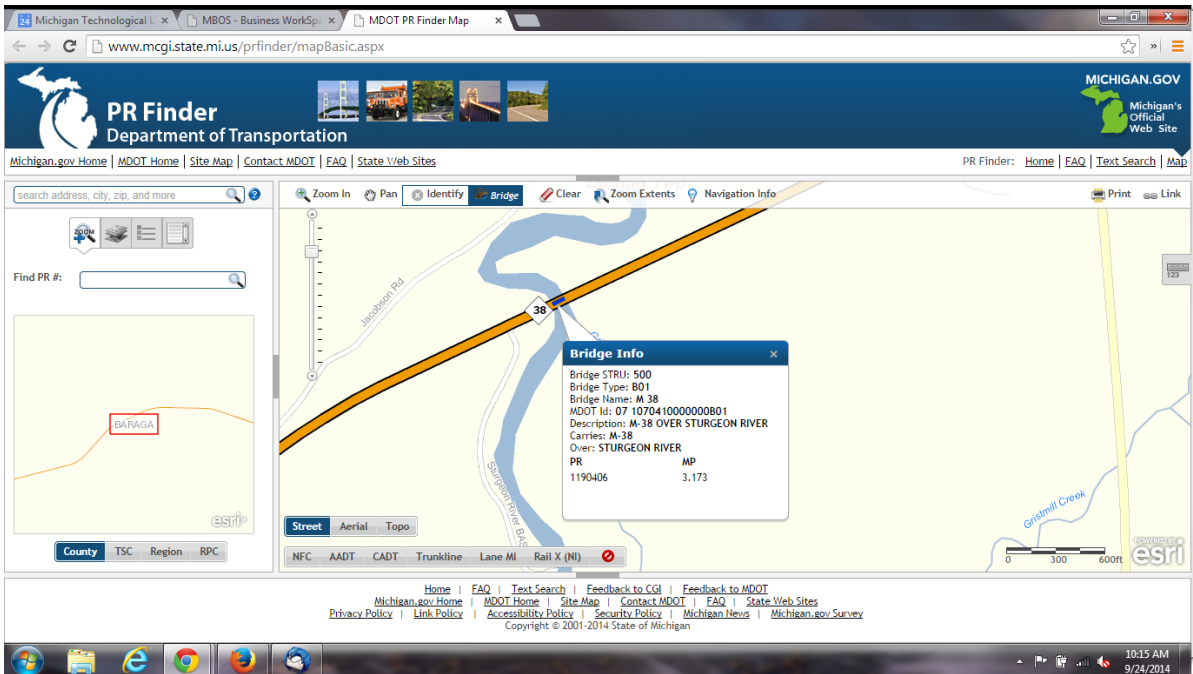


Fig. 10.10: MI Bridge 2 location.

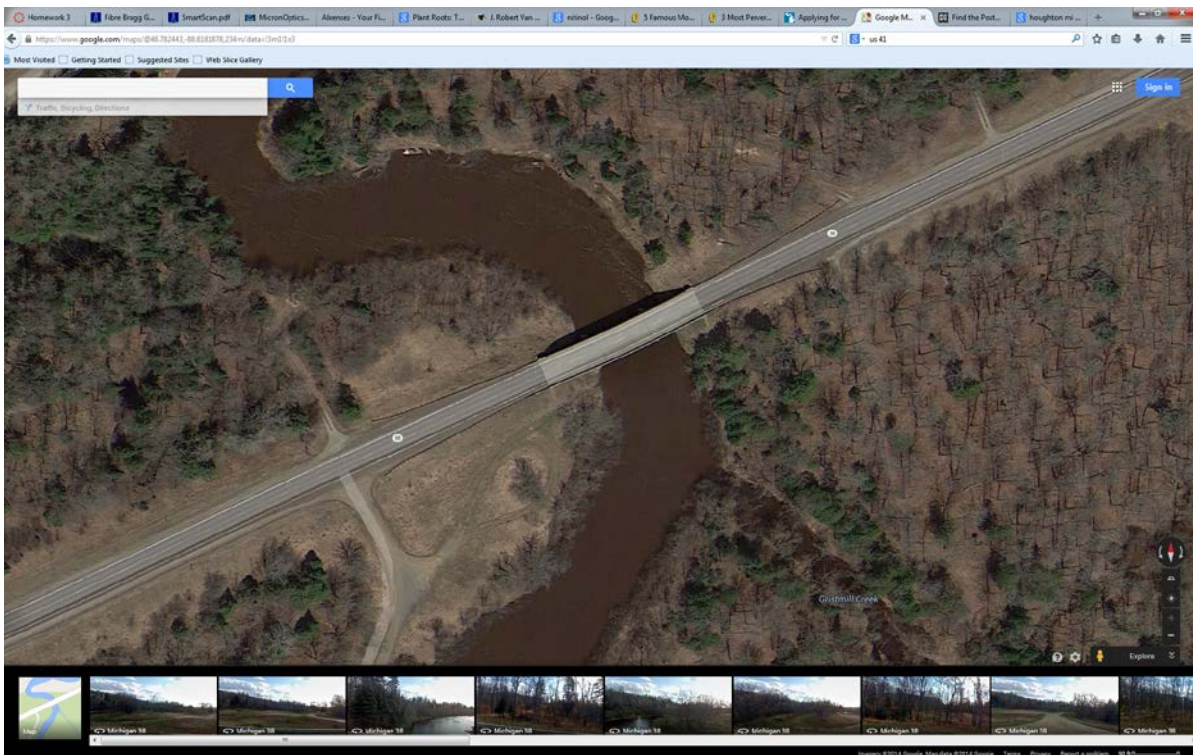
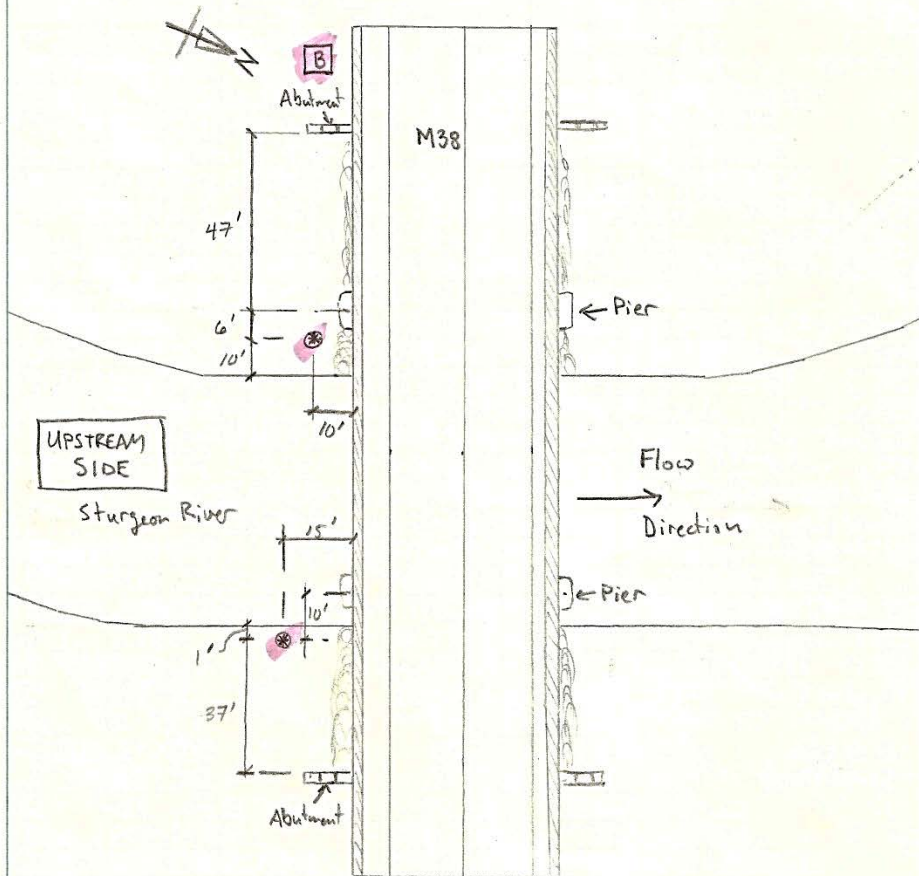


Fig. 10.11: Bridge 2 satellite image.

≈ 1/8" : 9' 3"

STURGEON RIVER BRIDGE / 38 CROSSING



Locations for digging

- ⊗ Proposed scow post (2)
- ⓑ Proposed Base Station Location (1)
(location is flexible)

Fig. 10.12: Bridge 2 installation schematic.



Fig. 10.13: 13. View of bridge 2, South (working) side (facing East)



Fig. 10.14: Alternate views of bridge 2, South (working) side (facing East)



Fig. 10.15: Proposed scour monitoring post location 1



Fig. 10.16: Proposed scour monitoring post location 2



Fig. 10.17: Sturgeon River site, looking West

10.2 Installation

The two bridge sites instrumented are scour critical bridges managed by MDOT. The first is the US41 crossing of the Pilgrim River. The second is the M38 crossing of the Sturgeon River (Fig. 10.18).



(a)



(b)

Fig. 10.18: Michigan bridge sites; (a) Pilgrim River bridge; (b) Sturgeon River bridge.

The Pilgrim River bridge is a single-span bridge with minimal scour countermeasures located very near Michigan Tech's main campus making it a useful site for the frequent site visits needed to debug sensor and data collection issues that arise during the field validation stage. The riverbed and banks are largely loamy soil with significant organic content. Posts were placed on the upstream side of each abutment just on the edge of the

riverbank where early scour attack may occur. The posts themselves were designed to stick out of the ground far enough to allow the wireless sensor units ground/snow clearance enough to successfully communicate with each other as well as the base station (Fig. 10.19).



Fig. 10.19: Top of one scour sensing post at the Pilgrim River site.

Installation of the posts was accomplished using an auger system (Fig. 10.20).



(a)



(b)

Fig. 10.20: Auger installation of the scour sensing posts; (a) MDOT Auger truck; (b) MDOT personnel leveling the auger post.

This approach was sufficient to allow the posts to be buried 10 ft below the water line before friction and hydrostatic pressure made additional depth impossible. Deeper

depths were not needed at this site, but could be accomplished using a pile-driving system.

The base station, consisting of a single board computer (SBC), power manager unit, solar panel, battery, cellular modem, and low-power wireless modem was installed in a weatherproof case on a sign post located high enough above the ground to improve wireless communications and discourage vandalism (Fig. 10.21).



Fig. 10.21: Base station at the Pilgrim River site.

The Sturgeon River site has a 3 span bridge that is located in largely sandy soil. The bridge has two piers with one pier that is seasonally dry. Taking advantage of this fact, the team installed one post upstream of one of the abutments, and the second upstream of the seasonally-dry pier (Fig. 10.22).



(a)

(b)

Fig. 10.22: Sturgeon River post sites; (a) Pier; (b) Abutment.

The auguring approach was similarly effective for installing these posts at the Sturgeon River site.

The Sturgeon River site is somewhat remote (10 miles west of the Village of Baraga) and not presently covered as part of any major cellular service provider's data network. An additional directional antenna was required for the base station at this site in order to communicate with the FTP server in Ann Arbor (Fig. 10.23).



Fig. 10.23: Base station at the Sturgeon River site.

10.3 Operation – Problems Encountered

Initial operation at the M-38 (Sturgeon River) site indicated that the cellular network conductivity was poor in the valley, where the highway crossed the river, likely due to the local topology and the relative remoteness of the nearest cellular transmission tower. A high-gain, directional antenna was acquired and installed, aimed at the local tower in order to increase the range of the cellular data modem that was part of this base station. This modification improved communication to acceptable levels. Also, one defective battery had to be replaced during the operation of the systems

Despite testing of the autonomous wireless data collection system in the laboratory, conditions in the field test affected the system in different ways and have led to some problems with reliability. The primary issue was an increase in dropped wireless data packets sent over the low-power, local wireless network that links the scour posts with the autonomous base station. Dropped packets are inevitable in any wireless data network and the system has been designed with fault handling algorithms in order to continue operation and collect all data despite some random loss. Field conditions (particularly snow) created additional packet loss and disrupted the timing of the network in a way that was not observed in the lab (developed in an earlier phase of the project). This issue manifested

itself in 2 ways. First, the power manager devices that synchronize the network and manage sleep mode for the system were not synchronizing correctly when one or more device did not establish good communications with the remaining devices. The existing algorithm was actually actively desynchronizing the network instead by as much as 15 minutes per day (under proper operation, all units are synchronized within 1 second of each other). This issue was fixed by rewriting the code to be more tolerant of these faults.

The second issue was with communication of data between the base station and the posts. Longer data transmission times caused the base station to reset, losing that day's data. The base station would wake up, establish a cellular data collection with the remote server in Ann Arbor, MI, create a directory to store data, initialize a scour detection test, but not complete it, leaving behind an empty folder on the remote server. That event demonstrated that the remote cellular communication is working correctly, but on site collection is not. The team debugged this issue by reprogramming the base station to upload a log of its activity to the remote server to illustrate which step it reaches before failing. Data collection tests were initialized correctly by the server, acknowledged by the scour sensor posts, but the results were not collected correctly 10 minutes later as they should.

Issues relating to communication and synchronization between the base station and on-site posts were resolved through changes in the on-site communication algorithm. Most significantly, changes to the synchronization algorithm that runs in the power manager device were made to allow the system to be more fault-tolerant when communication delays are encountered. The existing algorithm was actively desynchronizing the network by resetting timers on the base station power manager when communications from the posts were not properly received. This issue has been fixed by rewriting the code to require successful communications with the posts before resetting of the base station times was allowed. Observations have shown that these changes were effective. In addition, the time allowed for the tests has been increased in order to improve system reliability. Ten-minute daily windows have been increased to fifteen minutes, eliminating the phenomenon of empty data folders in the remote server.

10.4 Conclusions

Wireless scour sensing post networks composed to two posts and one base station were installed and validated during this portion of the study. These posts operated for nearly nine months in an autonomous mode. Some problems were encountered with synchronization of the wireless network in the field that led to data loss. Synchronization and timing algorithms were modified to be more fault tolerant (particularly for missed communications) to improve reliability.

11 Conclusions

In this study an automated remote flow detection arrays based on bio-inspired flow sensors were introduced for scour monitoring. The method is simple because it uses robust magnetostrictive sensors and low-power wireless sensors for data acquisition. The method takes advantage of a simple algorithm and pre-known depth and state of the sensors to determine the extent of scour.

The proof-of-concept experiments were performed in the laboratory and the field to validate the ability of an automated scour detection and monitoring system to successfully monitor scour. The laboratory results demonstrated that distinction between static and dynamic sensor signals can be made, and, with the knowledge of the depth of the sensor, scour can be measured and monitored. The laboratory tests established the automated characteristics of the system and displayed the ability of the system to successfully give a warning of impending bridge failure. The ability of the system under study to automatically capture and log peak scour events was shown. Furthermore, the algorithm used in this system is simple which aids its autonomy and the results that are relayed to the bridge owner are easy to comprehend.

The hardware components that make the system were discussed. It was evident that all the components involved in the system are relatively easily available and are inexpensive. This study also presented the simplicity of the procedure that was adopted for field installation which makes the system easy to handle and install and suitable for mass installation.

Significant effort was made to improve the robustness and sensitivity of the whisker sensors for the intended usage and environment. Corrosion protection through galvanization, use of rugged Alfenol alternatives, and development of the low-flow airfoil and magnetic sea weed sensor morphologies led to improvements in performance.

Field validation was carried out in two stages, first using wired posts and finally, leveraging the low-power wireless technology. Data from the remote systems was integrated into a decision support client that provides users with flexible alert conditions, network- and bridge-level views of alerts and conditions, and the option to view historical views as well.

12 References

- [1] Lagasse, P., Clopper, P., Pagan-Ortiz, J., Zevenbergen, L., Arneson, L., Schall, J., and Girard, L., [Bridge Scour and Stream Instability Countermeasures: Experience, Selection and Design Guidance. Volume 2], (2009).
- [2] Richardson, E. and Davis, S., "Evaluating Scour at Bridges . Federal Highway Administration, Hydraulic Engineering Circular No. 18," Publication FHWA NHI, 01-001 (2001).
- [3] Prendergast, L. and Gavin, K., "A review of bridge scour monitoring techniques," Journal of Rock Mechanics and Geotechnical Engineering, 6(2), 138-149 (2014).
- [4] Luke J. Prendergasta, K.G., "Monitoring of scour critical bridges using changes in the natural frequency of vibration of foundation piles – A field investigation," Transport Research Arena (2014).
- [5] Beatrice E. Hunt, P.E., M.ASCE1, Senior Hydraulics Engineer, "ESTABLISHING A SCOUR MONITORING," Geo-Frontiers Congress 2005 (2005).
- [6] Hunt, B.E., [Monitoring scour critical bridges], Transportation Research Board, (2009).
- [7] Swenson, D.V. and Ingraffea, A.R., "The collapse of the Schoharie Creek Bridge: a case study in concrete fracture mechanics," International journal of fracture, 51(1), 73-92 (1991).
- [8] Frangopol, D.M., Strauss, A., and Kim, S., "Bridge reliability assessment based on monitoring," Journal of Bridge Engineering, 13(3), 258-270 (2008).
- [9] Friedland1, R.T.a.I., "'Status of Scour Instrumentation Development'," Proceedings of the Hydraulic Engineering sessions at Water Forum '92 American Society of Civil Engineers (August 2–6, 1992.).
- [10] Zheng, W., [Instrumentation and Computational Modeling for Evaluation of Bridge Substructures across Waterways , Final Report for State Study-229] FHWA/MS-DOT-RD-13-229, MS-DOT-RD-13-229, (December 2013).
- [11] Lagasse, P., Richardson, E., and Schall, J., "Fixed instrumentation for monitoring scour at bridges," Transportation Research Record: Journal of the Transportation Research Board, 1647(1), 1-9 (1998).
- [12] Lefter, J., "Instrumentation for measuring scour at bridge piers and abutments," NCHRP Research Results Digest(189), (1993).
- [13] Yankielun, N. and Zabilansky, L., "Laboratory investigation of time-domain reflectometry system for monitoring bridge scour," Journal of Hydraulic engineering, 125(12), 1279-1284 (1999).

- [14] Ettema, R., Nakato, T., and Muste, M.V.-I., [An illustrated guide for monitoring and protecting bridge waterways against scour] IHR-Hydroscience & Engineering, University of Iowa, (2006).
- [15] Zarafshan¹, A., Iranmanesh², A., and Farhad Ansari, M.A., “Vibration-Based Method and Sensor for Monitoring of Bridge Scour,” *Journal of Bridge Engineering*, ASCE, (2012).
- [16] Mueller, D.S., Abad, J.D., García, C.M., Gartner, J.W., García, M.H., and Oberg, K.A., “Errors in acoustic Doppler profiler velocity measurements caused by flow disturbance,” *Journal of hydraulic Engineering*, 133(12), 1411-1420 (2007).
- [17] Placzek, G. and Haeni, F., [Surface-geophysical techniques used to detect existing and infilled scour holes near bridge piers], US Department of the Interior, US Geological Survey, (1995).